THESIS

LIBRARIES
MICHIGAN STATE UNIVERSITY
EAST LANSING, MICH. 48824

This is to certify that the

dissertation entitled

Excited State Proton Transfer

presented by

Nahid Shabestary

has been accepted towards fulfillment
of the requirements for

Ph.D. degree in Chemistry

M. A. El-Bayoumi
Major professor

Date May 10, 1982

MSU is an Affirmative Action/Equal Opportunity Institution

O-12771

MSU
LIBRARIES

RETURNING MATERIALS:
Place in book drop to remove this checkout from your record. FINES will be charged if book is returned after the date stamped below.

EXCITED STATE PROTON TRANSFER

By

Nahid Shabestary

A DISSERTATION

Submitted to
Michigan State University
in partial fulfillment of the requirements
for the degree of

DOCTOR OF PHILOSOPHY

Department of Chemistry

1982

ABSTRACT

EXCITED STATE PROTON TRANSFER

By

Nahid Shabestary

Excited state proton transfer represents one of the simplest photoreactions that is expected to occur when the acidity or the basicity of a functional group is enhanced upon excitation. Phenomenologically, excited state proton transfer manifests itself usually by the appearance of a new fluorescence band which has a large Stokes shift. For example, methyl salicylate in hydrocarbon solvents exhibits two fluorescence bands, one at 340 nm and the other with a large Stokes shift of 10,000 cm^{-1} at 450 nm. The latter fluorescence band results from a tautomer produced in the excited singlet state as a result of an intramolecular proton transfer. The methoxy derivatives which cannot undergo excited state proton transfer exhibit a normal fluorescence, i.e., a band at $\sim$340 nm. The first chapter deals with examples of excited state proton transfer in solution, the solid phase and the vapor phase. Several aspects related to

the mechanism of excited state proton transfer are summarized. The question of whether the emission results are explained in terms of an excited state equilibrium or in terms of equilibrium between different ground state conformers is discussed.

We have studied the absorption and luminescence properties of p-amino salicylic acid (PAS) and N,N dimethyl p-amino salicylic acid (DPAS) and their methyl esters (PASE, DPASE), under various conditions. Effects of the medium, pH and substituents helped in the interpretation of the absorption spectra which are dominated by "charge-transfer transitions. In the "charge transfer" states of these molecules the hydroxyl and amino groups act as electron donors while the carboxyl group acts as an electron acceptor. The emission spectra clearly reveal the occurrence of proton transfer from the hydroxyl group to the carbonyl oxygen during the lifetime of the first excited singlet state. In the case of DPAS the charge transfer state where the hydroxyl group acts as an electron donor (O)CT, is lower in energy than the (N)CT where the amino group acts as an electron donor. The N,N dimethyl amino group has a lower ionization potential than the NH_2 group. Thus in the case of DPAS an energy level reversal occurs which has an important consequence on the emission spectrum of DPAS. A unique excitation wavelength dependence has been observed. In the (N)CT state, the basicity of the

oxygen of the carboxyl group is expected to be larger than that of the ground state, but the acidity of the hydroxyl group is not expected to change appreciably. In this case no proton transfer is expected for the hydroxyl group as a result of excitation of the (N)CT state. In contrast, for the excitation of the (O)CT state, both the acidity of the phenol group and the basicity of the oxygen of the carboxyl group are expected to be increased relative to their values in the ground state. Experiments show that in the case of DPAS a longer excitation wavelength (330 nm) leads to emission at 354 nm while a shorter excitation wavelength (300 nm) gives rise to an emission at ∿460 nm as well as at 354 nm. In the case of DPAS, we are dealing with excitation of two different electronic states of the same conformer. In contrast, the emission of MSA is varied as a result of excitation of different conformers which are at equilibrium in the ground state. All these results have been discussed in detail in Chapter II. Our studies show that PAS also exhibits excited state proton transfer in the solid phase. The crystal structure of PAS shows intra- and intermolecular hydrogen bridges.

Studies of 1-azacarbazole in the solid phase, also shows that excited state double proton transfer accounts for the observed emission. The crystal structure, as determined by x-ray diffraction methods, shows that the crystal contains cyclic dimers only. A summary of these results is given in Chapter III.

Chapter IV summarizes experimental procedures and purification of solvents and compounds and Chapter V gives a brief conclusion with some suggestions for future work.

To Yasha

ACKNOWLEGMENTS

I wish to express my deep appreciation to my advisor, Professor M. Ashraf El-Bayoumi for his guidance, encouragement and friendship during the course of this study.

I am grateful to professor James L. Dye. for presiding as my second reader and for the editorial assistance in improving my writing skill. I also thank Professor Andrew Timnick and Professor Michael W. Rathke. for serving on my committee.

To Dr. Paul Hunter goes my thanks for being such a good friend and coworker throuhg my many terms of teaching.

I would also like to thank Dr. D.W. Ward for his great help in defining crystal structure.

Many thanks go to Mr. Ron Hass and Scott K. Sanderson for their expert assistance in electronics. Special thanks to my good friends and colleagues, Khader Ahmad Al-Hassan and Kamal Ismail. The author wishes to express her thanks to the chemistry department of MSU for the assistantships providing finacial support.

The author is particularly grateful to her husband, Abbas, for his constant encouragement and understanding.

TABLE OF CONTENTS

Chapter		Page
LIST OF TABLES.		viii
LIST OF FIGURES		x
CHAPTER I - EXCITED STATE PROTON-TRANSFER		1
1.	Introduction.	1
2.	Theoretical Models of Hydrogen-Bond	4
3.	Proton Transfer in the Ground State	5
4.	Hydrogen-Bonding in the Excited State . . .	13
5.	Excited State Acidity and Basicity.	17
6.	Proton Transfer in the Excited State. . . .	27
	A. Intramolecular Proton Transfer.	28
	Salicylic Acid and Its Derivatives. . .	28
	Salicylamide and Salicylanilide	47
	Naphthoic Acid and its Derivatives. . .	55
	B. Intermolecular Proton Transfer.	64
	Naphthol-Triethylamine Systems.	64
	3-Hydroxypyrene-TEA System.	71
	7-Azaindole Dimers (Double Proton Transfer)	72
	7-Azaindole-Alcohol Complexes	78
	C. Kinetic Isotope Effects in Proton Transfer Reactions.	82
	Isotope Effect in Excited State Proton-Transfer in 7-Azindole (7AI) Dimers.	85
	D. Proton Tunnelling	88

Chapter Page

Experimental Evidence in 7AI Dimers . . 91

E. Excited State Proton Transfer in the Vapor Phase, Methyl Salicylate. 92

F. Excited State Proton Transfer in the Solid Phase, Acridine Derivatives 97

CHAPTER II - EXCITED STATE PROTON TRANSFER IN P-AMINO SALICYLIC ACID DERIVATIVES . . 103

A. Introduction. 103

B. Excited State Proton Transfer in p-Amino Salicylic Acid (PAS) and its Methyl Ester (PASE). 105

1. Solvent Effect on the Absorption Spectra of PAS and PASE 114

2. pH Effect on the Absorption Spectra of PAS and PASE 120

3. Emission Spectra of PAS and PASE as a Function of pH at Room Temperature. . . 126

4. Fluorescence Spectra of PAS and PASE in Different Solvents at Room Temperature. 131

C. Excited State Proton Transfer in Solid Phase of p-Amino Salicylic Acid (PAS) . . . 140

D. Excited State Proton Transfer in N,N-Dimethyl p-Amino Salicylic Acid (DPAS) and its Methyl Ester (DPASE). 145

1. Solvent Effect on the Absorption Spectra of DPAS and DPASE 145

2. pH Effect on the Absorption Spectra of DPAS and DPASE 148

3. Emission Spectra of DPAS and DPASE As a Function of pH at Room Temperature. 156

Chapter Page

4. Fluorescence Spectra of DPAS and DPASE in Different Solvents at Room Temperature. 159

E. A Unique Excitation Wavelength Dependence of Excited-State Proton-Transfer. 163

CHAPTER III - EXCITED STATE DOUBLE PROTON TRANSFER IN 1-AZACARBAZOLE HYDROGEN-BONDED DIMERS, ITS ACETIC ACID COMPLEX AND IN THE SOLID PHASE. 170

A. Introduction. 170

1. Excited State Double Proton Transfer in 1-Azacarbazole Hydrogen-bonded Dimers. 171

2. Phosphorescence Spectrum of 1-Azacarbazole. 181

3. Excited State Double Proton Transfer in 1-Azacarbazole-Acetic Acid Complex . 183

4. Excited State Double Proton Transfer in 1-Azacarbazole in the Solid Phase. . 186

Crystalographic Data. 186

Room Temperature UV Absorption and Fluorescence Spectra of 1-Aza-carbazole in the Solid Phase. 188

CHAPTER IV - EXPERIMENTAL 193

A. Experimentally Studied Molecules. 193

1. Para Amino Salicylic Acid (PAS) 193

2. Methyl Para Amino Salicylic Acid (PASE). 193

3. N,N Dimethyl Para Amino Salicylic Acid (DPAS) 193

4. Methyl N,N Dimethyl Para Amino Salicylic Acid (DPASE). 193

5. 1-Azacarbazole (1AC). 194

Chapter Page

6. N_1-Methyl 1-Azacarbazole Tautomer . . . 194

B. Solvents. 195

1. 3-Methylpentane (3MP) 195

2. Ethanol 196

3. Ether 196

4. Water 196

5. Cyclohexane 196

6. Hexane. 196

C. Spectral Measurements 197

1. Absorption Spectra. 197

2. Emission Spectra. 197

3. Infrared Spectra. 198

4. Mass Spectra. 198

5. NMR Spectra 198

CHAPTER V - CONCLUSION AND FUTURE WORK. 199

REFERENCES. 204

LIST OF TABLES

Table		Page
1	pK_a and pK_a^* Values for Selected Molecules	19
2		53
3	Room Temperature Absorption Maxima (nm) and Spectral Shifts (cm^{-1}) Relative to 3MP for PAS in Different Solvents. . . .	116
4	Room Temperature Absorption Maxima (nm) and Spectral Shifts (cm^{-1}) Relative to 3MP for PASE in Different Solvents.	120
5	Room Temperature Absorption and Emission Maxima for PAS at Different pH Values, Ground and Excited States Species	121
6	Room Temperature Absorption and Emission Maxima for PASE at Different pH Value, Ground and Excited State Species . .	122
7	Emission Maxima in nm for PAS in Different Solvents	134
8	Emission Maxima in nm for PASE in Different Solvents	134

Table		Page
9	Room Temperature Absorption Maxima (nm) and Spectral Shifts (cm^{-1}) Relative to 3MP for DPAS Acid in Different Solvents.	147
10	Room Temperature Absorption Maxima (nm) and Spectral Shifts (cm^{-1}) Relative to 3MP for DPASE in Different Solvents.	147
11	Room Temperature Absorption and Emission Maxima for DPAS at Different pH Value, Ground and Selected States Species	152
12	Room Temperature Absorption and Emission Maxima for DPASE at Different pH Value, Ground and Excited States Species	155
13	Room Temperature Emission Maxima in nm for DPAS in Different Solvents.	159
14	Room Temperature Emission Maxima in nm for DPASE in Different Solvents	161

LIST OF FIGURES

Figure		Page
1	Absorption spectra of Schiff base (PLP 7 x 10^{-5} M, n butylamine 2.5 x 10^{-4} M) in various solvents; dioxane, ΔΔΔ DMF, —— H_2O, the dotted line represents decomposition of this spectrum.	7
2	Potential energy diagrams for the motion of the proton in a hydrogen bond A-H...B.	9
3	Hypothetical potential energy curves for the formation of a H-bond A-H...B in Ground and excited state, (1) $W_g > W_e$, (2) $W_g < W_e$	16
4	Effect of pH on the fluorescence of an aqueous solution of indole at 25°C . . .	25
5	Absorption and fluorescence spectra of salicylic acid and 2-methoxybenzoic acid in methanol at 20°C	29
6	Absorption and fluorescence spectra of methyl salicylate in methylcyclohexane (——) and fluorescence spectrum of	

Figure Page

methyl 2-methoxy benzoate in the same solvent (---) 31

7 Fluorescence spectra (uncorrected) of methyl salicylate, 10^{-4} mole ℓ^{-1} in methanol; at different excitation wavelengths 35

8 Fluorescence excitation spectra of methyl salicylate, 10^{-4} mole ℓ^{-1} in methanol 36

9 Fluorescence spectra of 2×10^{-4} mole cm^{-3} methyl salicylate in cyclohexane (——), ethanol (– – –), methanol (----), and 2,2,2-trifluoroethanol (....). The spectra are shown in relative numbers of quanta vs. wavenumber in μm^{-1}. The excitation wavelength is 286 nm 38

10 Excitation spectra of methyl salicylate in methylcyclohexane. Solid dots represent the 450-nm band, while open circles represent the 350 nm fluorescence . 42

11 Temperature variation of the fluorescence spectrum of methyl salicylate in cyclohexane (1.4×10^{-4} M). As temperature increases the short wavelength emission intensity raises and the long wavelength

Figure Page

intensity decreases. Temperatures (°C): 21.2, 29.6, 39.1, 48.3, 57.3, 67.5. 46

12a Fluorescence spectra of salicylamide: (a) 2.4 x 10^{-4} M in ethanol, λ_{ex} = 265 nm; (b) 1.3 x 10^{-5} M in cyclohexane, λ_{ex} = 300 nm; (c) 1.0 x 10^{-4} M in water, λ_{ex} = 265 nm. 49

12b Effect of excitation wavelength on the fluorescence spectrum of 2.5 x 10^{-5} M salicylamide in ethanol: (a) λ_{ex} = 290 nm; (b) λ_{ex} = 310 nm. 50

13 Fluorescence decay curve of 10^{-3} M aqueous salicylamide (all emission above 400 nm) excited at 265 nm; sweep speed 16 PS channel^{-1}. The upper curve is a semi-log plot. 52

14 Fluorescence of salicylamide in D_2O (1.7 x 10^{-4} M). Excitation wavelengths (nm): (a) 330; (b) 330; (c) 265 54

15 Fluorescence excitation spectra for salicylamide in D_2O. Emission wavelengths (nm): (a) 350; (b) 430. 56

16 Fluorescence of methyl 3-hydroxy-2-naphthoate in cyclohexane: (a) 1 x 10^{-5} M

Figure Page

(b) 1 x 10^{-4} M, λ_{ex} = 260 nm, (c) 1 x 10^{-4} M, λ_{ex} = 390 58

17 Fluorescence excitation spectra of methyl 3-hydroxy-2-naphthoate in cyclohexane (a) short wavelength emission and (b) long wavelength emission. 59

18 Change of the absorption spectrum of β-naphthol in cyclohexane produced by added TEA (15°C). Concentration of β-naphthaol: 2 x 10^{-4} mole ℓ^{-1}. Concentration of TEA: (1) 0 mole ℓ^{-1}, (4) 1.12 x 10^{-2} mole ℓ^{-1} (6) 1.80 x 10^{-1} mole ℓ^{-1} 65

19 Fluorescence spectra of β-naphthol in methylcyclohexane at different concentrations of triethylamine (1) 0.000 M; (2) 0.002 M; (3) 0.004 M, (4) 0.008 M; (5) 0.020 M; (6) 0.10 and 0.15 M; (7) as solvent. 67

20 Fluorescence spectra of β-naphthol in methylcyclohexane +0.14 M triethylamine at different temperatures 69

Figure

21 Fluorescence spectra of β-naphthol under various conditions. The time-resolved spectra of the β-naphthol-TEA system in toluene at 25°C observed 0 ns (curve a) and 10 ns (curve b) after the fluorescence of free β-naphthol reached the maximum intensity. The concentration of β-naphthol and TEA are 1.2 x 10^{-4} M and 0.705 x 10^{-2} M, respectively. Curve C is the steady state fluorescence spectrum of the toluene solution of 3-naphthol (0.705 x 10^{-4} M) 70

22 Room temperature absorption (left) and fluorescence (right) of 7-azaindole in 3MP at 1.0 x 10^{-5} M (——) and 1.0 x 10^{-2} M (---). Excitation wavelength 285 nm. Front surface excitation was used for the concentrated sample. The signals were arbitrarily adjusted to give comparable intensity in the F_1 region. 75

23 Corrected room temperature fluorescence spectra of 7AI in EtOH (——) and 7AI in EtOD (-·-·). 79

Figure		Page
24	Model barrier for proton tunnelling calculation	90
25	Vapor phase fluorescence spectra (uncorrected) of MSA at 50°C, equilibrium pressure under N_2, excitation wavelengths indicated. The experimental conditions are identical for both spectra	93
26	Vapor phase fluorescence of MSA, under N_2, as a function of temperature (indicated in °C). Insert: semilogarithmic plot of the intensity ratio of short-to-long wavelength emission vs. reciprocal temperature.	94
27	Fluorescence spectra of a solution of 9-(p-hydroxy) phenylaridine in ethanol at different pH values. Curve 1-pH 8; curve 2 - pH 2	99
28a	Fluorescence spectra of a film of 9-(p-hydroxy) phenylacridine in vacuum at -180°C. Curve 1 - before exposure; curve 2 - after exposure for 10 min to the total radiation of an SVDSH-250 lamp; curve 3 - after regeneration at room temperature; curve 4 - acetic acid vapor; curve 5 - in pyradine vapor.	99

Figure Page

28b Potential energy curve scheme for proton phototransfer in films at -180°C. 99

29 Room temperature absorption spectra of p-nitroaniline in different solvents: (...) methylcyclohexane, (-.-.-) ether, and (----) ethanol (concentration in alcohol = 6.52 x 10^{-5} gm moles lit^{-1}). 108

30 Room temperature absorption spectrum of tri-1-naphthylboron in methylcyclohexane (dashed line); and same after bubbling in dry ammonia gas (solid line). 109

31 Qualitatively molecular orbital energy level for benzene, phenol and lowest vacant orbitals of substituent 111

32 Room temperature absorption spectra of salicylic acid (SA) in different media: (———) N/10-HCl; (-.-.-) N/20-NaOH; (-...-) 5-n NaOH; and methyl salicylate in (----) N/20-NaOH. 113

33 Room temperature absorption spectra of PAS in different solvents: (———)

Figure Page

3MP, (----) ether, (-.-.-) ethanol, and (....) H_2O (pH = 2) 115

34 Room temperature absorption spectra of PASE in different solvents: (——) 3MP, (----) ether; (-.-.-) ethanol; and (-..-..) H_2O 119

35 Room temperature absorption spectra of PAS at different pH values: (----) 0.85, (——) 2.0, (-.-.-) H_2O (2.9-12.1); and (-..-..-) 13.1. 123

36 Room temperature absorption spectra of PASE at different pH values: (----) 1.3; (——) H_2O (2.3-10.3); and (....) 11.0 124

37 Room temperature fluorescence spectra of PAS at different pH values: (----) 0.85, (——) 2.0, (-.-.-) H_2O, and (-..-..-) 13.1. 127

38 Room temperature fluorescence spectra of PASE at different pH values: (----) 1.3, (——) H_2O, and (....) 11.0. 128

39 Room temperature fluorescence spectra of PAS in different media: (——) 3MP; (----) ether; (-.-.-) ethanol; and (....) H_2O (pH = 2) 132

Figure Page

40 Room temperature fluorescence spectra of PASE in different media: (——) 3MP; (----) ether; (-.-.-) ethanol; and (....) H_2O. 133

41 Ground-state conformers of methyl salicylate: (a) "ether bonded", (b) "open ring" (trans), and (c) "closed ring" (cis) 138

42 Room temperature fluorescence spectrum of PAS in KCl pellet. 143

43 Room temperature absorption spectra of DPAS in different solvents: (——) 3MP; (----) ether; (-.-.-) ethanol; and (....) H_2O (pH = 2.4) 146

44 Room temperature absorption spectra of (——) N,N-dimethyl p-amino salicylic acid, (....) N,N-dimethyl p-amino benzoic acid, and (----) salicylic acid in their neutral form in H_2O 149

45 Room temperature absorption spectra of DPASE in different solvents: (——) 3MP; (----) ether; (-.-.-) ethanol; and (-..-..) H_2O 150

46 Room temperature absorption spectra of DPAS at different pH values: (----) 0.8;

Figure Page

(——) 2.4, (-·-·-) H_2O (4.1-12.5) and (-··-··-) 13.6. 153

47 Room temperature absorption spectra of DPASE at different pH values: (----) 1.1, (——) H_2O; and (....) 11.9. 154

48 Room temperature fluorescence spectra of DPAS at different pH values: (----) 0.8, (——) 2.4, (-·-·-) H_2O, (-··-··-) 13.6. 157

49 Room temperature fluorescence spectra of DPASE at different pH values: (----) 1.1, (——) H_2O, and (....) 11.9. 158

50 Room temperature fluorescence spectra of DPAS in different solvents: (——) 3MP; (----) ether; (-·-·-) ethanol, (....) H_2O (pH = 2.4) 160

51 Room temperature fluorescence spectra of DPASE in different solvents: (——) 3MP; (----) ether; (-·-·-) ethanol; and (....) H_2O. 162

52 Room temperature fluorescence spectra of DPAS in 3MP at two different excitation wavelengths: (----) λ_{ex} = 300; (——) λ_{ex} = 330. 164

Figure Page

53 (a) Energy level diagram for DPAS (change in emission due to excitation of different electronic state of the same conformer) 166
(b) Energy level diagram for two conformers of MSA (change in emission due to excitation of different conformers). 166

54 Room temperature excitation spectra of DPAS in 3MP (uncorrected spectra) (——) represents the 354 nm band, while (----) represents the 464 nm fluorescence. 169

55 Room temperature fluorescence spectra of 1-azacarbazole in 3MP at two different concentrations 172

56 Room temperature ultraviolet absorption spectra of 1-azacarbazole (2 x 10^{-5} M) in different media: (----) cyclohexane; (——) ether; and (....) ethanol 173

57 Ultraviolet absorption spectra of 1-azacarbazole (2.5 x 10^{-5} M) in 3-methylpentane at room temperature (——); 77°K (----) 175

Figure Page

58 Room temperature fluorescence spectra of 1-azacarbazole at different pH values 176

59 Effect of pH on the fluorescence spectra of 1-azacarbazole at room temperature 178

60 Room temperature absorption spectra of 1-azacarbazole in 3-methylpentane at different concentration. 179

61 Qualitative double minimum potential energy diagram illustrating excited-state double proton transfer in 1-azacarbazole hydrogen-bonded dimers 182

62 Phosphorescence spectrum of 1-azacarbazole (6×10^{-4} M) in ether at 77°K excited at 330 nm. 184

63 Room temperature absorption spectra of 1-azacarbazole (2×10^{-5} M) in hexane, in presence of variable amounts of acetic acid, 0, 1.66×10^{-6}, 3.32×10^{-6}, 4.98×10^{-6}, 6.64×10^{-6}, 8.30×10^{-6}, 9.96×10^{-6}, 1.16×10^{-5} M in 10 cm cell. . 185

64 The emission of 5×10^{-4} M of 1-azacarbazole in 3-methylpentane in the absence (——), presence of excess acetic acid (----). 187

Figure Page

65 Stereoscopic view of a hydrogen-bonded dimer molecule 189

66 Stereoscopic views of the packing of dimer molecules into the unit cel 190

67 Room temperature fluorescence spectrum of 1-azacarbazole in the solid phase 192

CHAPTER I

EXCITED STATE PROTON-TRANSFER

1. Introduction

Proton transfer (PT) represents one of the simplest chemical reactions. Unlike electron transfer which involves mainly the exchange of charge between reactants, the transfer of a proton also results in the transport of mass. Because of their simplicity, reactions involving protons are ubiquitous. They have been studied in a large number of systems ranging from the base catalyzed decomposition of nitramide to the dissociation of water.[1,2] A large proportion of our knowledge about equilibria, chemical kinetics, isotope effects, mass transport in solution, free energy relationship, and chemical reactivity has developed from the study of proton transfer reactions. Reactions involving protons are not only very common and instructive but are found in a number of processes important to our everyday existence. In biology, protons are involved in a host of enzymatic reactions, the most important of which is the synthesis of ATP in mitochondria and chloroplasts.[3]

The rates of proton reactions have been shown to span at least 15 orders of magnitude.[4] A wealth of kinetic

data has produced a good qualitative description of the proton transfer process in the form of reaction mechanisms.[5] Detailed theories of proton transfer reactions are still developing. However, these are often based on information obtained from gas phase reactions (i.e., molecular beam studies) which are free of solvent participation.[6]

NMR, rapid mixing and perturbation techniques have been the most useful in the study of hydrogen ion reactions and transport. Since stopped flow is limited to the study of relatively slow reactions, most of our information about rapid proton transfer reactions such as those between oxygen or nitrogen atoms is due either to NMR or to perturbation techniques.[7,8]

The perturbation methods of course utilize a change in the equilibrium constant to observe the kinetics. Equilibrium is often perturbed by a rapid change in temperature or pressure. For a number of reactions, including those involving protons, light can be used to quickly change the equilibrium constant.[9] The perturbation arises from the fact that the ground state properties of a molecule are different than those of the excited state. The excited state properties, such as the dipole moment, ionic dissociation constant and hydrogen bonding ability may undergo dramatic changes upon electronic excitation. Many aromatic compounds in their first excited singlet states (S_1) display acidities very different from those

in the ground state due to changes in electronic distribution. In some cases the pH at which the absorption and the fluorescence spectra undergo a sudden change differ by six units or more. These studies indicate clearly that P.T. takes place during the lifetime of the first excited state (S_1).

Since molecules absorb a photon in 10^{-15} sec, in principle it is possible to perturb the equilibrium on this time scale. Thus, it is possible to rapidly initiate proton release or uptake with the absorption of a photon.

The study of the energetics and dynamics of excited state proton transfer is of great interest both experimentally and theoretically. It serves as a model photochemical reaction for which potential energy surfaces may be calculated. It appears also that excited state proton transfer occurs as a primary step in a number of photobiological processes such as vision.[10] The occurrence of excited state proton transfer in some enzymes may reveal interesting information regarding the nature and structure of their active sites.[11-13] Depending on the molecular system and the medium, intra- or intermolecular excited state proton transfer may occur.

In this review, a brief discussion of hydrogen-bonding in the ground and excited state is given. Examples of proton transfer in the ground state as well as in the

excited state are discussed. Kinetic data using nano- and picosecond techniques provide rate constants for excited state proton transfer and the mechanism of excited state proton transfer is discussed for intramolecular and intermolecular proton transfer in derivatives of salicylic acid and naphthaic acid, 7-azaindole dimers and hydrogen-bonded complexes. Evidence for the possibility of proton tunneling and values of energy barrier heights are reviewed. Examples of solvent effects on the fluorescence spectra and rate constants of systems that undergo excited state proton transfer are provided. Finally, examples of excited state proton transfer in the solid and in the vapor phase are given.

2. Theoretical Models of the Hydrogen-Bond

Various models are used for H-bonding, the subject was reviewed recently.[14,15]

In the electrostatic model, the energy of the hydrogen bond is calculated in terms of dipole interaction. Coulson and Danielson[16] used a valence-bond approach in which the hydrogen-bond is treated as a four electron problem. Other variations of this method were attempted, nevertheless, the conclusions reached are similar. The electrostatic forces, the short-range repulsion forces, and the charge-transfer forces, are all of the same order of magnitude but are of different signs. Often the second

and third effects cancel each other which explains the success of electrostatic theories. The amount of charge transferred from O_B to O_A is found to be nonnegligible (but small) for short bonds and negligible for long bonds; thus the long bonds are essentially electrostatic. The charge-transfer approach of H-bonding is analogous[17] to the charge-transfer theory of molecular complexes. The contribution of the charge-transfer term increases as the ionization potential of the lone pair becomes smaller. Since a fraction of an electron is replaced on the antibonding O_AH orbital ν, the O_AH bond is thus weakened. This is just what is observed experimentally. The large migration increases the polarity of the O_A-H...O_B systems and intensifies the ν_{OH} IR bands. In the SCF-MO theory, the complex AH...B is considered as a single large molecule and is treated by the SCF-MO and CI techniques. Although the electrostatic interaction appears to be the principal interaction, the dipole-dipole term is also important.

3. Proton Transfer in the Ground State

A proton transfer reaction in which a proton involved in an H-bond A-H...B is transferred from A to B, belongs to the broad classification of acid-base reactions. The transfer may occur along a potential energy curve similar to the ones depicted in Figure 2 by two mechanisms, direct

transfer over the barrier and/or through quantum mechanical tunneling through the potential barrier separating the two minima. The phenomenon of tunnelling will be discussed later.

The transition from an H-bonded complex A-H...B to a proton transfer complex $A^-...H-B^+$ in a nonpolar solvent is accompanied by significant changes. For example, in the IR spectra, the disappearance of ν_{OH}(A-H) bands and the appearance of $\nu_{OH}(B^+-H)$ bands have been observed in the IR spectra of mixtures of some carboxylic acids ranging from acetic (the weakest, pK_a = 4.76) to trifluoroacetic (the) strongest, pK_a = 0.23) with pyridine in $CHCl_3$.[18]

Evidence for ground state proton transfers has also been found in ultraviolet absorption studies. Baba et al.[19] investigated the absorption spectra of the p-nitrophenol-triethylamine system as a function of amine concentration and found absorption bands corresponding to an H-bonded complex and a proton transfer complex. The appearance of two absorption bands of Schiff bases of pyridoxal 5' phosphate (PLP) in certain media have been attributed to the presence of two tautomeric forms: an enol-imine absorbing at 330 nm and a keto-enamine absorbing at 410 nm. (See Figure 1). The following equilibrium is solvent dependent, which explains the spectral changes that occur due to a change of the dielectric constant of the medium.

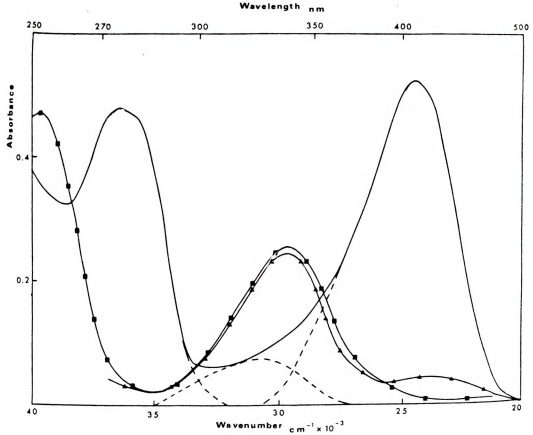

Figure 1. Absorption spectra of Schiff base (PLP 7 x 10^{-5} M, n butylamine 2.5 x 10^{-4} M) in various solvents; dioxane, ΔΔΔ DMF, —— H_2O, the dotted line represents decomposition of this spectrum.[20]

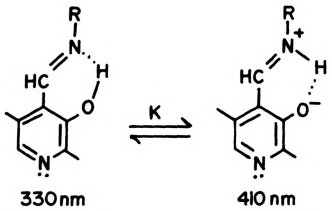

The keto-enamine tautomer is formed due to a proton transfer from the phenolic group to the azomethane nitrogen if the enol-imine is intramolecularly H-bonded. However, if intermolecular H-bonds are formed with the solvent, a double proton transfer involving the solvent molecules is required to form the keto-enamine tautomer.

The Double-Minimum Potential

Evidence for a double minimum unsymmetrical potential energy curve (Figure 2b) where the lower of the two minima corresponds to an H atom located near the donor atom was provided by vibrational spectroscopy. In 1959 Bell and Barrow[21] showed that the first and second overtone O-H stretching vibrations of ethanol, phenol, and p-nitrophenol exhibit a pair of bands in the presence of bases. The energy of the second potential minimum was shown to depend on the strength of the proton donor and the acceptor

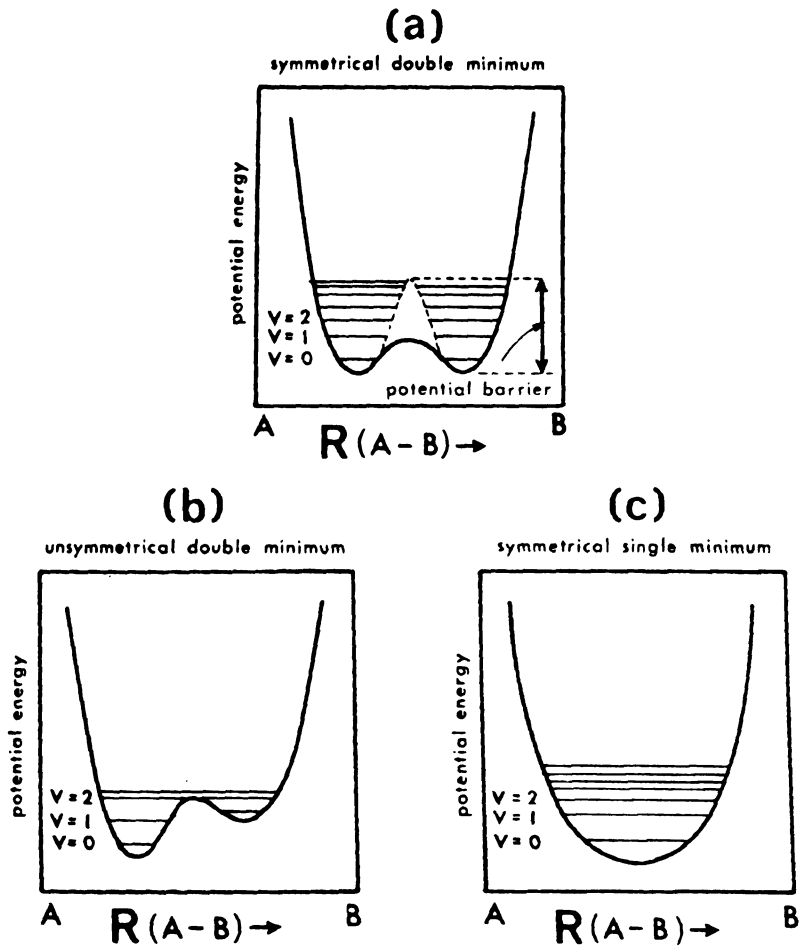

Figure 2. Potential energy diagrams for the motion of the proton in a hydrogen bond A-H...B.

strength of the base.[22] The same concept was used to interpret the splitting of the first overtone of the NH_2 symmetric stretching vibration band in a number of intramolecularly H-bonded ortho-anilines.[23] Some of the basic criteria for the existence of a double-minimum potential in an H-bonded system, with the second minimum at about the $\nu = 2$ level, are (1) a splitting of the ν_{02} but not the ν_{01} band; (2) an increase in the magnitude of the splitting with an increase in the strength of the H-bond; (3) a reduction of the splitting upon deuteration; (4) a temperature independent intensity ratio for the pair of bands resulting from the splitting of ν_{02}, since both transitions originate in the ground state. The band splitting is concentration independent in an intramolecularly H-bonded system, since the effect originates in the monomer.

Some of the strongest evidence supporting a double-minimum potential comes from neutron diffraction studies. For example, neutron diffraction studies of KH_2PO_4 show the proton as an elongated shape between the two oxygen atoms which are separated by 2.49 Å.[24] This distribution could be interpreted in either of two different ways: as a centrally located proton with a very anisotropic motion or, more likely as a disordered distribution of the protons between two possible positions, one on each side of the mid-point between the oxygen atoms. In the

case of ice the O-O distance is much longer, being 2.76 Å, and the two possible hydrogen positions are much farther apart (about 0.74 Å). Because of this the disordered protons appear as separate well-defined peaks. Other indirect evidence of double-minimum potentials in H-bonded systems comes from dielectric saturation experiments,[25] from data on compressibility,[26] thermal expansion,[27,28] the change in the bond energy,[29] change of intermolecular distance upon deuteration[30] and NMR studies.[31]

At this point it should be mentioned that the interpretation of the above experiments is not as decisive as might be desired. For example even one of the best pieces of evidence, i.e., the split of the IR bands, could be due to an overtone of the AH bending mode, enhanced by Fermi resonance with ν_{Str}.[32]

One of the early views of H-bonding was the concept of "mesohydric tautomerism" according to which the H was thought to resonate very rapidly between two equally probable positions, one near the donor atom, and the other near the acceptor atom. This concept would require that the potential energy function for the H-atom either passes two equal potential minima with a low barrier between the two (Figure 2a) or be symmetrical, with one broad minimum (Figure 2c).

Hadzi and collaborators[33] have classified hydrogen bonds of the O_A-H...O_B type into four groups. In group

A are included the symmetric single minimum H-bonds; in group B, the symmetric double minimum H-bonds with small potential barrier, in group C, the symmetric double minimum H-bonds with a potential barrier higher than in group B; and in group D, the H-bonds with an asymmetric double minimum potential curve. The H-bonds of type A and B are uniformly very short, with R ($O_A...O_B$) varying from 2.4 to 2.6 Å. Some typical single minimum H-bonds are observed in KH maleate, NaH diacetate, KH dibenzoate, KH bisphenylacetate. The IR spectra are characterized by the absence of a ν_{01} (O-H) band in the region above 1800 cm^{-1}, the NMR signals are narrow and weak and remain unchanged at low temperature. The H-bonded compounds belonging to type B (KH_2AsO_4, $NH_2H_2PO_4$, $CaHPO_4$, $NaHCO_3$) exhibit two O-H bands in the 1900-3000 cm^{-1} region, separated by 300-500 cm^{-1}; the PMR signals are strong and narrow at room temperature and only slightly broader at -180°C.[34,35] Group C includes various carboxylic acid dimers and group D includes various phenols.

A very interesting investigation, through ab initio techniques, of the double well picture of the hydrogen bond was performed by Clementi et al.[36] The study was on the DNA base pair Guanine-cytosine and the motivation was the theory put forward by Löwdin[37] on the possible importance of quantum mechanical tunnelling for the interconversion between different tautomeric forms. Although

there was a noticeable shoulder where the second minimum might have been expected no second minimum was found. Clementi and coworkers gave various possible sources of error in their prediction of the lack of a double minimum. The most important is that no simultaneous motion of two hydrogen bridges was considered. To test this possible error source, Clementi and coworkers carried out calculations on the formic acid dimer[36] which has two hydrogen bonds. First only the motion of a single hydrogen bridge was considered. Using the Guanine-Cytosine basis set only a single minimum was found. When a larger basis set was used, a very pronounced shoulder was predicted but no minimum. It was only when the coupled motion of the two hydrogen bridges was considered and a double-zeta basis set was used that the calculation yielded a double minimum.

4. Hydrogen-Bonding in the Excited State

A molecule in its first excited singlet state has a different electronic distribution than the molecule in its ground state. If the chromophoric portion of the molecule is involved in H-bonding one would expect changes in its strength. In this way, electronic absorption and emission spectroscopy may provide experimental evidence about H-bonding. Kasha[38] pointed out that absorption bands corresponding to $n \rightarrow n^*$ transitions are "blue shifted" in H-bonding media. This is due to the decreases in charge

density on the lone pair atom as a result of lone pair promotion. Thus, the H-bond is always stronger in the ground state. Bayliss and McRae[39] considered H-bonding interactions to be a special case of dipole-dipole interactions. However, Pimental[40] pointed out that dipole induced- dipole and dipole-dipole interactions produce small solvent shifts compared with those due to H-bonding. He discussed the importance of H-bonding effects compared with other solvent effects and pointed out the role of the Franck-Condon principle in H-bonding. Solvent shifts due to H-bonding can be formulated as follows (See Figure 3):

$$\Delta\nu_a = \nu_a - \nu_o = W_g - W_e + w_e$$

$$\Delta\nu_f = \nu_f - \nu_o = W_g - W_e - w_g$$

where:

$\Delta\nu_a$ is the energy shift in the absorption maximum,

$\Delta\nu_f$ is the energy shift in the emission (fluorescence) maximum,

ν_a is the energy of the absorption maximum,

ν_f is the energy of the emission (fluorescence) maximum,

ν_o is the energy of the absorption maximum in the gas phase,

W_g is the enthalpy contribution in the ground state from H-bonding interaction of the solvent with

the solute,

W_e is the enthalpy contribution in the excited state from H-bonding interaction of the solvent with solute upon excitation; and

w_e and w_g are the energies implied by the Franck-Condon principle and are always positive.

Since w_e and w_g are always positive, the shift in absorption and emission will depend on whether W_g is greater or less than W_e.

When $W_g > W_e$, i.e., the H-bond is stronger in the ground state than in the excited state as shown in Figure 3, a blue shift $\Delta\nu_a > 0$ which exceeds $W_g - W_e$ by w_e will be observed in the absorption spectrum. Similarly, in emission a shift less than $W_g - W_e$ by w_g will be observed (either a red or blue shift depending on the electronic magnitudes of $W_g - W_e$ and w_g).

When $W_e > W_g$, i.e., the H-bond is stronger in the excited state than in the ground state as shown in Figure 3, both absorption and emission spectra will show a red shift, which is less than $W_g - W_e$ by w_e for absorption and is less than $W_g - W_e$ by w_g for emission.

The well characterized H-bonds have energies in the range 1-7 Kcal mol^{-1} (350-2500 cm^{-1}). According to the above discussion, a blue shift in absorption may exceed the ground state H-bonding energy, hence, the blue shift

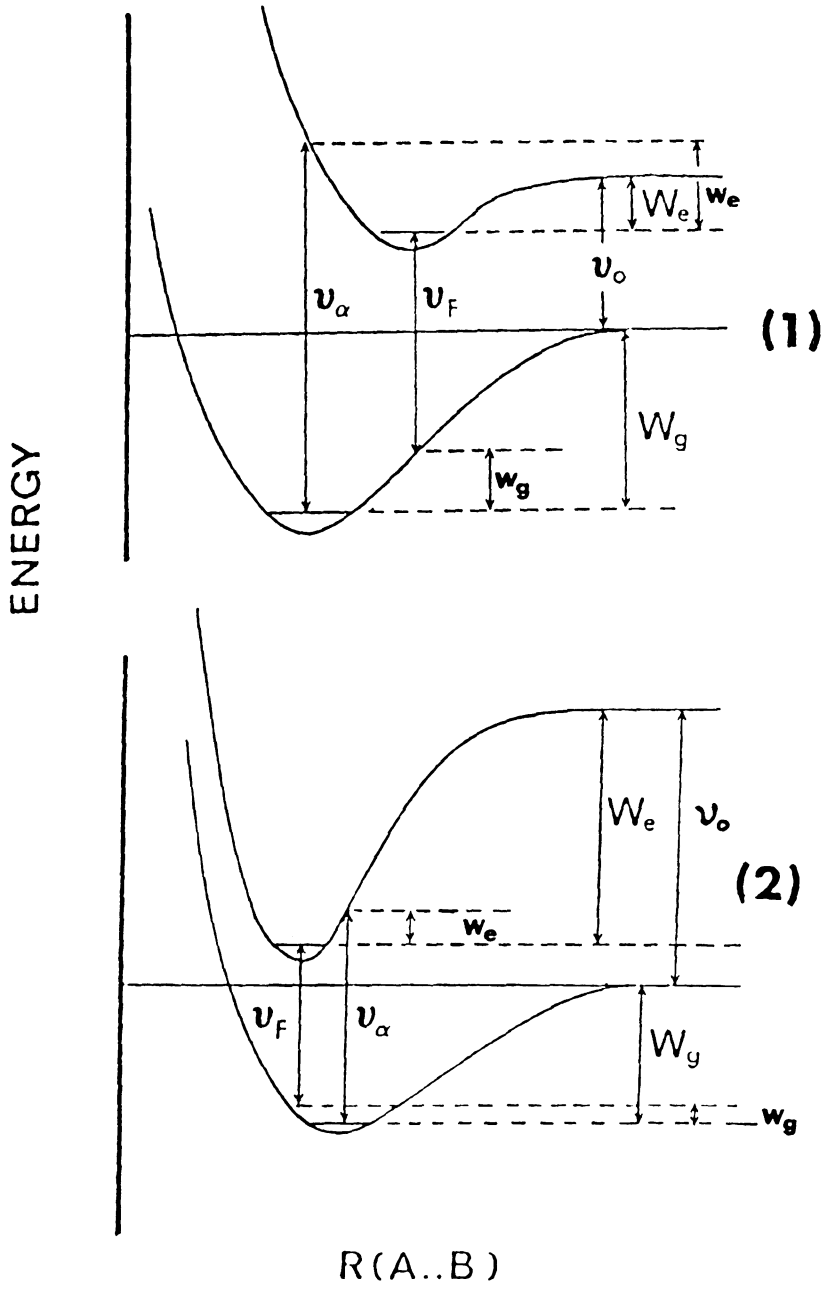

Figure 3. Hypothetical potential energy curves for the formation of a H-bond A-H...B in ground and excited state, (1) $W_g > W_e$, (2) $W_g < W_e$.

is expected in the range of 350-2500 cm^{-1} or even larger than 2500 cm^{-1}. But a red shift in absorption should never be as large as W_g, so should not be larger than 2500 cm^{-1}.

A red shift in the absorption spectrum indicates that the H-bonding is stronger in the excited state. This may indicate an increase in the acidity or basicity depending on the functional group at the chromophore involved in H-bonding. The spectra of nitrogen heterocyclic bases in which the lowest transition is $\pi \rightarrow \pi^*$ have been found to undergo a red shift upon H-bonding. This is due to an increase in the charge density of the H-bonded nitrogen, which increases its basicity and in turn increases the H-bond energy in the excited state.

5. Excited State Acidity and Basicity

In 1931, Weber[41] noticed that the fluorescence of 1-naphthylamine-4-sulfonate changed color as the pH of the solution was altered, although no corresponding change in absorption was observed. Similar observations were made[42-44] which were interpreted by Förster[45-47] in terms of a change in the acid-base equilibrium upon electronic excitation, i.e., an excited state proton transfer had occurred.

As with other chemical properties the acid-base properties of molecules (pK values) depend on the electronic

charge distribution. Since charge densities are often modified by electronic excitation (new species), one might expect a change in the acidity or basicity of a molecule in a different electronic state.[48,49]

Compounds that change their pK values as a result of excitation can be divided into two groups: one group in which the pK_a value decreases (increased acidity) upon excitation, such as ArOH, ArNHR, $ArN^{+}HRR'$, ArSH[42,50,51] where Ar is an aromatic group, the other group in which the pK_a value increases (decreased acidity), such as ArCOH, $Ar\overset{R}{\underset{|}{C}}=O$, $Ar-\overset{R}{\underset{|}{C}}=N\diagup^{R}$, $Ar\overset{\diagup}{\underset{\diagdown}{N}}:$.[52,53]

For hydroxy naphthalene derivatives, and hydroxy- and aminopyrene sulphonates, the pH at which the absorption and fluorescence spectra change is usually different by a factor of 6 or more and thus the acidity constant in the ground and first excited singlet state (S_1) differs by 10^6 or more (see Table 1). In these cases, a proton transfer takes place during the first excited singlet state lifetime at a pH value where proton transfer does not occur in the ground state.

Weller discussed methods of determining the excited-singlet state dissociation constants, pK*, from spectroscopic data.[9,43,54] Jackson and Porter[55] have applied the same techniques to determine the pK of molecules in the lowest excited triplet state. Their results showed that the pK of the lowest triplet is usually close to that

Table 1. pK_a and pK_a^* Values for Selected Molecules.

	pK	pK*	pK-pK*
Phenol	10	5.7	4.3
α-naphthol	9.23	2.0	7.23
β-naphthol	9.46	2.5	6.95
β-hydroxy pyrene 5,8,10-trisulphonate	7.30	1.0	6.30
4-ammoniumpyrene (in ethanol)	3.7	-1.8	5.5
1-naphthoic acid	3.7	7.7	-4.0
2-naphthoic acid	4.2	6.6	-2.4
9-anthroic acid	3.0	6.5	-3.5
Acridinium cation	5.45	10.3	-4.85
1-naphthoic acid cation	-6.9	1.5	-8.4

of the ground state rather than to that of the lowest excited singlet state.

Various methods are used for the determinations of pK*. The subject was reviewed recently.[56,57]

a. Förster Cycle Determinations

The Förster cycle method offers a simple method to estimate pK* values, the method is based on a thermodynamic cycle. This method requires a study of the emission and absorption spectra as a function of pH. The change in acidity as a result of excitation can be detected only if the rate constant of excited state proton transfer is comparable to or greater than the rate of fluorescence decay. In such cases, the absorption spectrum exhibits a pH dependence different from that of the fluorescence spectrum, i.e., the ground and excited states have different pK_a values. From the spectral shifts in absorption and emission spectra,[43,58] Weller estimated the change in the pK value ($pK_a^* - pK_a$) by using the equation:

$$pK^* - pK = \frac{\Delta E_2^{R^-} - E_1^{RH}}{2.303RT} \quad , \quad \text{or}$$

$$pK_a^* - pK_a = 2.1 \times 10^{-3} \, (\bar{\nu}^{R^-} - \bar{\nu}^{RH}) \text{ at } 298°K.$$

In deriving this equation it was assumed that $\Delta S^* \simeq \Delta S$. The equation does not take into account the fact that

equilibrium may not be reached before deactivation and that the lifetime of S_1 is too short to allow protolytic reaction to reach equilibrium. It can, in principle, also be applied to higher excited singlet states.

To obtain pK* it is necessary to know the ground state equilibrium constant, pK (S_0) for the reaction in question and to have some measure of the energy difference between the lowest vibrational level of the ground and the excited state in both the RH and R^- forms, i.e., ΔE_1 and ΔE_2. Absorption spectroscopy is commonly used to determine the ground state pK.[59] It is not always easy to obtain a good value for the energy of 0-0 transitions except for those cases in which the molecule shows vibrational fine structure in its absorption and fluorescence spectra.

There are three approaches[60-62] which can be used to obtain a 0-0 energy approximation: (a) the use of the absorption maxima, (b) the use of fluorescence maxima, and (c) the averaging of the absorption and fluorescence maxima of each form[43,63] according to:

$$\Delta E_1 = h\nu_1 = (h\nu_1^{abs.} + h\nu_1^{fluo.})/2 \quad \text{for RH}$$

$$\Delta E_2 = h\nu_2 = (h\nu_2^{abs.} + h\nu_2^{fluo.})/2 \quad \text{for } R^-$$

One must realize that $\Delta\nu$ obtained from absorption and fluorescence maxima are only approximate due to the Franck-Condon factors in the excited and ground states because of

the effect of solvation on 0-0 transition. Since the electronic charge distribution is significantly different in the S_1 and S_0 states, the equilibrium orientation of the solvent cage necessary to keep a minimum of free energy[64] must be different in the two states. Reorientation of the solvent shell does not occur during the absorption process and thus a Franck-Condon state of higher energy than the equilibrium excited state is reached. The energy of a 0-0 absorption band corresponds the algebraic sum of the 0-0 transition observed in the gas phase, the stabilization of the ground state and the Franck-Condon energy in the excited state. There is no reason to believe that for two species electronically as different as a dissociated and an undissociated acid these solvent effects will be identical and cancel out in the calculation of $\Delta\bar{\nu}$.

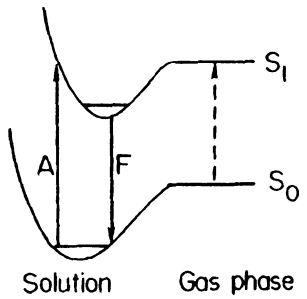

Energy of an electronic transition measured in the gas phase and in solution.

In solution, the lifetime of the Franck-Condon state being much smaller than that of the S_1 state, reorientation of

the solvent cage will occur before fluorescence occurs. After emission the molecule reaches a Franck-Condon ground state, the overall result being that fluorescence is shifted to the red compared to absorption. Therefore $\Delta\bar{\nu}$ cannot be obtained from the absorption or fluorescence spectra, only the average of these energies provides, a "best value" of the energy gap between the ground and S_1 states. In general a satisfactory agreement is obtained[63, 65] between methods (a) and (c), but method (b) leads to larger pK* (S_1) values that are relatively close to the pK (S_0) values.

The limitations of the Förster cycle have often been discussed.[61,66] To put the value of Förster cycle in perspective, one should state that "as with many other rough rules in physical organic chemistry, it can serve as a good guide even if it is not absolutely reliable quantitatively and it can at least indicate the direction of the pK-shift".

b. Fluorescence Titration

The change in molecular fluorescence with acidity gives information about the protolytic behavior of the excited singlet state of a compound. A pK* (S_1) value calculated from the Förster cycle gives an indication of the acidity range in which a fluorescence change is expected, but, since no account is taken of the relevant rates of the

particular processes involved, the Förster cycle does not indicate whether or not proton transfer in the excited state is kinetically feasible. Improved instrumentation has made fluorescence techniques more available and extended the range of compounds accessible to the method because of improved sensitivity. The techniques of fluorescence spectroscopy are well known.[67-69]

If equilibrium is established during the excited state lifetime then the pK_a^* and pK_b^* values can be determined in a way analogous to the spectrophotometric determination of the ground state pK's, by fluorometric titration. For example, the fluorescence intensity of indole[70] as a function of pH, shows that at both low and high pH the indole fluorescence is quenced (Figure 4). In the high pH region the quenching is ascribed to the ionization of the pyrrolic hydrogen according to the reaction:

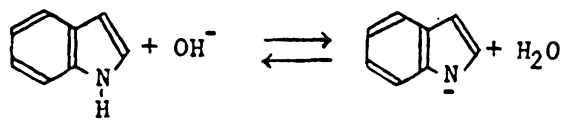

From the midpoint of the titration curve one gets $pK_b^* = 12.3$. Exactly the same number was obtained by E. vander Donckt.[71] The excited state $pK_b^* = 12.3$ should be compared to the ground state $pK_b = 16.97$[72] which shows that indeed the pyrrolic hydrogen acidity has considerably increased in the excited state.

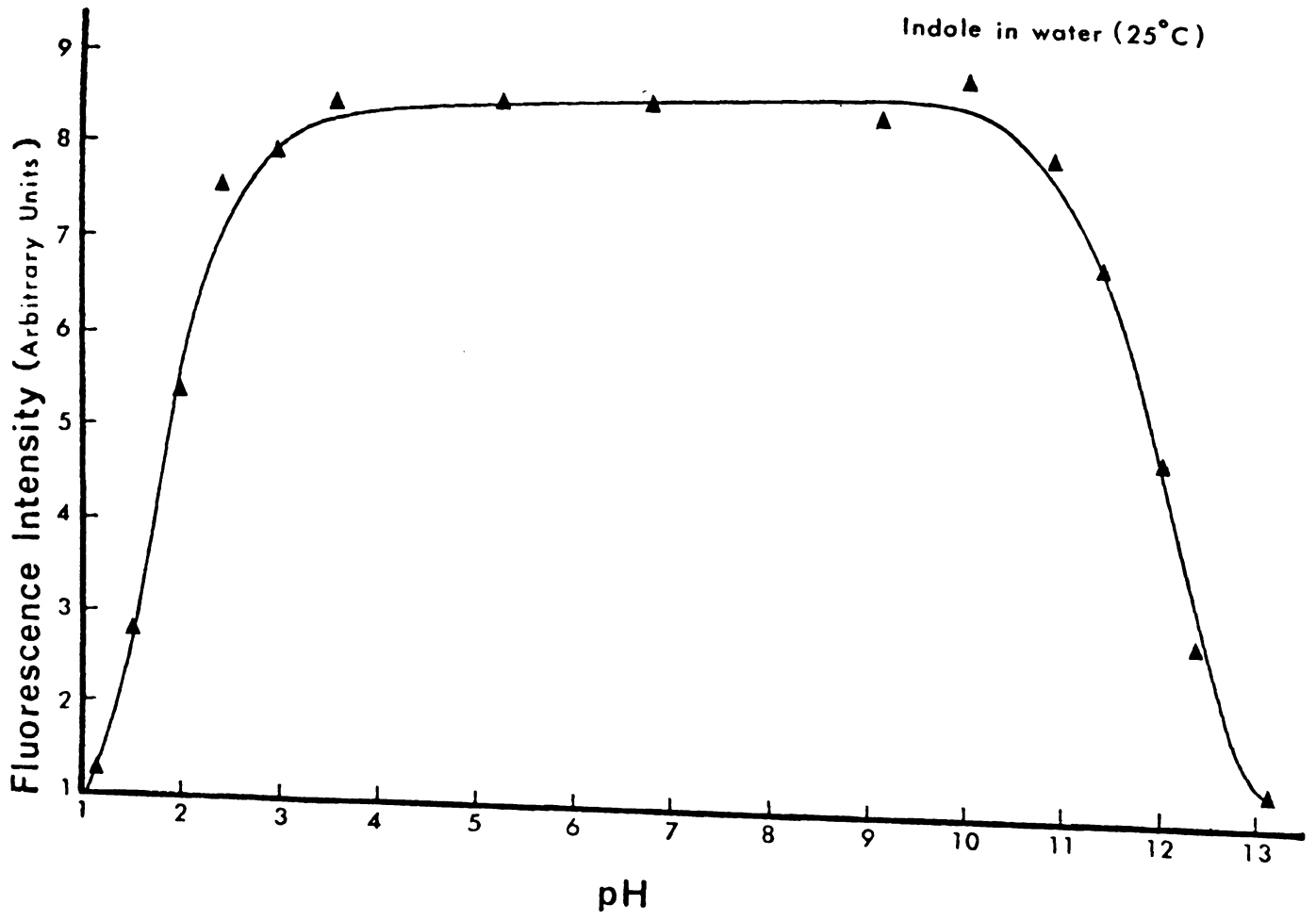

Figure 4. Effect of pH on the fluorescence of an aqueous solution of indole at 25°C.[70]

In the low pH region, the quenching is considered to be due to protonation of pyrrolic nitrogen according to the reaction:

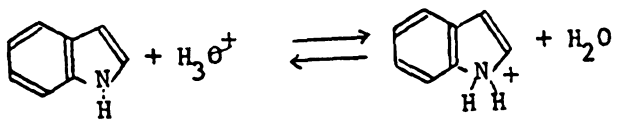

In the same way one gets a pK_a^* = 1.8, in very good agreement with the value pK_a^* = 1.7 obtained by Bridges and Williams.[73]

c. Photopotentiometry

Photopotentiometry[74] is based on the measurement of the potential developed between one illuminated electrode and one dark electrode in a solution. This potential, which is primarily a function of the various species in solution, was used to produce data leading to pK_a^* values. The values found were -2.89 and 12.3 for 2-naphthylamine cation and anion, respectively. These values compare reasonably well with the values obtained (-1.5 and 12.2)[47] by using the Förster cycle. Other values obtained using this technique include, 13.5 for the 1-naphthylamine anion, 4.37 and 9.5 for 3-pyridinol anion and cation, respectively.

6. Proton Transfer in the Excited State

In the case of ground state proton transfer in ground state "tautomerism", both the enol and the keto forms may exist in equilibrium in solution. Excited state proton transfer "phototautomerism", may also occur giving rise to a tautomer with an emission shifted with respect to that of the original species. The relative intensities of these two emission bands depend on the efficiency of the proton transfer process and the quantum yields of the original molecule and its tautomer. For example, it has been found[75] that the shift of the fluorescence maximum of β-naphthol in C_6H_6 brought about by the addition of triethylamine (TEA) is quite large (4000 cm^{-1}) compared to the shift of the ^1L_b absorption band of β-naphthol caused by hydrogen bonding with TEA which is only 370 cm^{-1}. These results suggested strongly that ion-pair formation, due to a complete proton transfer rather than just stronger H-bond formation, occurs in the fluorescent equilibrium state.

Proton transfer may occur intramolecularly as in salicylic acid[76-78] or intermolecularly as in the 7-azaindole hydrogen bonded dimer.[79,80] A detailed discussion of various examples of molecular systems that undergo excited state proton transfer will be given.

a. Intramolecular Proton Transfer

Salicylic Acid (SA) and Its Derivatives - Studies of excited state pK values reveal a general trend in which aromatic alcohols become more acidic, while aromatic ketones become more basic in their excited states.(81) This gives rise to an interesting effect when both groups are present in the same molecule and are situated in ortho positions. In such cases an intramolecular hydrogen bond in the ground state is formed in non-hydrogen-bonding solvents. The enthalpy of formation of such a hydrogen-bond is estimated from infrared data to be in the range of 7-8 Kcal $mole^{-1}$ indicating a strong hydrogen-bond and a red shift of emission even larger than in aromatic molecules with just one functional group is observed due to intramolecular proton transfer. For example, in methyl salicylate the fluorescence maximum is red shifted by about 10,000 cm^{-1} from the absorption maximum, while in phenol the corresponding energy difference is about 4000 cm^{-1}.(76,82) Weller had observed that although the maxima of the long wavelength absorption bands of salicyclic acid (I) and 2-methoxy-benzoic acid (II) differ in wavelength by only about 1000 cm^{-1}, the maximum of their fluorescence bands differ by 5000 cm^{-1} (See Figure 5). The fluorescence maximum occurs in the blue at 434 nm for I but that of the ether II occurs in the ultra-violet at 357 nm. The large Stokes shift observed in the case of salicylic acid

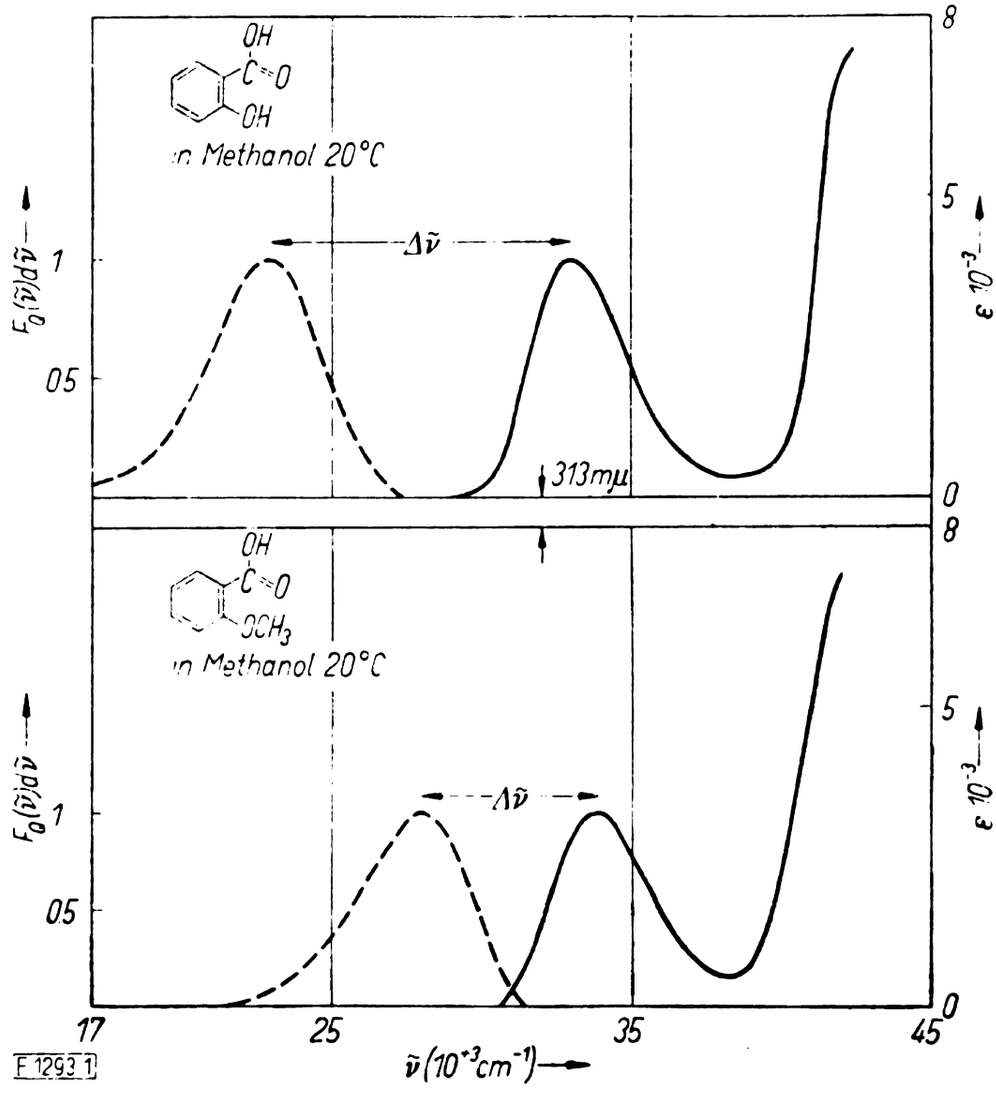

Figure 5. Absorption and fluorescence spectra of salicylic acid and 2-methoxybenzoic acid in methanol at 20°C.(76)

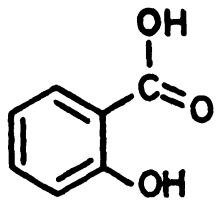

I

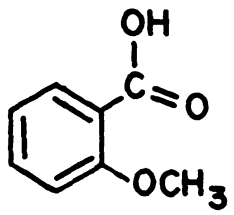

II

was interpreted[76,83] as arising from a tautomer formed in the excited state via an intramolecular proton transfer. To further confirm these results Weller made similar observations for methyl salicylate (MSA) in aprotic solvents where two fluorescence bands occurred at room temperature. The one at 340 nm is simply the mirror image of the lowest near UV absorption band, while the second fluorescence is strongly red shifted ($\sim$10,000 cm^{-1}) with a maximum near 450 nm and is much stronger than the other component at 340 nm (Figure 6). Proton transfer is driven by a pK change of about -6 for the phenolic oxygen[84,85] and a pK change which may be as large as +8 for the carbonyl oxygen of the carboxyl group.[65] Methyl 2-methoxy-benzoate with no transferable proton emits a single band at 320 nm with a normal Stokes shift. Furthermore, the emission of methyl salicylate in 0.1 M $NaOH/CH_3OH$ exhibits a maximum at 416 nm[86] which corresponds to the anion emission. Thus the 450 nm emission is assigned to a zwitterion formed via an intramolecular proton transfer in the excited state.

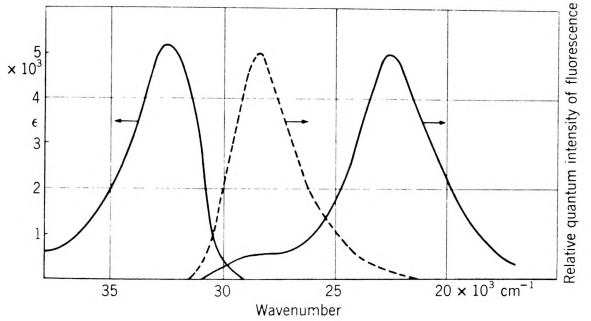

Figure 6. Absorption of fluorescence spectra of MSA in methyl cyclohexane (solid lines) and fluorescence spectrum of methyl 2-methoxy benzoate in the same solvent (dashed); fluorescence spectra after Weller.(83)

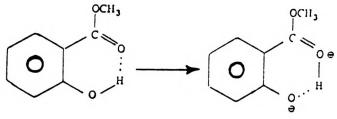

λ_{em} = 340 nm λ_{em} = 340 nm

Intramolecular proton transfers have also been reported for the salicylanilid I,[81,87,88] salicylamide II,[88,89] phenyl salicylate III,[90] and salicylaldehyde IV[91]

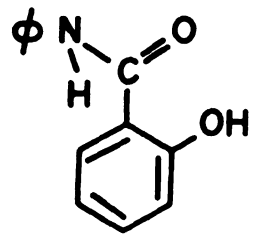

I

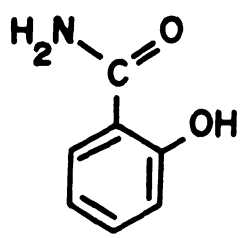

II

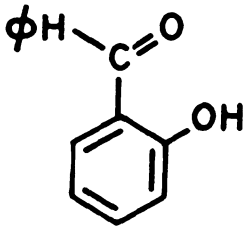

III

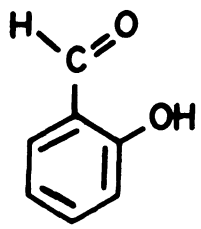

IV

Several studies designed to investigate the mechanism of excited state proton transfer led to many interesting findings. Quenching experiments using CS_2 (carbon disulfide)[76] demonstrated that at room temperature the 340 and 450 nm emission of methylsalicylate were equally quenched. This led to the speculation that the two forms of the excited molecule were in equilibrium, i.e., the proton transfer reaction in the excited state reached equilibrium in a much shorter time than the lifetime of the excited molecules. This set a lower limit of 10^8 S^{-1}

for the intramolecular proton transfer rate constant.

The relative contribution of the two components to the total fluorescence was strongly dependent on temperature. As the temperature was lowered, the intensity ratio of the 450 nm to the 340 nm emission bands increased. From the temperature dependence of this ratio in hydrocarbon solvents, Weller[9] calculated a difference in enthalpy of about $\Delta H^* = -1.0 \pm 0.5$ Kcal mole^{-1} (-0.7 Kcal mole^{-1})[92] between the neutral form and the zwitterion, and hence from the fluorescence spectral shift ($\Delta\bar{\nu} = 5100$ cm^{-1}) he deduced a ground state enthalpy change of 13.5 ± 0.5 Kcal mole^{-1}. The activation energy for proton transfer has been estimated[94] to be $E \leq 2$ Kcal mole^{-1} according to:

$$k_{PT} = \nu_{OH} \exp(-E/RT)$$

where ν_{OH} is the stretching frequency and is equal to 10^{14} sec^{-1}, $k > 1/\tau_0$ ($>10^8$ S^{-1}) and T = 77°K where proton transfer is still observed. From 4°K experiments an even smaller limit of $E \leq 0.1$ Kcal mole^{-1} is derived. A tunnelling mechanism was suggested as the actual transfer mechanism.[94] In acetonitrile, the ratio of the 450-340 nm emission is decreased.[92] This was interpreted in terms of a shift in the excited state equilibrium to form the neutral species. Because the neutral form has a large dipole moment in the excited state compared to the

zwitterion, it is stabilized to a large extent in acetonitrile.* This interpretation was modified as will be seen later.

Investigation by Klöpffer's group[86] showed that in hydrogen bonding solvents (methanol, ethanol, water, and acetic acid) there are two strong emissions with maxima at 450 and 355 nm, whose relative intensities depend on the excitation wavelength (Figure 7). At excitation wavelengths greater than about 310 nm, the 450 nm band dominates, while at excitation wavelengths below 310 nm, the 355 nm fluorescence is the stronger emission. This suggests that different ground state species are being excited. The excitation spectra of the two bands are shown in Figure 8. The excitation maximum of the blue fluorescence is at 310 nm, that of the UV component is at 300 nm. The excitation maximum at 349 nm is due to traces of the phenolate ion generated by ground state dissociation of methyl salicylate.

The study of multiple fluorescence of 2,6-dihydroxybenzoate[93] showed that the two emissions for methyl salicylate arise from species which are not in equilibrium in the excited state and which originate from different ground state species. In the case of 2,6-dihydroxybenzoate

---

*This strongly suggested considerable intramolecular charge transfer in the excited state of salicylic ester.

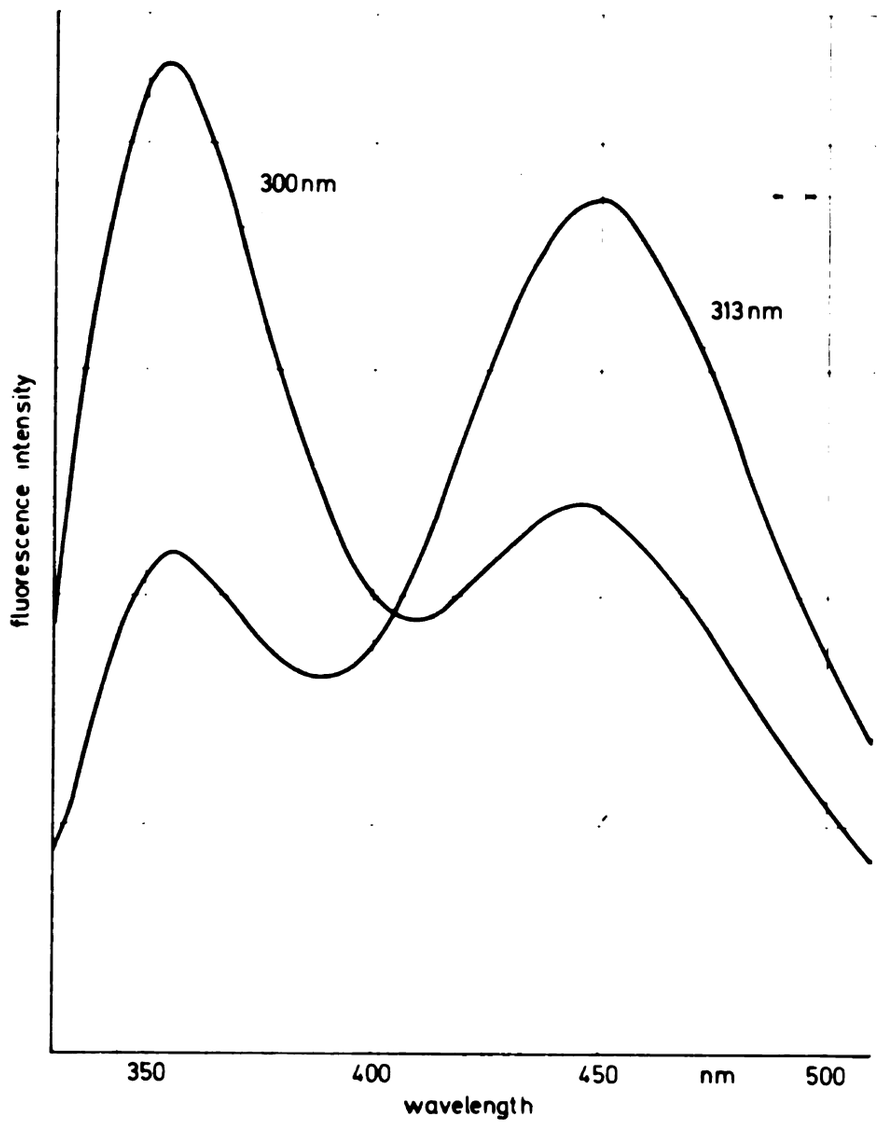

Figure 7. Fluorescence spectra (uncorrected) of MSA, 10^{-4} mol ℓ^{-1} in methanol; excitation wavelengths and emission slit width indicated; spectral excitation slit width 20 nm.(86)

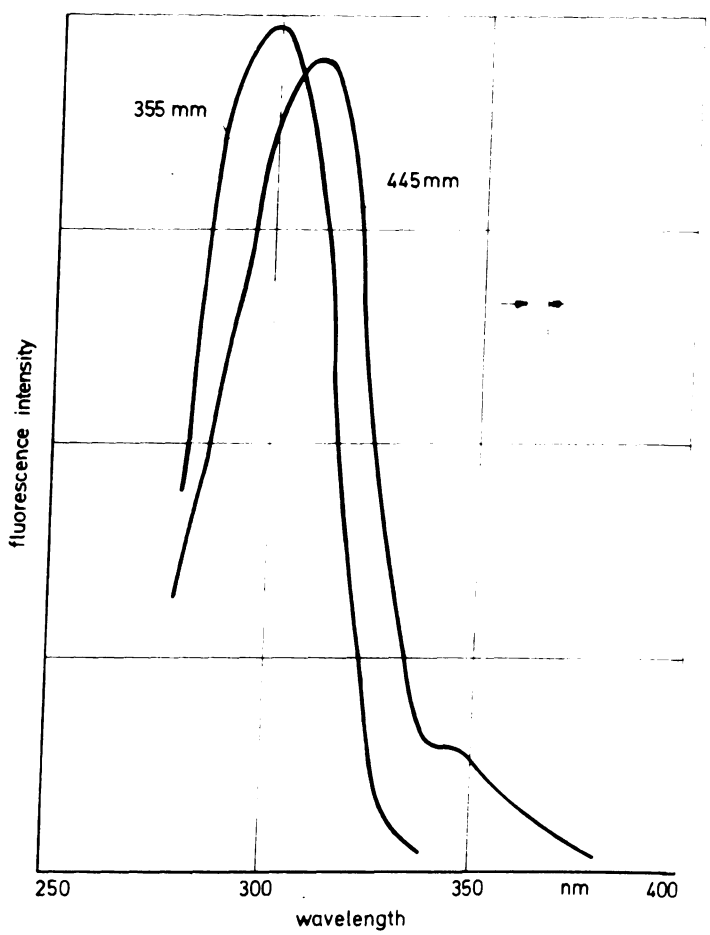

Figure 8. Fluorescence excitation spectra of methyl salicylate, 10^{-4} mole ℓ^{-1} in methanol.(86)

which cannot undergo intramolecular H-bonding through rotation around the ester-ring carbon-carbon bond, exhibits only short wavelength emission in polar solvents, but in non-polar solvents it emits only at longer wavelengths. If there were an equilibrium between the neutral and the zwitterion forms, one would have expected to observe both forms, especially in polar solvents in which methyl salicylate shows two emissions.

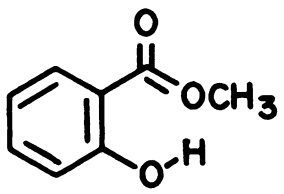

Methyl Salicylate

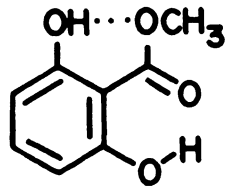

2,6-Dihydroxybenzoate

Sandros[94] found that the ratio of the UV to blue emission was very sensitive to the hydrogen-bonding ability of the solvent and the excitation wavelength (Figure 9). Contrary to the earlier findings,[92] this ratio is much greater in alcohol solvents than in cyclohexane. The position of the short wavelength emission is seen to be solvent dependent. The fluorescence maximum of methyl-2-methoxylbenzoate shows similar solvent shifts. The excitation wavelength dependence results from exciting different proportions of the ground state conformer.

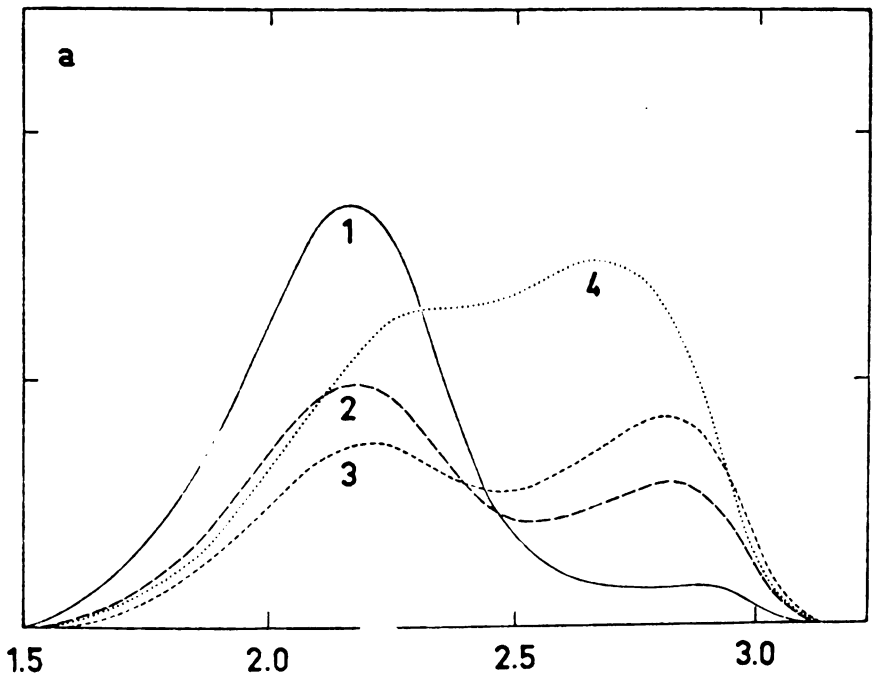

Figure 9. Fluorescence spectra of 2 x 10^{-4} mole cm^{-3} methyl salicylate in cyclohexane (——), ethanol (— — —), methanol (----), and 2,2,2-trifluoroethanol (....). The spectra are shown in relative numbers of quanta vs wavenumber in μm^{-1}. The excitation wavelength is 286 nm.(94)

Sandros proposed that a ground state equilibrium between cis and trans conformers rather than excited state equilibrium is responsible for the relative intensities of the two fluorescence bands.

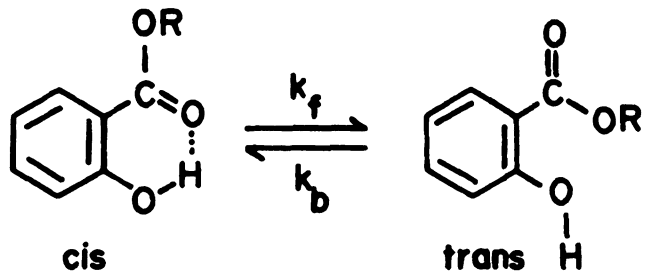

The excitation of the cis form gives rise to a rapid and virtually complete proton transfer, while the trans form does not undergo proton transfer.

Yasunaga et al.[95] performed a kinetic study at 25°C by using ultrasonic absorption techniques and obtained the rate constants for the interchange of the conformers:

$$k_f = 9.5 \times 10^5, \quad k_b = 2.6 \times 10^7\ S^{-1}, \quad K = 0.0365$$
$$\text{and } \Delta H = 2.5 \text{ Kcal mole}^{-1}$$

Thus, the cis-trans interconversion may be slow on the time scale of singlet state deactivation. The greater intensity of the short wavelength fluorescence band in H-bonding solvents can be attributed to stabilization of

the trans ground state by hydrogen bonding with the solvent. In non-H bonding solvents, the cis conformer is the preferred species due to the strong intramolecular H-bond.

An interpretation of the dual fluorescence of methyl salicylate[87] in terms of an emission from an intramolecularly hydrogen-bonded species and from a species in which the hydrogen-bond is ruptured in the excited state is very unlikely. The energy difference between the UV and blue emission bands is too great to be accounted for in terms of hydrogen-bond breakage.

Kaufmann[96] studied the picosecond time resolved fluorescence from MSA and SA in order to provide additional information on the mechanism of proton transfer in the excited state. Methylsalicylate in methylcyclohexane was excited with a 264 nm picopulse[96] (8 psec pulse) and the appearance of 450 nm fluorescence was measured with a streak camera. It was hoped that they could determine the rate of intramolecular proton transfer. The recorded fluorescence signal was a convolution of the apparatus function with the fluorescence from the sample. Deconvolution of the data indicated that the transfer rate constant must be greater than 10^{11} sec^{-1}. The data did not change even where the temperature was lowered to 4°K. Replacing the proton with a dueteron and cooling to 4°K also did not alter the data.[96] Therefore, they

could not confirm or deny whether the proton transfer proceeds via a tunnelling mechanism.[97,98] The lifetime measurement of methylsilicylate showed that the neutral excited state species had a fluorescence lifetime in methylcyclohexane three times larger and in acetonitrile 10 times larger than that of the excited state zwitterion at room temperature. The rapid formation of 450 nm emission and the very different lifetimes of the fluorescence components would also indicate that two species are formed immediately after the absorption of a photon and that they originate from different ground state molecules, since the excitation spectrum of the two emissions is different (Figure 10). These results indicate that the ground state equilibrium rather than the excited state equilibrium is responsible for the distribution of the fluorescence intensity between two wavelengths.

The case of salicylic acid is more complicated than that of methyl salicylate since it can exist in several ionic forms in the ground state and excited state. In addition, it can form dimers.

Methyl-5-ethoxysalicylate I also shows two fluorescences,[92] but in this case the neutral form is favored in the excited state. The enthalpy has been determined to be $\Delta H^* = +0.9$ Kcal mole^{-1}. Thus, increasing the temperature now favors the zwitterion. Time resolved studies are needed to unravel the dynamics of such ethoxy derivatives.

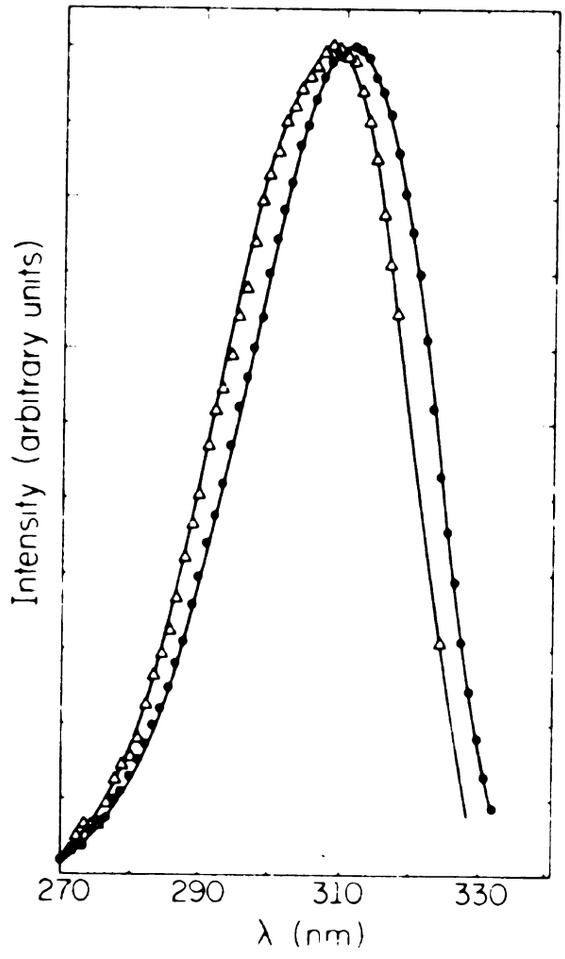

Figure 10. Excitation spectra of methyl salicylate in methylcyclohexane. Solid dots represent the 450-nm band, while open circles represent the 350 nm fluorescence.(96)

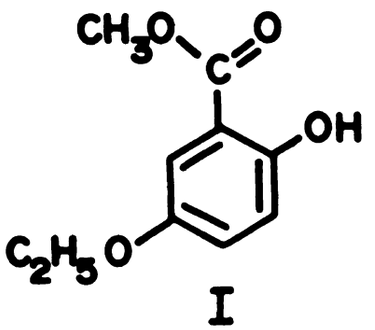

I

Recently, a quenching study of methylsalicylate by carbon tetrachloride[90] showed that the quenching of the short wavelength band is much more marked, the quenching of the long wavelength band being barely detectable (contrary to the previous result).[76] Moreover the short wavelength emission may contain contributions from two "slowly" interconverting ground state conformers that are not equally quenched. Preliminary fluorescence decay measurements using single photon counting appear to verify these results. A single exponential decay with a lifetime of 131±10 PS[90] was observed for the long wavelength emission band of methylsalicylate in methanol (in methylcyclohexane the corresponding lifetime is 280 PS).[96] Therefore there exist at least three distinct ground state conformers: I, II and III.

In non-H-bonding solvents such as cyclohexane, we would expect II to be the major ground state precursor of short wavelength emission, due to stabilization by

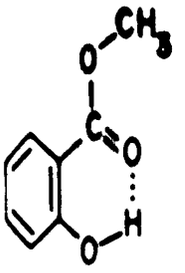

I

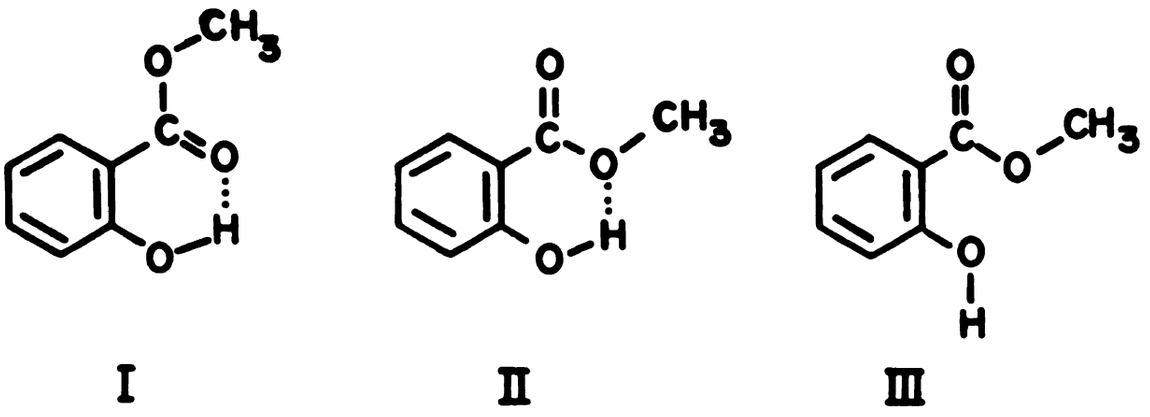

I II III

the intramolecular H-bond while I is expected to be the precursor of the zwitterion emission at longer wavelengths. In methanol, however, there will be a stabilization of structure III due to H-bonding with the solvent. Structure III contributes a significant component to the short wavelength emission in methanol: such a component is more quenchable by CCl_4 (i.e., has a larger Stern-Volmer constant). Structure II contributes also to the short wavelength emission band. One should notice that the relative intensity of the short wavelength emission increases as the solvent proton's ability to form H-bonds increases.

Mori et al.[99] concluded from IR data that structure (I) was the most stable; a fact confirmed in a later study[100] which used the CNDO/2 method and gave the calculated stability order I > II > III. The calculated energy differences of (II) and (III) as compared with the most stable ones, (III), are 1.8 and 12.7 Kcal $mole^{-1}$ respectively. In another study using the INDO[101] method a difference in energy of 18.3 Kcal $mole^{-1}$ between

I (cis) and III (trans) has been obtained which suggests that a strong intramolecular H-bond must be present.

The effect of temperature on the fluorescence spectrum of methylsalicylate in cyclohexane excited at 280 nm also has been studied by Ford et al.[90] (Figure 11). The essential feature is that a decline in the intensity of the long wavelength band as the temperature is raised is accompanied by an increase in the short wavelength band. Weller[92] had earlier observed a similar but apparently smaller effect. In contrast to the results of Ford et al. Smith and Kaufmann reported that the intensity of the short wavelength band remains substantially constant with temperature in methylcyclohexane. Ford et al. have noted one possible explanation for this discrepancy. The two fluorescence bands overlap appreciably, so that if spectra are recorded with a large emission monochromator slit width then the bands will be less well resolved and an apparent insensitivity to the relative intensities will occur.

The detailed interpretation of temperature effects is quite complex, because the nonradiative rates for each of the excited state species and the ground state equilibria between the three conformers are temperature dependent. Moreover, the quantum yields of different emitting species are different. It appears certain however, that the short wavelength emission intensity increases with increasing

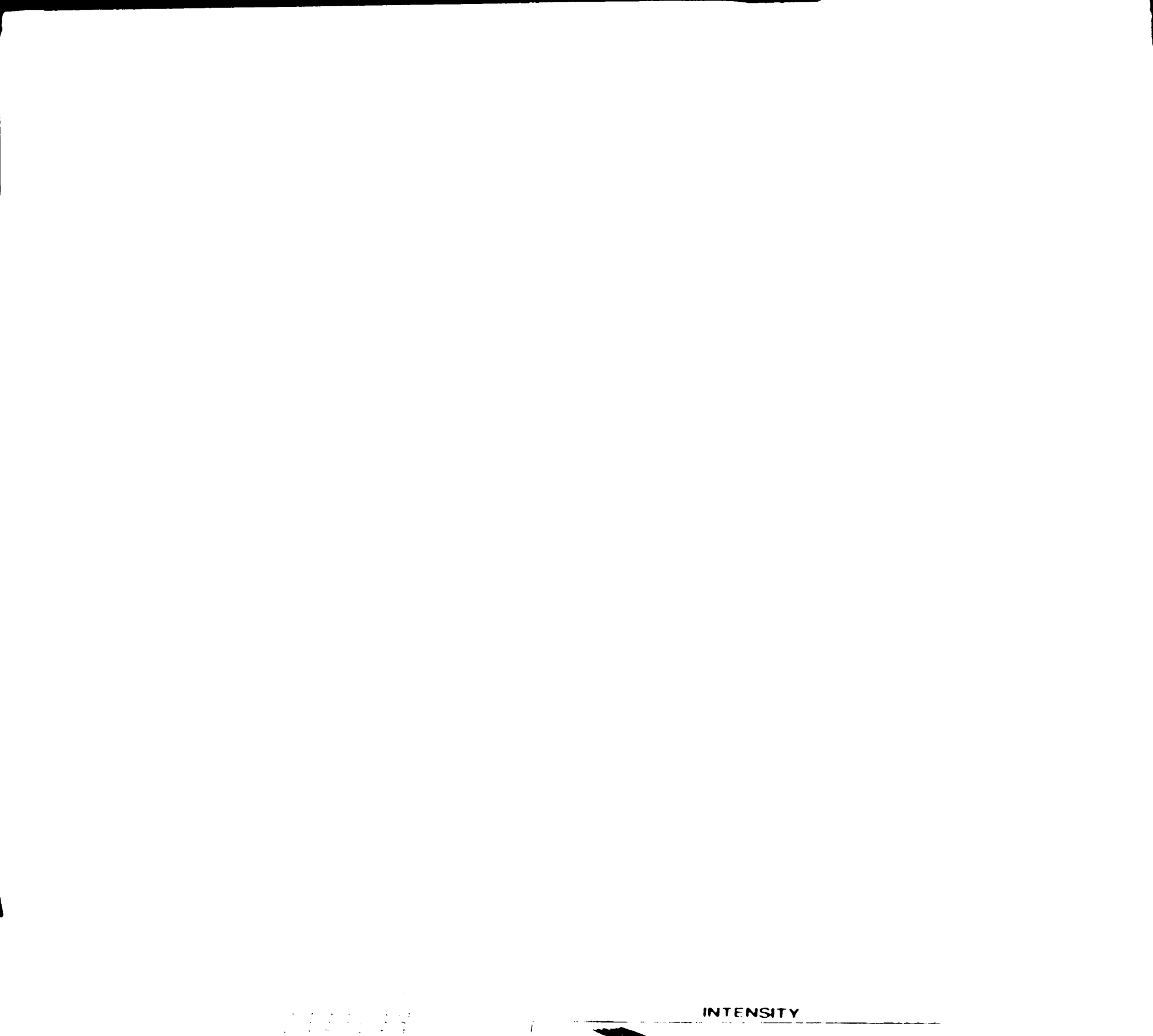
INTENSITY

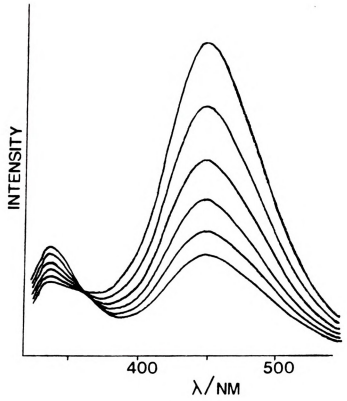

Figure 11. Temperature variation of the fluorescence spectrum of methyl salicylate in cyclohexane (1.4×10^{-4} M). As temperature increases the short wavelength emission intensity raises and the long wavelength intensity decreases. Temperatures (°C): 21.2, 29.6, 39.1, 48.3, 57.3, 67.5.(90)

temperature indicating a shift in the ground state equilibria, since the rates of radiationless processes seldom decrease with increasing temperature.

The pH dependence of the intramolecular proton transfer in salicylic acid was examined,[85] the following ionization scheme was postulated for the ground and excited singlet state. Very similar behavior was found for salicylamide and salicylanilide.[102]

Salicylamide and Salicylanilide - In contrast to methylsalicylate in cyclohexane, salicylamide in cyclohexane shows only a single fluorescence band at ~450 nm assigned to the zwitterion species with a Stokes shift comparable to the long wavelength band for methylsalicylate (ca. 10150 cm^{-1}) (Figure 12a). This behavior is similar to that of salicylanilide which also gives a single band at 469 nm[81] in non polar solvents. In ethanol the fluorescence of salicylanilide consists of a single band at 420 nm attributed to the phenolate anion form. Salicylamide exhibits two emission bands one at 342 nm due to the neutral form and the other at 426 nm which is a composite band due to zwitterion and phenolate emission generated by exciting different ground state conformers (Figure 12b). In water at pH 5.6 where salicylamide exists in its neutral form, a single fluorescence band at 420 nm is observed. The fluorescence decay curve for salicylamide in water

Ground state

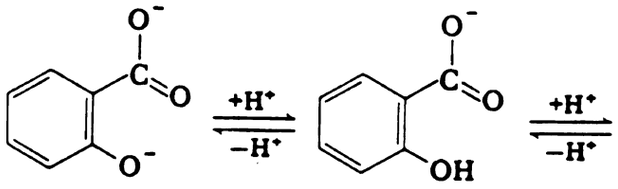

$pK(S_0) = 14$ $pK(S_0) = 3{\cdot}0$

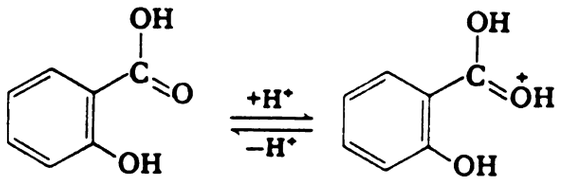

$pK(S_0) = -8{\cdot}0$

Lowest singlet state

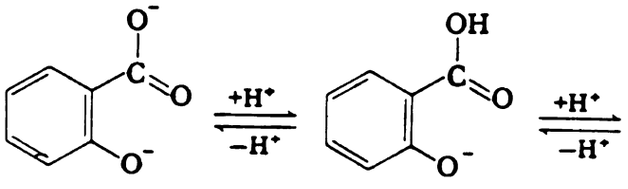

$pK(S_1) = 16{\cdot}0$

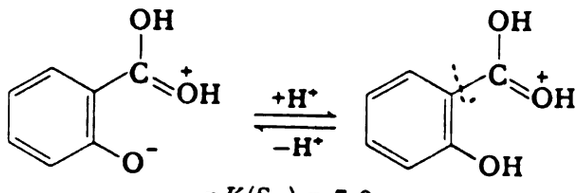

$pK(S_1) = 7{\cdot}0$

Ionization Scheme for Salicylic Acid[85]

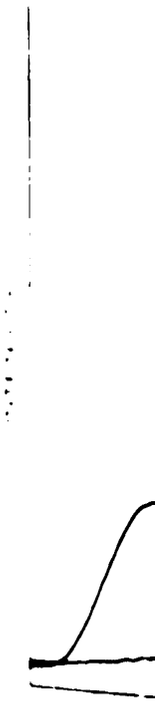

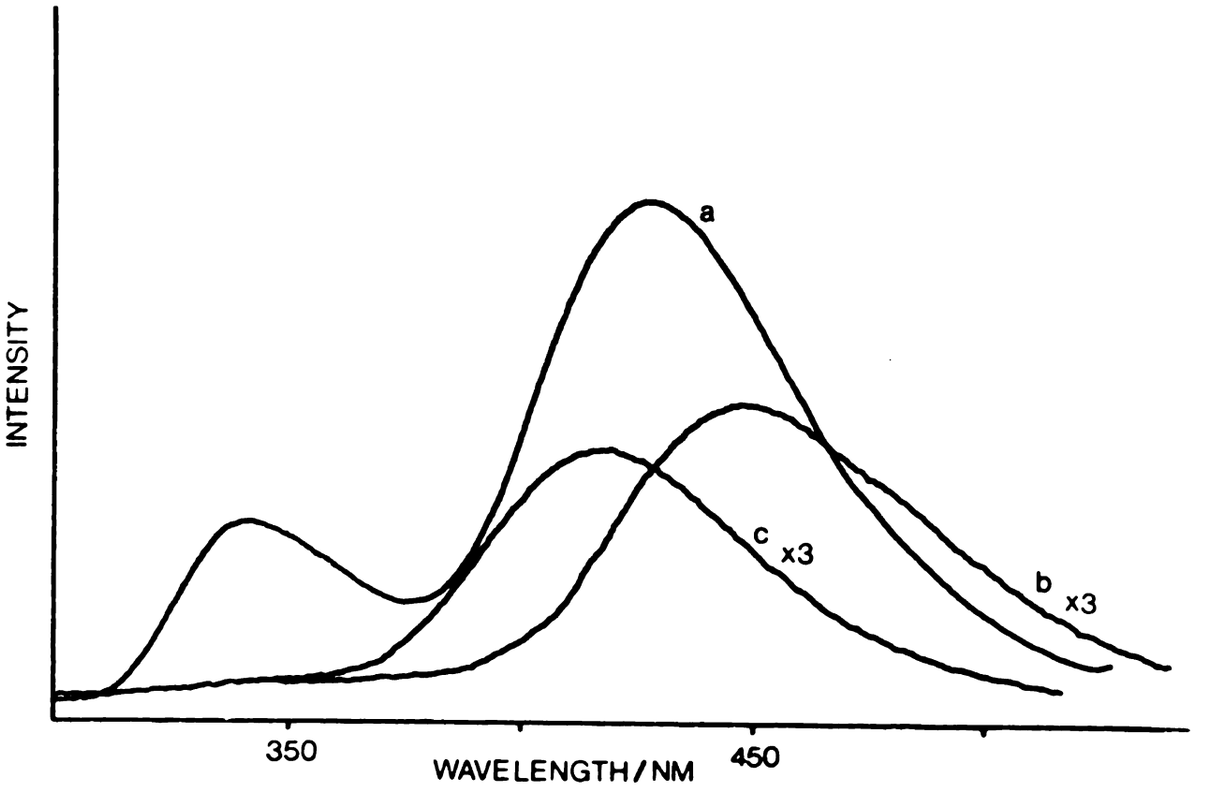

Figure 12a. Fluorescence spectra of salicylamide: (a) 2.4×10^{-4} M in ethanol, λ_{ex} = 265 nm; (b) 1.3×10^{-5} M in cyclohexane, λ_{ex} = 300 nm; (c) 1.0×10^{-4} M in water, λ_{ex} = 265 nm.(89)

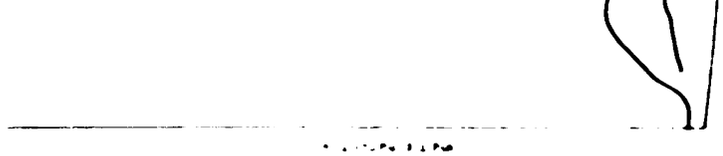

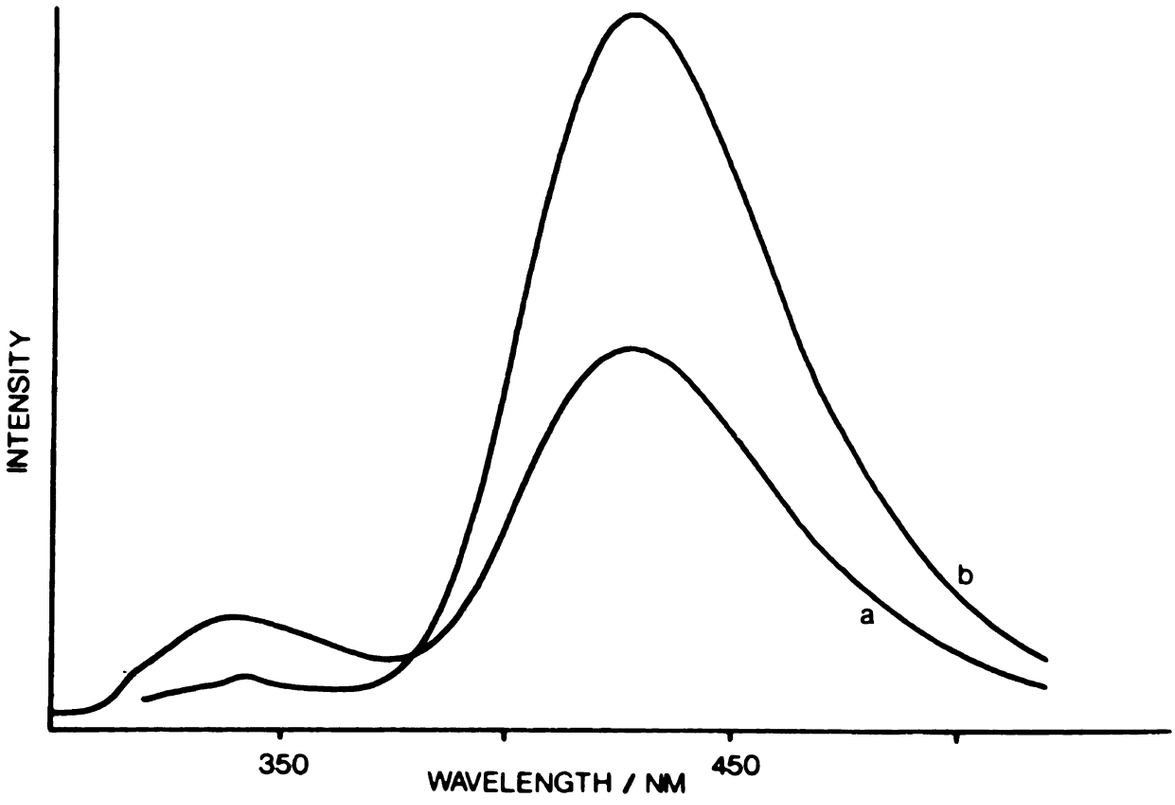

Figure 12b. Effect of excitation wavelength on the fluorescence spectrum of 2.5 x 10^{-5} M salicylamide in ethanol: (a) λ_{ex} = 290 nm; (b) λ_{ex} = 310 nm.[89]

obtained by observing the whole fluorescence band from 400 nm upwards by picosecond spectroscopy, with a streak camera, is shown in Figure 13. The semi-log plot of the data (upper data points) clearly shows the nonexponential nature of the decay. The most obvious explanation of these observations is that the observed decay is the result of the simultaneous decay of the two species with lifetimes of 1.87±0.20 ns and 0.11±0.01 ns which have overlapping fluorescence spectra. The fluorescence decay curves have been recorded by observing different wavelength sections of the emission, isolated by suitable filters (Table 2).

The observation of the two lifetimes indicates two separately emitting species, while the fluorescence and excitation spectra in water give no indication that this results from excitation of different ground state species. Similar results were obtained for acidified solutions. The possibility that one of the two decay components observed with a lifetime of 6 ns is due to salicylate anion ($-COO^-$) has been eliminated. However, the phenolate anion ($-O^-$) of salicylamide gives a single exponential with a lifetime of 1.9±0.12 ns which coincides with the long lifetime component of the decay curve. This suggests that the phenolate anion is a major contributor to the long wavelength emission band of aqueous salicylamide. Furthermore, the trend in the value of the fraction of

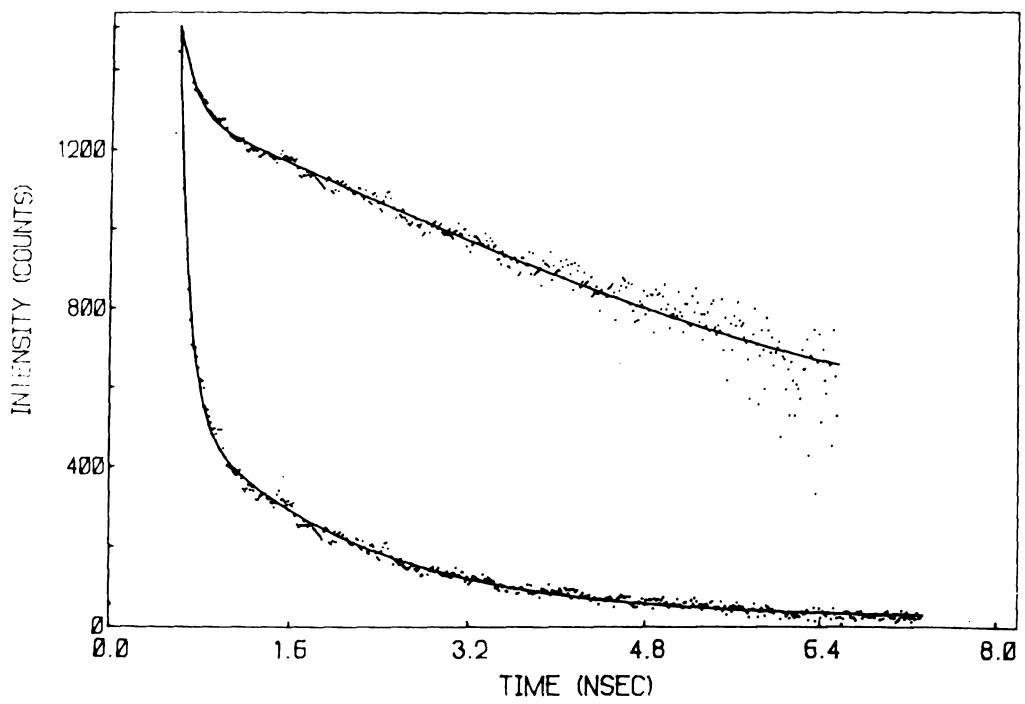

Figure 13. Fluorescence decay curve of 10^{-3} M aqueous salicylamide (all emission above 400 nm) excited at 265 nm; sweep speed 16 PS channel^{-1}. The upper curve is a semi-log plot.(89)

Table 2.

Wavelength Band	Fraction of Fast Component
400 nm	0.34 ± 0.09
440 nm	0.59 ± 0.05
>495 nm	0.80 ± 0.02

short-lived component with emission wavelength indicates that the zwitterion fluorescence lies to the red of that of phenolate anion. The most plausible explanation of the results in water is that following excitation there is an immediate loss of a proton from the phenolate group. Some of these protons are transferred to the carbonyl group to give the zwitterion species. The fast decaying fluorescence can then be attributed to the zwitterion species, while the slow component arises from the excited phenolate anion. Whether the transfer of the proton lost from the phenolate group to the carbonyl group depends on the ground state conformation of salicylamide molecule in water is not clear, although this appears reasonable.

The fluorescence spectra for salicylamide in D_2O (PD 0.5) at various excitation wavelengths are shown in Figure 14. In changing from H_2O to D_2O, a large

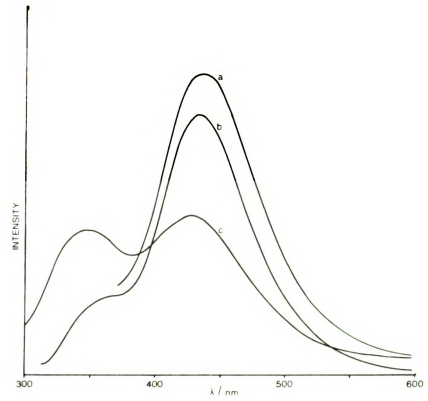

Figure 14. Fluorescence of salicylamide in D_2O (1.7×10^{-4} M). Excitation wavelengths (nm): (a) 330; (b) 330; (c) 265.[88]

increase in the intensity of the 355 nm emission band relative to that of the long wavelength band is observed. The zwitterion concentration remains constant on deuteration. The intramolecular proton transfer is expected to be so rapid that even when slowed by deuteration, the zwitterion yield is unaffected. The increased intensity of the neutral molecule emission makes it possible to record the excitation spectra of the neutral and zwitterion species (Figure 15). As expected, the ground state trans conformer of excited neutral salicylamide absorbs at shorter wavelengths than the cis ground state conformer, the latter can lead to excited state zwitterion formation.

Naphthoic Acid and Its Derivatives - 3-Hydroxy-2-naphthoic acid (I) [87,103-105], and the corresponding methoxy derivative (II) have been investigated.

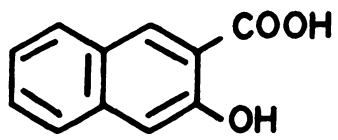

I

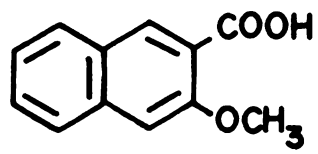

II

The infrared (and NMR) data suggested a relatively strong intramolecular hydrogen bond.[81] The ultraviolet absorption spectra of these derivatives show this bond to be red shifted compared with the corresponding methoxy-derivatives which lack the hydrogen bond.[105-107]

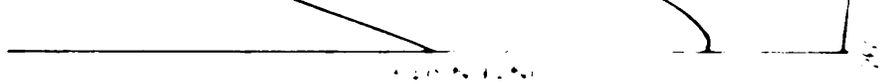

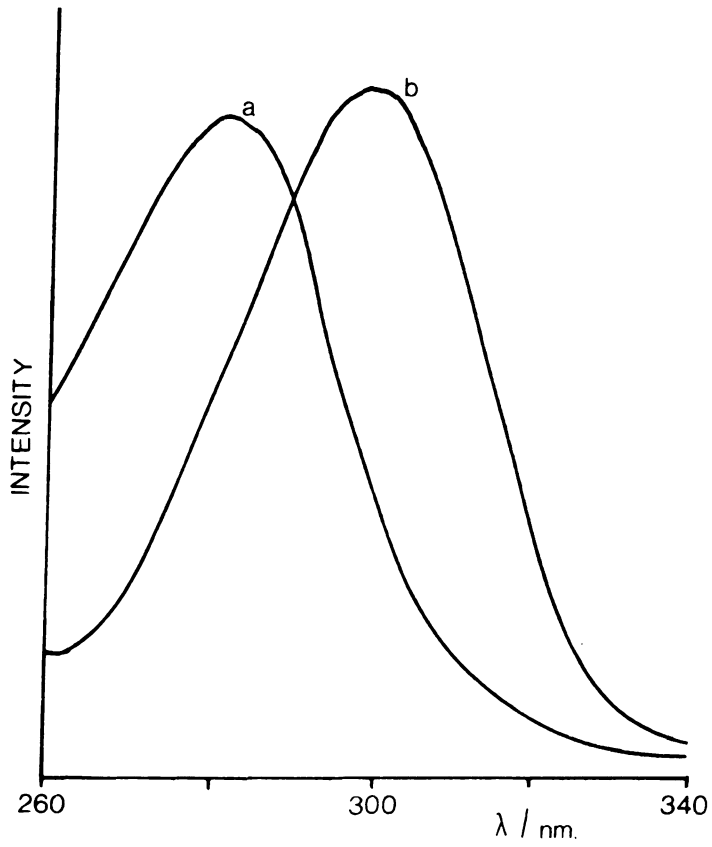

Figure 15. Fluorescence excitation spectra for salicylamide in D_2O. Emission wavelengths (nm): (a) 350; (b) 430.[88]

The fluorescence spectrum of methyl-3-hydroxy-2-naphthoate is the subject of some controversy. A fluorescence band at ca. 420 nm, corresponding to a normal Stokes shift (3200 cm^{-1}) of emission is observed. Naboiken[105] and co-workers have observed a weak, long wavelength emission (ca. 650 nm) in hydrocarbon solvents in concentrated solutions where there is a noticeable quenching of the short wavelength fluorescence band. The interpretation of this band at 650 nm as being due to impurities, dimers or excimers was refuted;[105] instead it was attributed to an intramolecular proton transfer. The fluorescence decay of this band[108] gave a single exponential lifetime of 60±6 PS.

The 650 nm band has not been observed by some workers[77,104] in either the methyl ester or in the free acid. More recently, a band at 605 nm was observed[108] (Figure 16). As we see in Figure 16 this band is more apparent in concentrated solutions and at longer excitation wavelengths.

The fluorescence excitation spectra (Figure 17) of the short wavelength emission has two maxima and lies at shorter wavelength than the featureless excitation spectrum of the 608 nm emission band. Neither excitation spectrum bears a close relationship to the absorption spectrum, but this is hardly surprising, since the absorption spectrum is a superposition of the spectra of at least two distinct

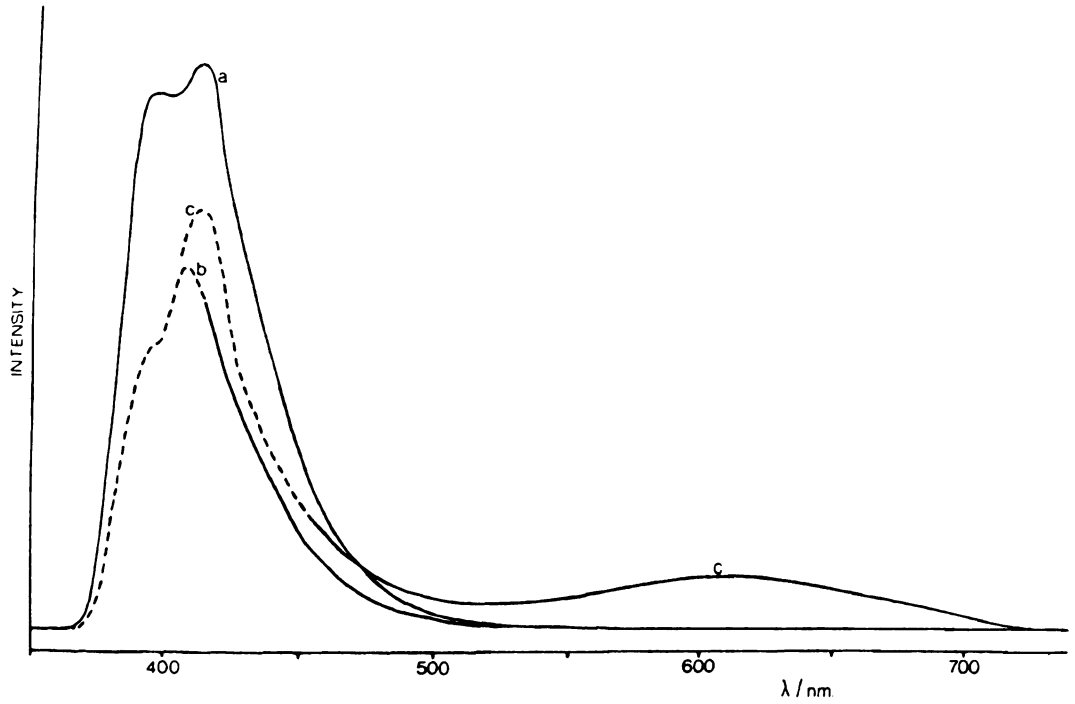

Figure 16. Fluorescence of methyl 3-hydroxy-2-naphthoate in cyclohexane: (a) 1 x 10^{-5} M, (b) 1 x 10^{-4} M, λ_{ex} = 260 nm, (c) 1 x 10^{-4} M, λ_{ex} = 390.[108]

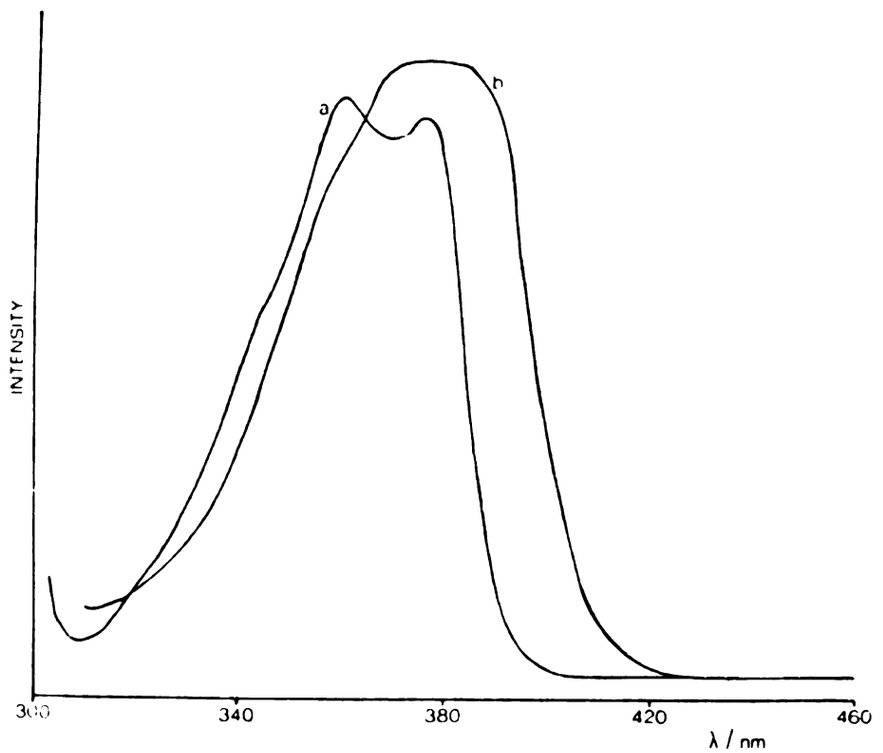

Figure 17. Fluorescence excitation spectra of methyl 3-hydroxy-2-naphthoate in cyclohexane (a) short wavelength emission and (b) long wavelength emission.(108)

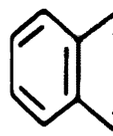

III

ground state species, as evidenced by the excitation spectra. The long wavelength emission can be attributed to a zwitterion species formed by intramolecular proton transfer in the first excited singlet state. The ground state precursor of the zwitterion is an intramolecularly H-bonded conformer, III. The anion of the ester emits at

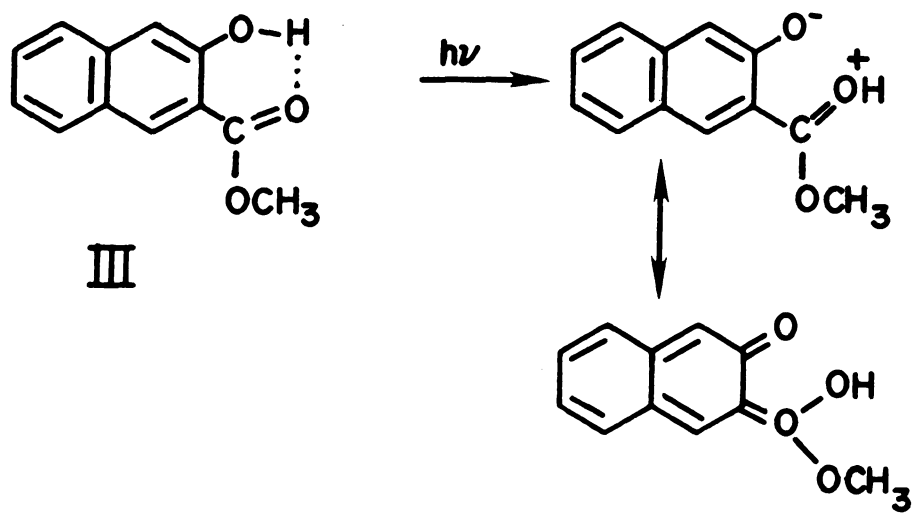

III

18,200 cm^{-1} (550 nm) in alcoholic NaOH, corresponding to an absorption maximum near 25,000[105] cm^{-1}.

The short wavelength emission band of methyl-3-hydroxy-2-naphthoate in cyclohexane is characterized by a non-exponential and concentration-dependent fluorescence decay.[108] At a concentration of 10^{-4} M, the lifetimes that best fit a double exponential decay function are 23.3±0.2 ns and 5.1±0.9 ns. As the concentration is increased, the longer of the two lifetimes is progressively

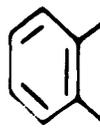

reduced. This observation suggests that there are two distinct contributions to this short wavelength band. Quenching evidence for a dual contribution to the short wavelength emission of methyl salicylate has been given.(90)

The interpretation is in terms of two interconvertible ground-state conformers. Interconversion is sufficiently slow that it does not occur during the excited state lifetime. The suggested conformers are ones in which the hydroxylic proton is H-bonded to the "ether type" oxygen of the carboxyl group (IV) and an "open-ring" form containing no intramolecular H-bonds (V).

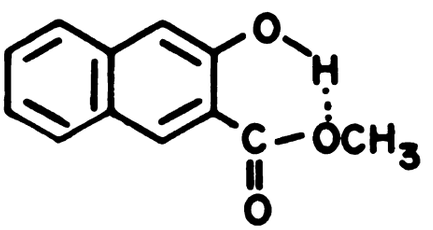

IV

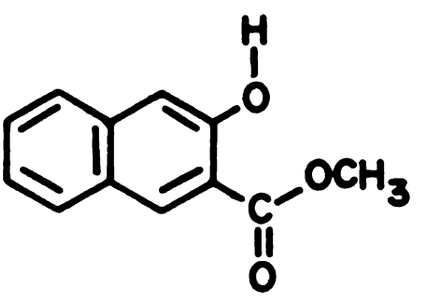

V

The 23.3 ns lifetime can be attributed to conformer IV and the 5.1 ns lifetime to V. A calculation of the following equilibrium constant from absorption data (ΔH = 5 Kcal mole^{-1}) yields a value of approximately 5 x 10^3. The equilibrium should therefore be almost entirely in favor of III. On this basis then, the absorption spectrum would bear a close similarity to the excitation spectrum of the long wavelength emission band which is

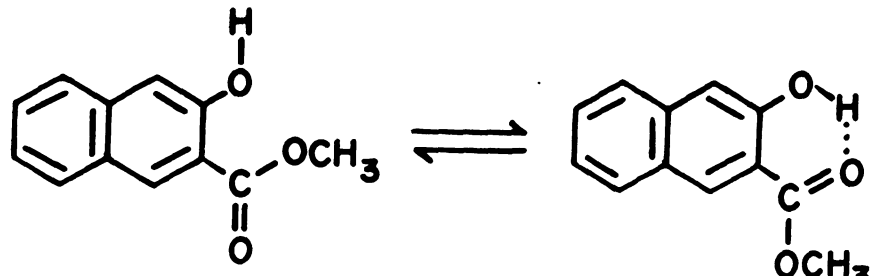

V III

clearly not the case. McTigue[109] has shown that H-bonds involving ether oxygen and carbonyl oxygens are of similar strength for intermolecular H bonding between H_2O and various organic ketones and ethers in CCl_4 solution. Thus conformers IV and III will be of similar energy. The absorption spectrum is virtually independent of temperature between 293 and 328°K in cyclohexane and between 160 and 280°K in methylcyclohexane. This is consistent with conformers III and IV being energetically similar, with conformer V making up only a very small proportion of the ground state mixture.

The study of 3-hydroxy-2-naphthoic acid[77] (free acid) shows that an anomalous long wavelength fluorescence appeared only in basic solvents or proton accepting solvents such as acetone, acetonitrile, and in aprotic solvents doped with small amounts of basic solvents, such as a mixture of toluene and pyridine,[77,104] whereas in benzene only normal fluorescence with its maximum near 23700 cm^{-1} (420 nm) is observed. Two fluorescence bands have been observed, one near 24000cm^{-1} (416 nm) and the

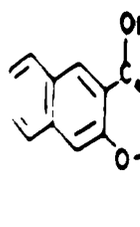

other at 19000 cm^{-1} (526 nm). These two bands have been interpreted by Hirota in analogy to those of methyl salicylate. From the temperature dependence of the relative intensity $\Delta H^* = -3.1$ Kcal $mole^{-1}$ has been calculated.(77) Recently the hypothesis of true intramolecular proton transfer in the excited state of 3-hydroxy-2-naphthoic acid has been refuted by Ware *et al.*(104) who employed fluorescence quenching and singlet-state lifetime measurement techniques in a variety of solvents to show that photoautomerization in the lowest excited singlet state involves intermolecular H-bonding with the solvent in the ground electronic state. According to Ware,(104) pyridine acts as static quencher by forming a ground state complex. The proposed mechanism of the anomalous fluorescence

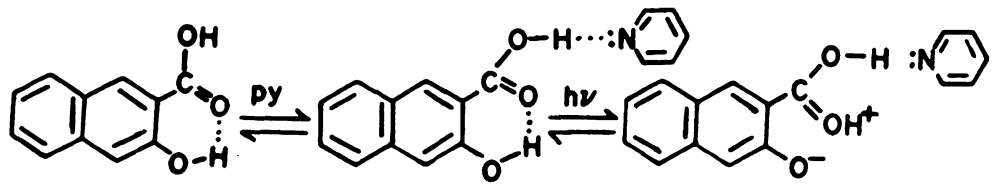

of this acid consists in the formation of the H-bonded complex, followed by absorption of a photon and intramolecular proton transfer. Thus the enthalpy ($\Delta H = -3.1$ Kcal $mole^{-1}$) measured by Hirota should be attributed to the enthalpy of formation of this complex. At high concentrations of this acid, complex spectral behavior is

observed due to association and to quenching by H^+ ions.[103]

The effect of pH on the absorption and fluorescence spectra of 3-hydroxy-2-naphthoic acid has been investigated.[110] Although the ground-state behavior was similar to that of salicylic acid, the molecules differed in the prototropic reactions of the S_1 state, phototautomerism occurred only partially in the anion and not at all in the neutral molecules. Similar experimental evidence has been obtained for 1-hydroxy-2-naphthoic acid and 2-hydroxy-1-naphthoic acid.[111] In these cases the neutral molecules undergo intermolecular phototautomerism to form the zwitterion but, unlike 3-hydroxy-2-naphthoate the anions do not react in this way.

b. Intermolecular Excited State Proton Transfer

Naphthol-Triethylamine Systems - Nagakura and Gouterman[112] have demonstrated that both α- and β-naphthol form quite strong H-bonds with triethylamine (TEA). The change of absorption caused by H-bonding in the case of the β-naphthol-TEA system in cyclohexane is shown in Figure 18. The ground and excited state equilibrium constants for this system in cyclohexane have been estimated to be 180 and 3300 respectively. The dipole moment[113] of naphthol, its hydrogen-bonding ability and its acidity are greater in the first excited singlet state than in the

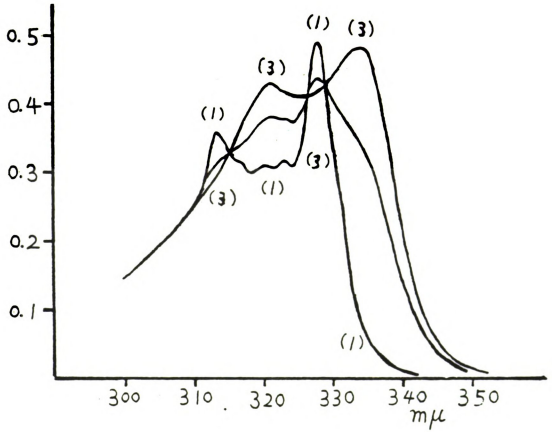

Figure 18. Change of the absorption spectrum of β-naphthol in cyclohexane produced by added TEA (∿15°C). Concentration of β-naphthaol: 2×10^{-4} mol ℓ^{-1}. Concentration of TEA: (1) 0 mole ℓ^{-1}, (2) 1.12×10^{-2} mole ℓ^{-1} (3) 1.80×10^{-1} mole ℓ^{-1}.(75)

ground state ($pK_a = 9.1$ and $pK_a^* = 2.8$).[114] These facts have been ascribed to the increased migration of π-electrons on the oxygen to the vacant π-MO's of the naphthalene ring in the excited electronic state.[113,115,116] In view of the above facts, one might expect proton transfer in the excited state of the naphthol-TEA system in nonpolar solvents.

The change in the fluorescence spectrum of β-naphthol caused by the addition of TEA in methylcyclohexane[92] is shown in Figure 19. Up to about 0.1 M TEA, the change undoubtedly is due to hydrogen-bond formation. However, the broadness of the spectrum observed at and above 0.1 M triethylamine, when practically all excited naphthol molecules are complexed, indicates that this spectrum is due to more than one emitting species. Comparison with the fluorescence spectrum in pure TEA suggests that the contact ion-pair (III) is the other component. The shift in the fluorescence spectrum due to ion-pair formation is about 5500 cm^{-1}. The observed phenomenon is interpreted as due to a strong charge-transfer from the nitrogen nonbonding orbital to naphthol in the Franck-Condon excited state, which is followed by almost complete proton transfer from oxygen to nitrogen in the excited equilibrium state. Fluorescence quenching with oxygen showed that both components are equally quenched.[92] This indicates that the proton transfer equilibrium between II and III

1·0
0·5
0

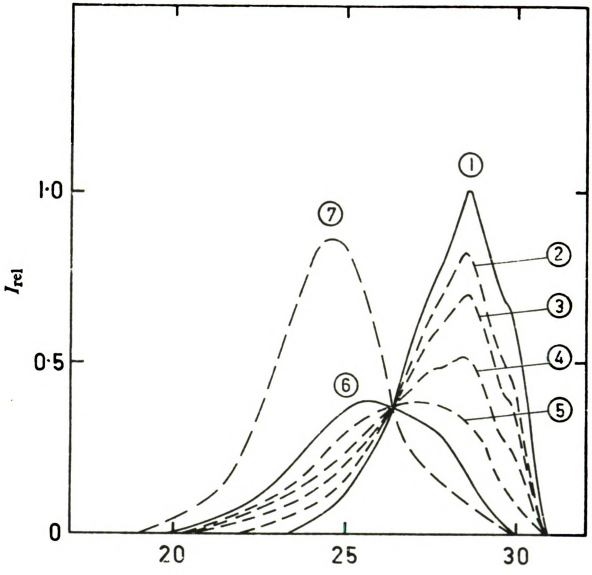

Figure 19. Fluorescence spectra of β-napthol in methylcyclohexane at different concentrations of triethylamine (1) 0.000 M; (2) 0.002 M; (3) 0.004 M, (4) 0.008 M; (5) 0.020 M; (6) 0.10 and 0.15 M; (7) as solvent.(92)

is fully established in a time shorter than the lifetime of the excited molecules.

$$\underset{\text{I}}{ArOH} + NR_3 \rightarrow \underset{\text{II}}{Ar^*OH...NR_3} \overset{K^*_{23} = 1.5}{\rightleftarrows} \underset{\text{III}}{Ar^*O^-...\overset{+}{H}NR_3} \qquad (1)$$

Lowering of the temperature, however, changes the fluorescence spectrum of the H-bond complex in favor of the ion-pair III, as shown in Figure 20. From the intensity ratio at separate frequencies (22,500 cm^{-1} and 28,000 cm^{-1}) the equilibrium constant, K^*_{23} has been found to be 1.5 and from the temperature dependence of K^*_{23}, the enthalpy, ΔH^*_{23} of the excited state equilibrium is -0.9 Kcal $mole^{-1}$.

The interaction of β-napthol in the excited state with triethylamine was studied by measuring nanosecond time-resolved fluorescence spectra and by analyzing the decay fluorescence bands due to the free and complexed proton doners. The time-resolved fluorescence spectrum has a new band at 410 nm in addition to the band of the free β-naphthol molecule at 355 nm. The former corresponds to the band found in the steady-excitation fluorescence spectrum of the β-naphthol-TEA-benzene system and ascribed to ion-pair formation by Mataga and Kaifu.[75,117] This band decays more rapidly than the band at 355 nm (Figure 21).[118] Using the Stern-Volmer equation,[119] the

1·0
0·5
0

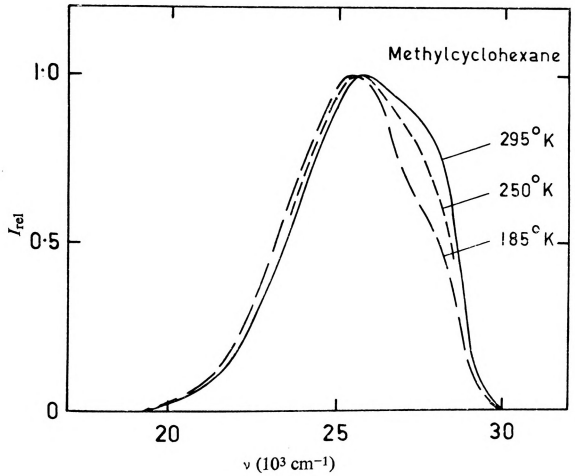

Figure 20. Fluorescence spectra of β-naphthol in methylcyclohexane +0.14 M triethylamine at different temperatures.(92)

Fluorescence Intensity

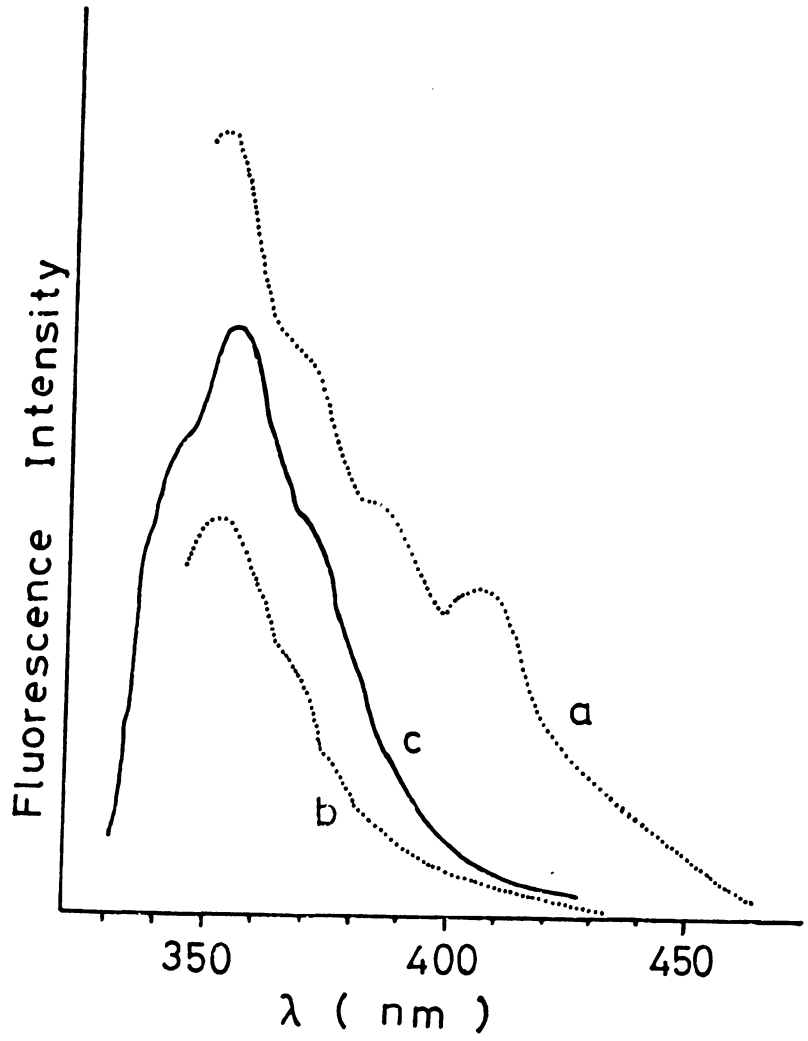

Figure 21. Fluorescence spectra of β-naphthol under various conditions. The time-resolved spectra of the β-naphthol-TEA system in toluene at 25°C observed 0 ns curve (a) and 10 ns (curve b) after the fluorescence of the β-naphthol reached the maximum intensity. The concentrations of β-naphthol and TEA are 1.2×10^{-4} M and 0.705×10^{-2} M, respectively. Curve c is the steady state fluorescence spectrum of the toluene solution of β-naphthol (0.705×10^{-4} M).(118)

lifetime of β-naphthol and the rate constant for complex formation in the excited state were determined at 30°C to be 11.6 ns and (2.17±0.01) x 10^9 $M^{-1}s^{-1}$, respectively. From the temperature dependence of the rate constant an activation energy E_a and a frequency factor A were determined as follows:

$$E_a = 1.64 \pm 0.11 \text{ Kcal mole}^{-1}$$

$$A = (3.05 \pm 0.12) \times 10^{10} \text{ M}^{-1}\text{s}^{-1}$$

This E_a value is comparable to the activation energy for the diffusion of toluene as determined from the temperature coefficient of its viscosity.[120] The rate constants obtained from analysis of the fluorescence quantum[121,116d] yield and by using Somoluchowski's equation[122,123] are 2 ∿ 3 x 10^9 $M^{-1}s^{-1}$ and 3 ∿ 8 x 10^9 $M^{-1}s^{-1}$, respectively, which are in good agreement with the results of time-resolved fluorescence spectra.

3-Hydroxypyrene-TEA System - The change in the fluorescence spectrum in methylcyclohexane[92] upon lowering the temperature is much less significant in this case than with β-naphthol and can be interpreted as a slight sharpening of the structure. Thus ΔH^*_{23} is either around zero or strongly positive. The latter assumption implies that the spectrum in methylcyclohexane is solely due to

the form (II). In toluene, evidently the ion-pair (III) is favored over from (I) and the same is true in pure triethylamine. The relative values of the equilibrium constant K^*_{23} in methylcyclohexane, toluene and triethylamine, calculated from the intensity ratio at 21,000 cm^{-1} and 25,600 cm^{-1}, are <1, 10 and 7.6, respectively.

7-Azaindole Dimers (Double Proton Transfer) - Biprotonic phototautomerism in 7-azaindole hydrogen-bonded dimers was first discovered by Taylor, El-Bayoumi, and Kasha[124] when they examined the fluorescence spectrum of 7-azaindole (7AI) in 3-methylpentane (3MP) as a function of concentration. It was known from earlier work by El-Bayoumi[125] that in carbon tetrachloride an appreciable fraction of the 7AI molecules is present in the form of doubly hydrogen bonded dimers. The equilibrium constant for this self-association was estimated to be 118 M^{-1} based on an infrared study in CCl_4, at 35°,[125] 1.8×10^3 and 2.5×10^2 M^{-1} in 3MP and CCl_4, respectively, at 25°C, based on absorption spectra,[79] at 315 nm. These correspond to $\Delta G°$ values of -4.5 and -3.3 $Kcal mol^{-1}$ at room temperature. The lower association constant in CCl_4 can be rationalized on the basis of the high polarizability of this solvent relative to 3MP. By studying the effect of temperature on the association constant in 3MP, ΔH = -9.6 $Kcal mol^{-1}$ and ΔS = -18 e.u. have been estimated. Using

the value of 1.8×10^3 M^{-1} for the association constant in 3MP at 25°, only about 4% of 7AI molecules are dimerized at 10^{-5} M while 85% are dimerized at 10^{-2} M. Thus the solid curve in Figure 22 is due mainly to the monomer while the dashed curve represents the dimer. Because of the large negative value of ΔH, the extent of dimerization will increase dramatically on cooling. This was confirmed by measuring the absorption spectrum in 3MP at 77°K, where the spectra were identical at 10^{-4} and 10^{-2} M.

In Figure 22, the room temperature fluorescence spectrum of 7AI in 3MP is seen to consist of two fluorescence bands. The first band, F_1, has a maximum at about 325 nm and is attributed to the normal fluorescence of the monomer with possibly a small contribution from the dimer. The second band F_2, has a maximum at about 480 nm and an intensity relative to F_1 which depends on concentration, excitation wavelength and temperature. This second band was attributed by the authors to fluorescence from a new tautomeric species which forms in the excited state of the dimer by the simultaneous intermolecular proton transfer of the two pyrrolic hydrogens, as shown below. The authors took great care to eliminate alternative explanations of F_2 such as impurities, excimers, and photodecomposition products.

Further evidence supporting this mechanism was provided by comparing[126] the fluorescence spectrum of 7AI

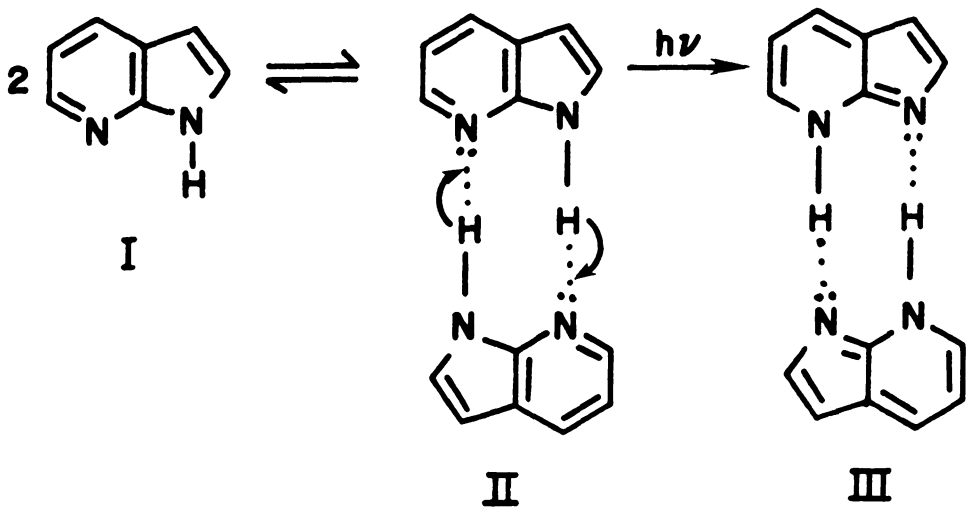

I II III

with that of its two N-methyl derivatives IV and V.

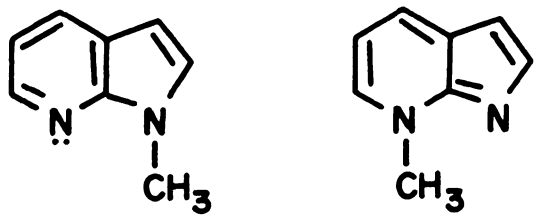

IV V

The fluorescence spectrum of IV exhibits only the normal fluorescence analogous to F_1 in the 7AI system. In particular the V compound, which has a formal electronic structure similar to species III, gives a fluorescence spectrum very similar to F_2.

An important question was the mechanism by which this double proton transfer takes place (whether the reaction is thermal or proceeds through quantum mechanical

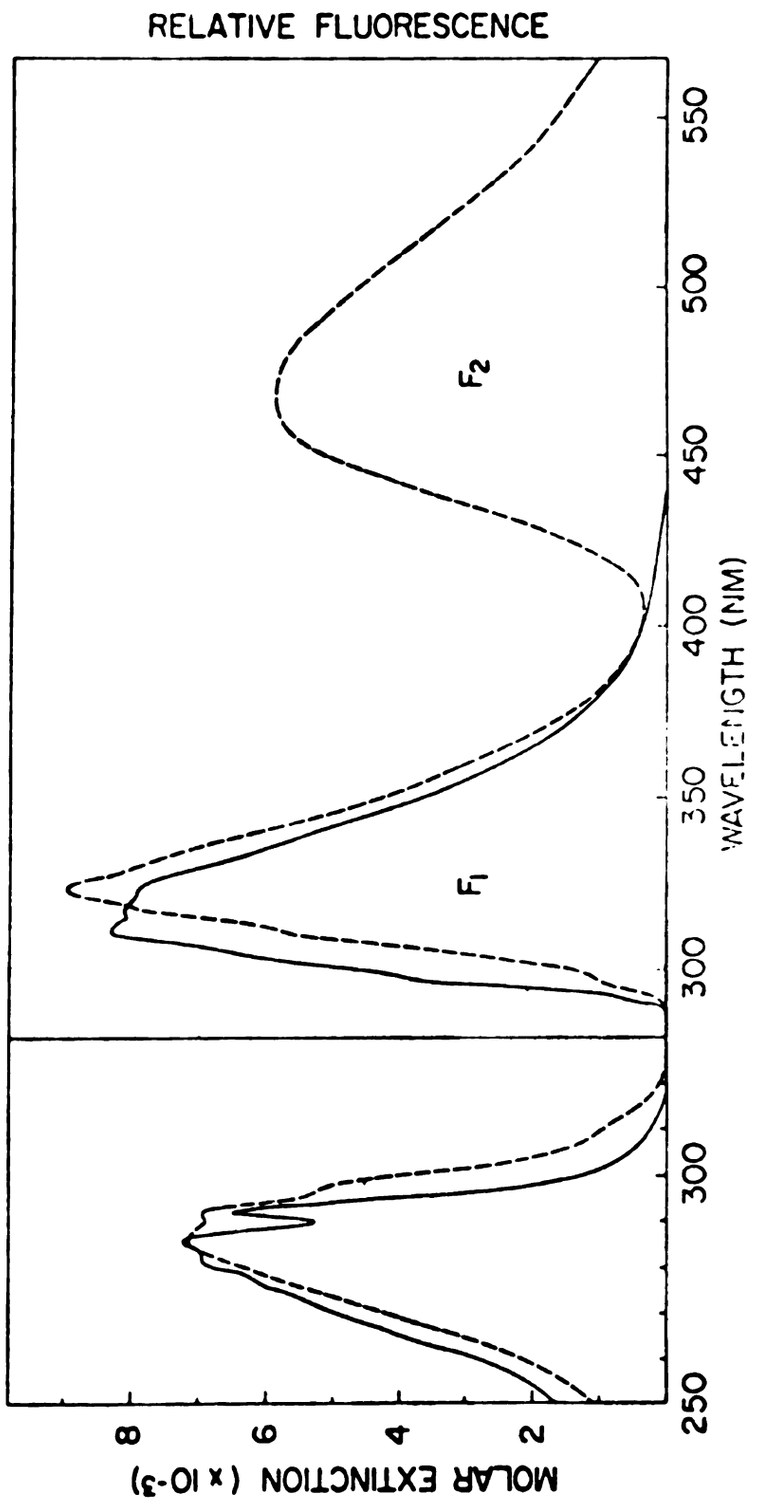

Figure 22. Room temperature-absorption (left) and fluorescence (right) of 7-azaindole in 3MP at 1.0 x 10-5 M (——) and 1.0 x 10-2 M (----). Excitation wavelength 285 nm. Front surface excitation was used for the concentrated sample. The signals were arbitrarily adjusted to give comparable intensity in the F_1 region.

tunnelling). By studying the effect of temperature on the relative intensities of the normal violet fluorescence (F_1) and the green tautomer fluorescence (F_2) in 3MP, a value of 1.4 Kcal mole^{-1} (500 cm^{-1}) was obtained as the potential energy barrier for double proton transfer. It was found, however, that the relative integrated intensities of the tautomer and dimer fluorescence are the same at 77 and 4.2°K,

$$\text{i.e.,} \quad (k_{PT})_{77K} \simeq (k_{PT})_{4.2K}$$

If the double proton transfer is a thermal process in which the two proton move over the energy barrier, then by assuming an Arrhenius behavior with a pre-exponential factor of $10^{12} - 10^{13}$ sec^{-1}, characteristic of unimolecular reactions, an energy barrier of the order 20 - 30 cm^{-1} for the reaction at 4.2°K is obtained.[80] Thus at this temperature thermal energy is not sufficient to allow appreciable transfer over the barrier. However, substantial F_2 is observed. Clearly these observations pointed strongly to quantum mechanical tunnelling. At higher temperature the proton transfer can take place by both tunnelling and thermal activation in which the two protons move over the energy barrier from high vibrational levels, populated according to a Boltzmann distribution, while at very low temperature tunnelling may be the only reaction pathway.

In order to obtain further support for the occurrence of proton tunnelling at low temperature, a sample of 7AI in which the hydrogen atom at the N^1 position was replaced by deuterium was used.[79] At 77°K where proton transfer over the barrier is presumably negligible, there is a large effect on the F_2/F_1 ratio. It was noted that deuterium substitution enhances F_1 at the expense of F_2 indicating that proton transfer is less efficient in the deuterated sample. The ratio of proton tunnelling rates for the deuterated and nondeuterated compounds was 2.9.

$$\frac{k_{PT}^h}{k_{PT}^d} = \left(\frac{F_2}{F_1}\right)^h \left(\frac{F_1}{F_2}\right)^d$$

Recently Bulska and Chodkouska[127] have studied the effect of temperature on the F_2/F_1 ratio by exciting the dimer specifically and they found that the ratio F_2/F_1 approaches zero at low temperatures where the phosphorescence was not yet observable. At low temperature the tautomeric fluorescence overlaps the isoelectronic monomeric phosphorescence. From these results they concluded that a tunnelling mechanism is not required to account for the observed experimental effects. The role of proton tunnelling in excited-state proton transfer is still an open question that requires further study.

The dynamics of double proton transfer in the excited state of the 7AI hydrogen-bonded dimer has been studied[80] in our lab by nanosecond time resolved spectroscopy, the rate constants for proton transfer in dueterated 7AI (N_1-D-7AI) at 77°K are

$$k_f^d = 1.9 \times 10^8 \text{ sec}^{-1}$$

$$k_b^d = 1.2 \times 10^7 \text{ sec}^{-1}$$

A picosecond study of the 7AI dimer by Eisenthal[128,129] shows dependence of the rate constant for excited state proton transfer upon wavelength which offers an explanation of the relatively slow risetime (4 ns) for the tautomer fluorescence observed in dueterated 7AI at 77°K.

7-Azaindole-Alcohol Complexes - The fluorescence spectra of 7AI in alcohols are composed of two bands completely analogous to those in hydrocarbon solvents.[124] Besides the normal fluorescence band of 7AI, F_1, another broad (excimer like) fluorescence, F_2, appears with a maximum at 450 nm (Figure 23). In the case of alcoholic solvents, the relative intensities of F_1 and F_2 depend only on temperature and not on concentration and excitation wavelength. The F_2 fluorescence in alcohols is not due to excimer formation since the F_2/F_1 intensity ratio is independent of concentration.

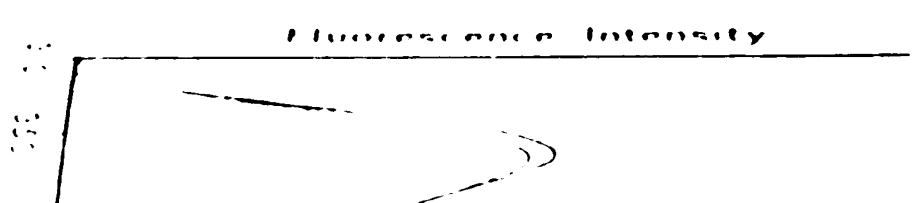
Fluorescence Intensity

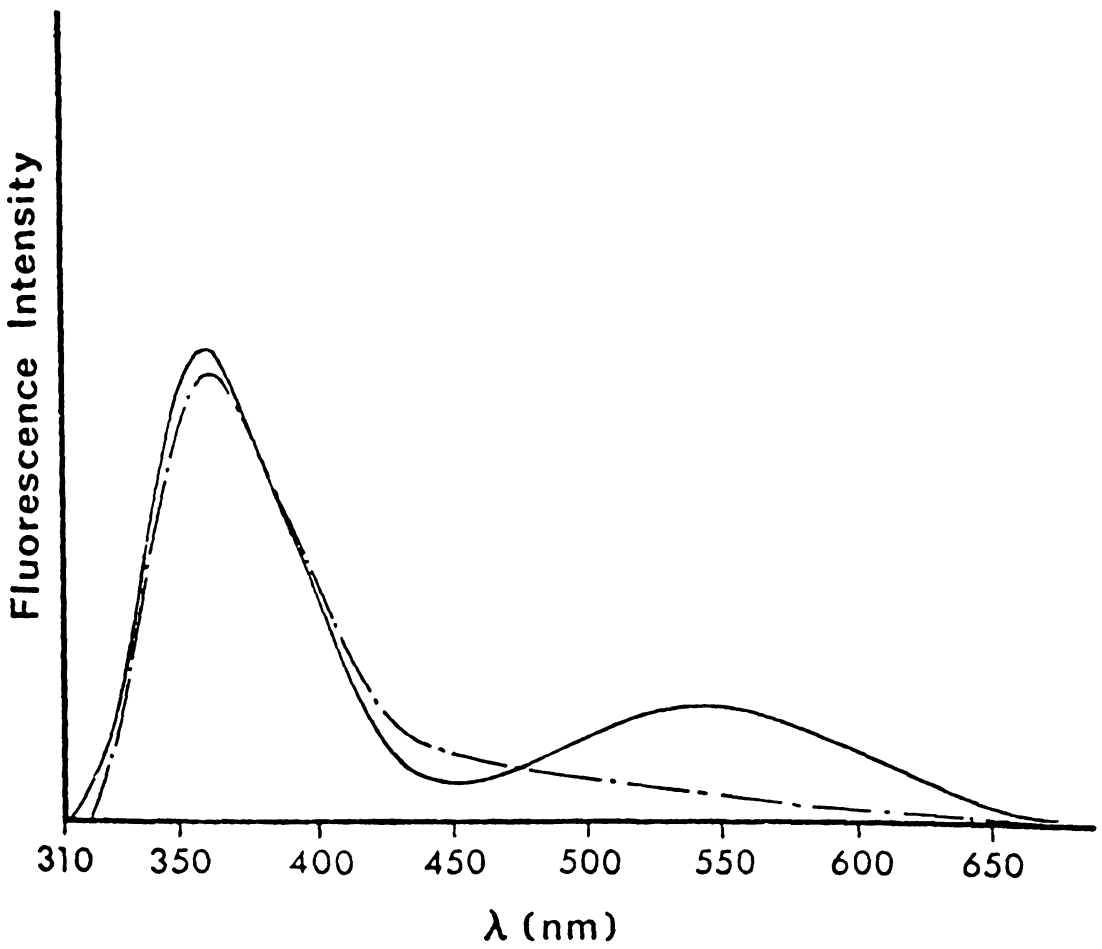

Figure 23. Corrected room temperature fluorescence spectra of 7AI in EtOH (——) and 7AI in EtOD (-·-·-).

Taylor et al. attributed the F_2 band to a tautomer resulting from a double proton transfer in the excited state between 7AI and an alcohol molecule in an analogous way to the tautomerization of H-bonded 7-azaindole dimers in hydrocarbon solvents. The tautomer is the same in both cases and only the mechanism of its production is different.

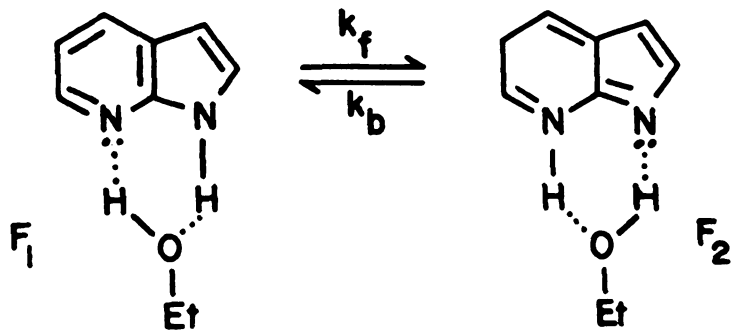

The effect of pH, temperature and solvent deuteration on the fluorescence spectra and quantum yields of 7AI and other model compounds in ethanol[130] gives some evidence supporting the above mechanism of excited state proton transfer between a 7AI molecule and an alcohol molecule.

One may visualize two kinds of complexes between 7AI and alcohol: a 1:2 complex (I) or a cyclic 1:1 complex (II).[131]

When small amounts of ethanol are added to a dilute (1.0×10^{-4} M) solution of 7AI in 3MP at room temperature,

O
H3C2

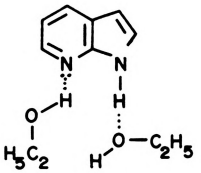

I

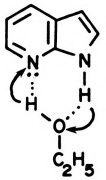

II

the absorption spectra are perturbed in the same way as during 7AI dimerization (red shifts). The absorption at 310 nm is due to primarily to the complex and can be used to determine the stoichiometry and the association constant of the complex. The results confirm the assumption of a 1:1 complex and an equilibrium constant of 49 M^{-1} is obtained. The association constant of the alcohol complex in 3MP is much smaller than the self-association constant of 7AI in 3MP which is 2.5 x 10^2 M^{-1} at 25°C. This has been attributed[79] to cooperative effects present in the self-dimer and is absent in the case of the 7AI-ethanol complex.

c. Kinetic Isotope Effects in Proton Transfer Reactions

Kinetic isotope effects are particularly common in the case of hydrogen isotope effects, partly because hydrogen is involved in so many reactions, and partly because such effects are much larger for hydrogen atoms than for the isotopes of heavier atoms. It is interesting to note that the rate differences between reactions of hydrogen and deuterium compounds are sometimes so large that the use of deuterium compounds has been proposed as a practical means for slowing down harmful reactions.

The starting point for most discussions of isotope effects is the implication of the Born-Oppenheimer approximation that nuclear substitution leads to no appreciable change in electronic energy. Of the other factors leading to energy differences between molecules it is a feature of primary hydrogen isotope effects that zero-point energy changes are usually much more important than differences in isotopic partition functions. The formalism of the kinetic isotope effect has been given by many workers.[132] Within the framework of transition-state theory, kinetic isotope effects may be expressed in terms of differences and ratios of isotopic zero point energies and partition functions between reactants and the transition state, i.e.,

$$k_H/k_D = MMI \cdot EXC \cdot TUN \cdot \exp\{(\Delta\varepsilon_R - \Delta\varepsilon^{\neq})/2KT\}$$

where MMI (masses and moments of inertia) and EXC (vibrational partition function) include reactant and transition-state partition functions, and $\Delta\varepsilon^{\neq}$ is the zero-point energy difference between transition states containing H and D. TUN is the 'correction' for quantum-mechanical tunnelling through the energy barrier to reaction. There are two qualitative manifestations of the importance of zero-point energy changes in the primary isotope effect. The first is the wide applicability of Swain's relationship[133] between deuterium and tritium isotope effects: $k_H/k_T = (k_H/k_T)^{1.442}$ (independent of the force constant change). The second factor is the common observation of an Arrhenius temperature-dependence,

$$k_H/k_D = (A_H/A_D)\ \exp[-(E_a^H - E_a^D)/KT]$$

with A_H/A_D close to unity.

These results should, of course, be put in perspective. Swain's relationship is not very sensitive to the presence of factors other than zero-point energy,[134-136] and deviations from linear Arrhenius dependences and values of $A_H/A_D < 1$ are found and normally are taken as indicating the presence of tunnelling.[137,138] Westheimer pointed out that for the two cases of $k_H = k_D$ and $k_H >> k_D$, the preexponential factor is near unity. The factor that determines the isotope effect is then just the difference

between the zero point energies.

The substitution of D for H is an elegant probe to use in the elucidation of chemical dynamics. In particular the solvent isotope effect is a powerful technique for investigating the role of the solvent. When H_2O is replaced by D_2O it is inevitable that we are dealing with the effects of substitution at many different sites. The effects of these substitutions can be described by fractionation factor theory[139] and, because many sites are involved, more information can be found if measurements are made in equimolar mixtures of H_2O and D_2O as well as in pure H_2O and in pure D_2O.[140] The two forms of water differ in structure[141-143] and differences exist as evident from differences in thermodynamic properties of the two liquids, in the heats of hydration and solubilities of salts in the two forms of water.[144,145] Swain and Bader[146,147] proposed a model which explains the solvent isotope effect in terms of zero point energies associated with hindered translations and hindered rotations (librations) of H_2O and D_2O (as well as the internal vibrations). The hindered translations are of very low frequency ($\sim$170 cm^{-1}) and are treated classically. The librational frequencies of H_2O and D_2O are different; for example, at 10°C $\bar{\nu}_{H_2O}$ = 710 cm^{-1} and $\bar{\nu}_{D_2O}$ = 530 cm^{-1}.

The conclusion is that solvent isotope effects can be calculated rather accurately by (1) determining the

internal vibrations of any molecules which have protons which would exchange with water and become deuterons in D_2O solution, (2) determining the librational frequencies of the water molecules solvating each molecule appearing in the reaction. As a crude generalization, it can be expected that ion-forming reactions will have a solvation isotope effect contribution to $k_{H_2O}/k_{D_2O} > 1$, corresponding to a net increase in structure breaking (net decrease in librational frequencies) on going from reactants to transition state, while effects <1 are expected for ion-destroying reactions, and effects close to unity are expected for reactions which do not produce or destroy ions. Solvation isotope effects will generally be small, probably no more than 20-30% except for small ions which can have a considerable effect on the water structure (librational frequencies).

Isotope Effects in Excited State Proton Transfer in 7-Azaindole Dimers - Let us consider the kinetic scheme of double proton transfer:

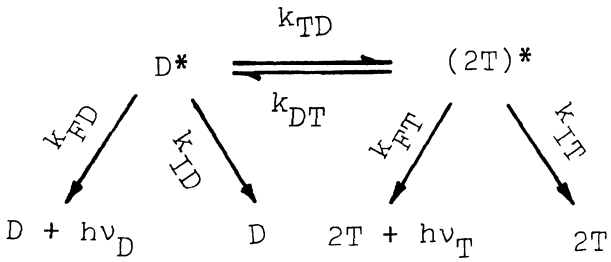

$$k_D = k_{FD} + k_{ID}$$

$$k_T = k_{FT} + k_{IT}$$

The kinetic description of the system under conditions of continuous illumination is as follows:

$$d[D^*]/dT = I_o - (k_D + k_{TD})[D^*] + k_{DT}[(2T)^*]$$

$$d[(2T)^*]/dT = k_{TD}[D^*] - (k_T + k_{DT})[(2T)^*] \quad (1)$$

Steady state conditions give $d[D^*]/dT = d[(2T)^*]/dT = 0$. By using the definition for quantum yields

$$\phi_{FD} = k_{FD}[D^*]/I_o \quad \text{and} \quad \phi_{FT} = k_{FT}[(2T)^*]/I_o \quad (2)$$

and since after correction for different instrumental sensitivity in the two different spectral regions

$$\phi_{FT}/\phi_{FD} = F_2/F_1 \quad (3)$$

we obtain from Equations 1, 2 and 3

$$F_2/F_1 = (k_{FT}[(2T)^*]/(k_{FD}[D^*]) = (k_{FT}k_{TD})/(k_{FD}(k_{DT}+k_T))$$

so

$$(F_2/F_1)_H/(F_2/F_1)_D = k^h_{TD}/k^d_{TD}\cdot(k^d_{DT}+k^d_T)/(k^h_{DT}+k^h_T) \quad (4)$$

since isotopic substitution is not expected to change the

radiative lifetimes. Further, since $k_T + k_{DT} \simeq k_T$ and since $k_T = k_{FT} + k_{nr}$, k_T^h is expected to be equal to k_T^d except in the improbable case of a very large and specific effect of one H/D atom on the non-radiative rates. Under these assumptions equation 4 can be simplified to

$$(F_2/F_1)_H/(F_2/F_1)_D = k_{TD}^h/k_{TD}^d \qquad (5)$$

The experimental isotope effect measured as in Equation 5, as the ratio of F_2/F_1 for protonated and deuterated 7-azaindole in 3MP matrix at 77°K is 2.9. So,

$$(k_{TD}^h/k_{TD}^d)_{77°K} = 2.9$$

Using the result for k_{TD}^d (8.6×10^7 s^{-1}) one can obtain $k_{TD}^h = 2.5 \times 10^8$ s^{-1}.(80) Further, as we discussed earlier, this kinetic isotope effect is connected to the zero-point energy difference (ZPE). So,

$$k_{TD}^h/k_{TD}^d = \exp(-ZPE/RT)$$

where

$$k_{TD}^h/k_{TD}^d = 2.9.$$

The ZPE thus obtained is around 60 cm^{-1}. If the

activation energy for double proton transfer is 500 cm^{-1} then the activation energy for the double deuteron transfer is around 560 cm^{-1}. This is in good agreement with the estimated activation energy of 500-600 cm^{-1} considering the double deuteron transfer at 77°K as a thermal process. It appears that a mechanism that involves motion of the deuterons over the potential barrier can explain the experimental data at 77°K because of the very small energy barrier.

d. Proton Tunnelling

One of the most unusual and interesting results of quantum mechanics is the prediction of tunnelling, i.e., the ability of a particle to exist in, or pass through, a region of space where its total energy is less than its potential energy. According to classical mechanics, such a phenomenon is impossible. As early as 1927[148] Hund discussed the probability of intramolecular rearrangements via tunnelling and Wigner[149] in 1932 discussed tunnelling with a view aimed at chemical kinetics. A tunnelling mechanism was proposed for the doubling of certain spectral bands of ammonia.[150] When proton transfer is very fast, such as in acid-base reactions in aqueous solutions, there exists the possibility that the proton in the incipient H-bonded complex A-A...B tunnels through the potential barrier between the two minima.

This possibility was pointed out by Bell in 1935. Since then, a great deal of indirect evidence has been accumulated which indicates the occurrence of proton tunnelling in ultrafast proton transfer.[151,152] Johnston[153] and Caldin[154] have provided reviews of various aspects of proton tunnelling in ordinary chemical reactions, and the significance of tunnelling to an understanding of the hydrogen-bond has been well described.[155-157] Löwdin[158] has discussed tunnelling as a possible mechanism of causing mutation and genetic error.

The JWKB method was used to obtain the transmission coefficient for an arbitrarily shaped potential. The JWKB solution has an oscillatory behavior in the "permitted" region and an exponential behavior in the forbidden region. In order to derive a formula for the transmission coefficient g (the probability of getting through the barrier) in general, we will consider a single incident wave hitting a barrier with two turning points (Figure 24). If the barrier is parabolic at its top (Figure 24), one can obtain for K_o,

$$K_o = (1/4\pi 2\pi/ha_o)(2m(V_2-E_o))^{1/2}$$

The factor $\pi/4$ comes here from the shape of the barrier.

If one measures the energy from the top as a fraction k of V_o, so that $E = V_2 - kV_o$ one obtains

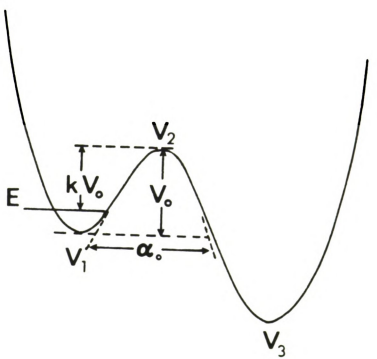

Figure 24. Model barrier for proton tunnelling calculation.

$$K = kK_o$$

and

$$g = \exp(-k\pi^2/ha_o)(2m(V_2-E_o))^{1/2}$$

Experimental Evidence in 7-Azaindole Dimers - By studying the effect of temperature on the fluorescence spectra of 7AI under conditions of continuous illumination a value of 500 cm^{-1} was obtained[79] as the potential energy barrier for double proton transfer. It was found, however, that the relative integrated intensities of the tautomer and dimer fluorescence are the same at 77°K and 4.2°K, i.e., $(k_{TD})_{77°K} \simeq (k_{TD})_{4.2°K}$ if one makes the reasonable assumption that the radiative and nonradiative (k_{ID}, k_{IT}) rates do not change from 77 to 4.2°K. If the double proton transfer is a thermal process where the two protons move over the energy barrier then by assuming an Arrhenius behavior with pre-exponential factors of $10^{12} - 10^{13}$ sec^{-1}, characteristic of unimolecular reactions we obtain energy barriers of the order of 20-30 cm^{-1} for the reaction at 4.2K. Clearly these observations point strongly to quantum mechanical tunnelling. At higher temperatures the proton transfer can take place by both thermally activated and tunnelling mechanisms, while at very low temperature tunnelling may be the only

reaction path. The effects of deuterium substitution of the pyrrolic hydrogen on the magnitude of F_2/F_1 ratio at 77°K are consistent with current theories of proton tunnelling. However, recent studies[127] of the effect of temperature on F_2/F_1 ratio appears to indicate that the proton-tunnelling mechanism is not necessary to account for the observed results. Further studies are required to examine the role of tunnelling in excited state proton transfer.

e. Excited State Proton Transfer in the Vapor Phase

Excited state proton transfer in the vapor phase was observed for the case of methyl salicylate[159] in 1924. At 110°C (17 mbar) two broad emissions of comparable intensity in the spectral range between 320 and 480 nm, similar to those in solutions of methylsalicylate have been observed.

The vapor-phase UV-absorption spectrum of methylsalicylate shows an absorption band with a maximum at 303 nm, probably an intramolecular charge transfer band,[81] and a structured absorption with a maximum at 234 nm (similar to the usual absorption of aromatic hydrocarbons).

Fluorescence spectra of MSA vapor in dry nitrogen at 50°C are shown in Figure 25 for two exciting light wavelengths: Methyl salicylate in the vapor phase clearly shows two different fluorescence bands whose relative

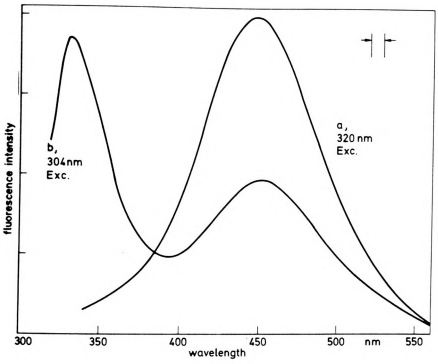

Figure 25. Vapor phase fluorescence spectra (uncorrected) of MSA at 50°C, equilibrium pressure under N_2, excitation wavelengths indicated. The experimental conditions are identical for both spectra.[160]

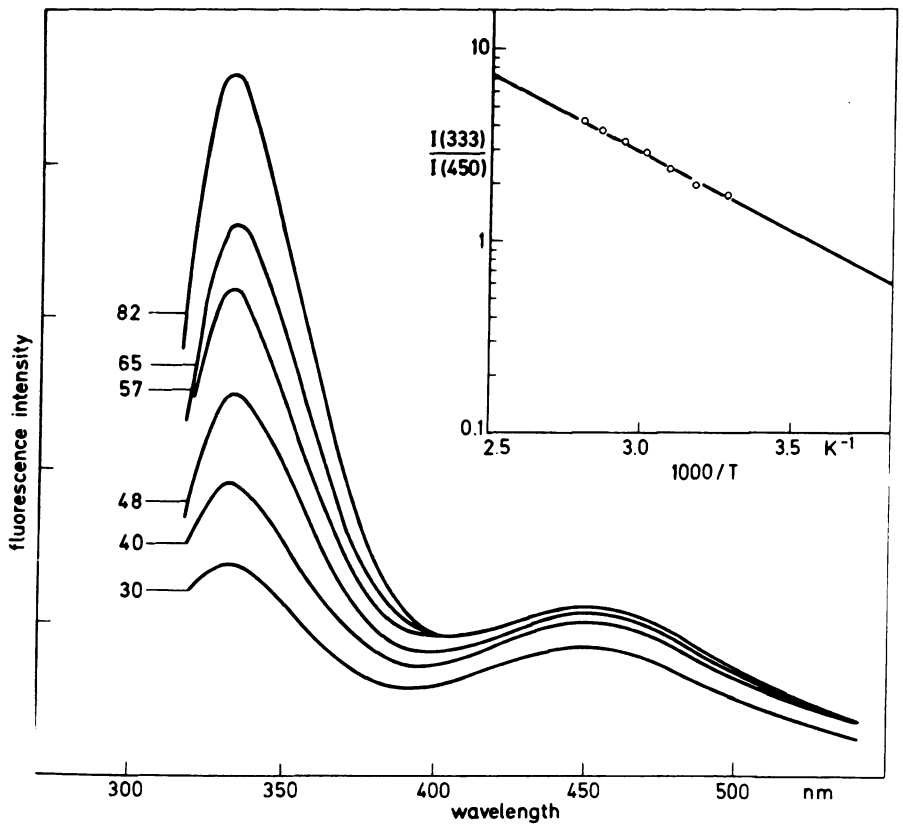

Figure 26. Vapor phase fluorescence of MSA, under N_2, as a function of temperature (indicated in ^{6}C). Insert: semilogarithmic plot of the intensity ratio of short-to-long wavelength emission vs. reciprocal temperature.[160]

intensity depends on the excitation wavelength and the temperature. These are a blue fluorescence (emission maximum 450 nm, excitation maximum 319 nm) and a UV fluorescence (emission maximum 335 nm, excitation maximum 303 nm).

The existence of distinctively different excitation maxima for the two emissions points to two ground state species as the origin of the two fluorescence bands rather than to an excited state equilibrium. The species responsible for the blue fluorescence corresponds to the form present in non-polar solvents, which is an intramolecularly H-bonded species (closed ring structure). The rate of excited state intramolecular proton transfer has been measured directly[98] for N-heterocycles containing intramolecular H-bonds, to be the order of $10^{10}s^{-1}$ and by a picosecond study for methyl salicylate in hydrocarbon solvent, to have a lower limit of $10^{11}s^{-1}$.[96] Proton transfer therefor effectively competes with other deactivation processes. The UV fluorescent species emit at shorter wavelengths than observed for the solvated form (355 nm), these species

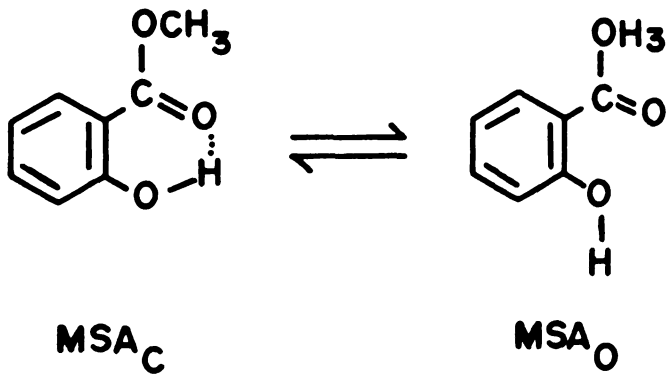

MSA_C MSA_O (1)

are most probably the open structure without a hydrogen bond. The equilibrium constant for this reaction occurring in the electronic ground state is given by:

$$K = [MSA_o]/[MSA_c]$$

Fluorescence obtained at different temperatures, using 290 nm excitation, are shown in Figure 26. Increasing the temperature strongly increases the short wavelength fluorescence intensity, whereas the blue fluorescence turned out to be nearly temperature independent. Lowering the temperature after heating again yields the spectrum characteristic of the lower temperature, only after an extended irradiation time do new peaks appear which can probably be attributed to irreversible photochemical reactions. The insert in Figure 26 shows that the intensity ratio of short-to-long wavelength fluorescence decreases exponentially with 1/T. The slope of the semilogarithmic plot in Figure 26 gives the enthalpy of the reaction (1). This quantity is found to be 3.59 Kcalmole^{-1} and corresponds to the energy needed for breaking the intramolecular hydrogen-bond. It is substantially smaller than the value estimated for the strength of the H-bond in MSA based on spectral shifts caused by C=O...H-O in stretching vibration bands of the C=O group (6.7 Kcalmole^{-1})[161] and in much better agreement with the results of a measurement

using ultrasonic relaxation in liquid MSA (2.5 Kcal mole^{-1}, K = 0.0365).[95] Since the entropy change, ΔS, of reaction (1) is most probably very small, we can estimate the equilibrium constant K to be 0.0025 at 25°C.

F. Excited State Proton Transfer in Acridine Derivatives - In 1946, a reversible color and fluorescence spectral change were detected in acridine at -180°C. The acridine was present as a minor constituent in a vacuum-sublimed crystalline organic acid such as oxalic, terphthalic, or succinic. The transition from the spectrum of the acridine cation to the spectrum of the neutral acridine molecule under illumination indicates clearly that a transfer of a proton occurred from the acridine cation back to the acid anion as a result of electronic excitation. The study[162] of the fluorescence and absorption spectra of acridine and its derivatives at different pH values in aqueous media showed that acridine has a higher affinity for the proton in the excited state than in the ground state. These results were in contrast to the observation[163] that the phototransfer of a proton occurs from an acridine cation to an acid anion. This may be attributed to the fact that the conditions were different; the acridine was contained in a crystalline acid at low temperature, and not in aqueous solution.

Further investigation on other compounds and media,

condensed together at low temperatures in a solid matrix gave similar results[164] (a film of acridine and an organic acid). Another study used "amphotoric" derivatives of acridine, which have acidic and basic groups in the same molecules,[164] one of these compounds is 9-(p-hydroxy)-phenylacridine, which forms chains by means of strong intermolecular H-bonds.[165] In aqueous media at low pH values the absorption maximum of the long wavelength absorption band undergoes a red shift into the visible region as in the case of acridine.[165] A similar effect was observed in the fluorescence spectrum of an ethanol solution of 9-(p-hydroxy)phenylacridine (Figure 28).

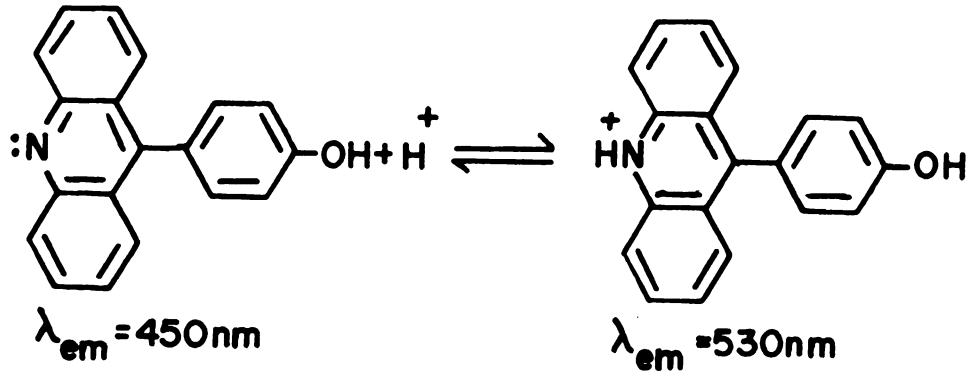

A film of 9-(p-hydroxy)phenylacridine, immediately after sublimation under vacuum at -180°C has a green luminescence with a maximum near 530 nm (Figure 28a), coinciding with the maximum observed for this compound in acid solution in Figure 27. This undoubtedly is due

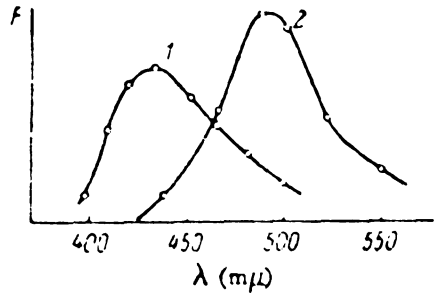

Figure 27. Fluorescence spectra of a solution of 9-(p-hydroxy) phenylaridine in ethanol at different pH values. Curve 1 - pH 8; curve 2 - pH 2.[164]

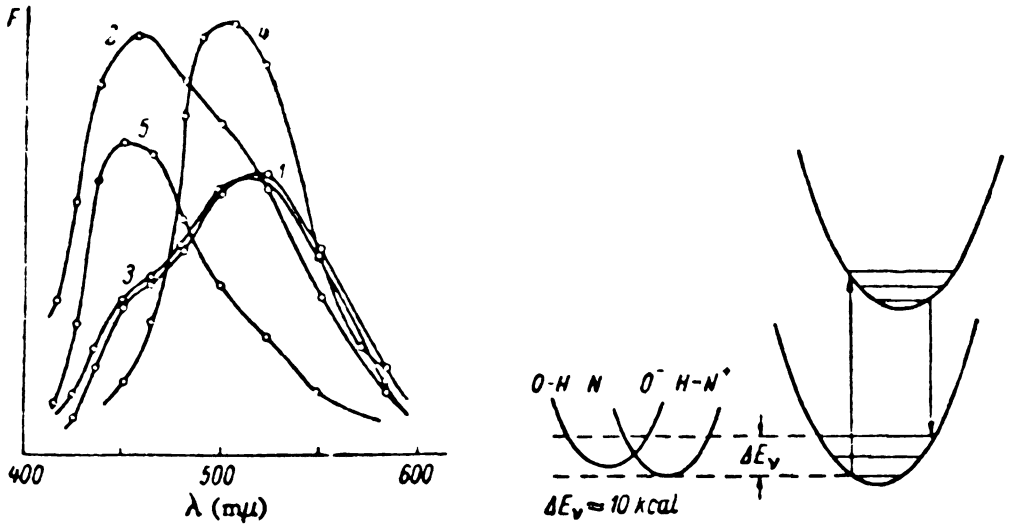

Figure 28 (a) Fluorescence spectra of a film of 9-(p-hydroxy) phenylacridine in vacuum at -180°C. Curve 1 - before exposure; curve 2 - after exposure for 10 min to the total radiation of an SVDSH-250 lamp; curve 3 - after regeneration at room temperature; curve 4 - acetic acid vapor; curve 5 - in pyradine vapor.

(b) Potential energy curve scheme for proton phototransfer in films at -180°C.[164]

to the combination of the proton of the phenol group with the nitrogen of the acridine ring (Structure 1):

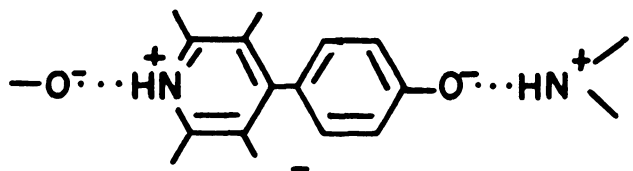

I

Upon irradiation at -180°C, the green luminescence is replaced by a blue luminescence in about 10 min, with a maximum near 450 nm. The latter luminescence is observed in 9-(p-hydroxy)phenylacridine in alcoholic solution, i.e., under conditions in which the phenol group is unionized (Figure 28). If the film is kept at room temperature for 2 to 5 hours, the green luminescence is restored, and this experiment can be repeated reversibly several times. Thus it appears that upon irradiation there is photo-transfer of a proton from the nitrogen atom (Structure II) to the negatively charged phenolic group.

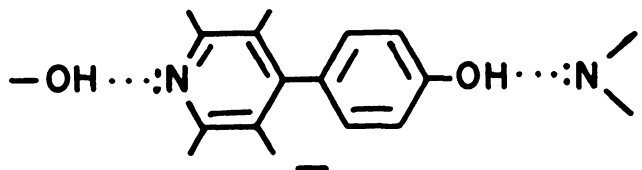

II

Therefore, it follows that in condense films, 9-(p-hydroxy)phenylacridine exists in the O^- (I) and not in the hydroxy form (II), as it does in neutral solvents.[165]

Here the proton transfer process uses the energy absorbed by the O^- form of the molecule of 9-(p-hydroxy)phenyl-acridine in the short wavelength absorption band. The return of the proton from the phenolic hydroxy group to the heterocyclic nitrogen is a thermal process. A similar phenomenon occurred in the two-component film (acridine + acid), in which the phototransfer of proton proceeded from an acridine cation to an acid anion.(163) Structure II, which has the higher energy, can be successfully stabilized at low temperatures.

The process described is apparently possible only in systems in which there is intimate contact between molecules and little probability of dissipation of the excitation energy into the thermal energy of the solvent. It was assumed that the transfer of a proton to the acid anion does not occur during the lifetime of the excited state of the fluorescing molecule, but after its transition to the ground electronic state at the expense of its high vibrational energy, which is acquired immediately after the emission of a light quantum. In fact, from the magnitude of the Stokes shift of the luminescence spectra of acridine, it follows that the emitting molecule in its ground state has initially a supply of vibrational energy approaching 11-12 Kcal $mole^{-1}$. The two minima in the potential energy of the proton near the ionized oxygen O^- of the phenol group on the one hand, and the nitrogen

atom of the acridine ring on the other (Figure are separated by an energy barrier of about 5 Kcal, as is characteristic of a strong hydrogen bond. In such a case, the vibrational energy liberated in the process of emitting a quantum of fluorescence should obviously be sufficient to overcome the indicated potential barrier. For the reverse process the potential barrier is lower, as follows from the rapid transfer of the proton to the nitrogen, even at room temperature. The same things occur in a 9-(p-hydroxy)phenylacridine, the ionized phenolic group of the neighboring molecule playing the role of the acid anion.

CHAPTER II

EXCITED STATE PROTON TRANSFER IN P-AMINO SALICYLIC ACID DERIVATIVES

A. Introduction

Excited state proton transfer reactions are among the most common adiabatic photoreactions; that is reactions in which the products are generated in an excited state. This fact allows the study of these phenomena by fluorescence spectroscopy.

This chapter deals with excited state proton transfer in hydrogen bonded systems both in solution and in the solid phase. The hydrogen bonded systems we have studied are p-amino salicylic acid (PAS) (I) and its N,N dimethyl derivative (DPAS) (II).

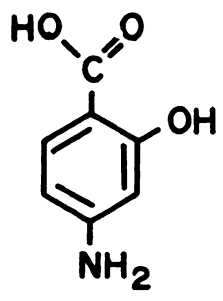

I

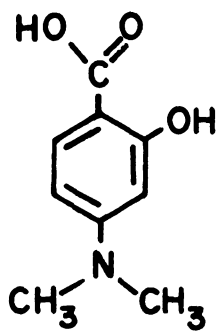

II

Absorption and luminescence properties of p-amino salicylic acid (PAS) derivatives were investigated under various conditions. The effect of medium, pH and substituents on the absorption spectra helped in the interpretation of the absorption bands which are dominated by "charge-transfer" transitions. In the "charge-transfer" states of these molecules the hydroxyl and amino groups may act as an electron-donors while the carboxyl group acts as an electron acceptor. The various species responsible for the absorption and emission at different pH values and the emission spectra in different solvents clearly reveal the occurrence of proton transfer in the excited state. Excited state proton transfer occurs either intramolecularly or intermolecularly depending on the medium. In order to get more information about proton transfer and to confirm the occurrence of proton transfer in PAS and DPAS we also synthesized the methyl ester of these compounds III, IV and we have studied their absorption and emission spectra under the same conditions.

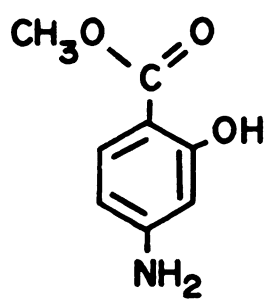

III

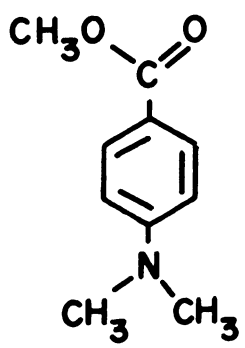

IV

The crystal structure of PAS[166] intra and intermolecular hydrogen bridges. We measured the fluorescence spectrum of PAS in the solid phase. Information from the solution spectra of PAS helped us to interpret the emission band in the solid phase of PAS in terms of an excited state intramolecular proton transfer. At the beginning of the chapter the spectrum of PAS is related to parent and related molecules, i.e., benzene, phenol and salicylic acid.

B. Excited State Proton Transfer in P-Amino Salicylic Acid (PAS) and its Methyl Ester (PASE)

Electronic absorption spectra of substituted benzenes are usually compared with the spectrum of benzene itself. This suggests that the differences in spectra of substituted benzenes reflect the perturbation effects of the various substituents. Such a picture is valid if orbitals are localized either on benzene or on the substituent and if no charge migration occurs between the substituent and benzene. However in order to interpret certain intense transitions which occur in the spectra of substituted benzenes but do not correspond to any benzene transition (B_{2u} (^1L_b), B_{1u} (^1L_a), E_{2u} (^1B), charge-transfer between the substituent and benzene orbitals must be considered. One may classify an excited electronic state

of a substituted molecule as either locally excited (LE) state or a charge-transfer (CT) state only as a zeroth-order description of the electronic state, since mixing between LE and CT states occur.

A locally excited state involves an excitation between different orbitals of the hydrocarbon, or between different orbitals of the substituent. Transitions involving LE states will appear in the substituted molecule at different energies than the corresponding transition of the unsubstituted hydrocarbon. Their intensities are also different due to the influence of the perturbing potential of the substituent.

A charge-transfer state involves the transfer of an electron between the hydrocarbon and the substituent. A CT transition gives rise to a CT band which is inherent to neither the hydrocarbon nor the substituent. Intense absorption bands have been observed frequently in complexes involving an electron-donating molecule and an electron-accepting molecule. A quantum-mechanical theory for these complexes has been developed by Mulliken[167]. (Excellent reviews of this subject have been given by McGlynn,[168] Briegleb,[169] Murrel[170] and Mulliken and Pearson[171]), which explains the observed band as an intermolecular CT transition. One would expect similar bands to be observed in the spectra of poly substituted benzene molecules, in which an electron-donor group and an

electron-acceptor group are parts of the same molecule. Transitions which result from CT interaction between these groups consequently are called intramolecular CT transitions.

Many examples of intramolecular CT transitions are known. For example, the long wavelength absorption band of p-nitro-aniline which is solvent sensitive, is characterized as an intramolecular CT transition involving charge migration from the amino- to the nitro-group (Figure 29). Arylboron compounds provide an interesting converse example where intramolecular CT transitions are expected to occur, thus the spectrum of tri-1-naphthylboron shows an intense absorption band at 3525 Å which was interpreted[172] as an intramolecular CT band in which the naphthyl group acts as the electron-donor and the boron atom as the electron-acceptor. Comparison of a given arylboron compound in methylcyclohexane as solvent before and after bubbling dry NH_3 gas through the solution shows that the band assigned as an intramolecular CT band disappears in the presence of ammonia. This was explained in terms of the formation of an additive compound with NH_3 in which the lowest vacant orbital of boron, involved in the intramolecular CT transition, is now filled with the nitrogen lone pair electrons (Figure 30).

The localized-orbital model is the most preferred model for the treatment of substituted benzene. One of the

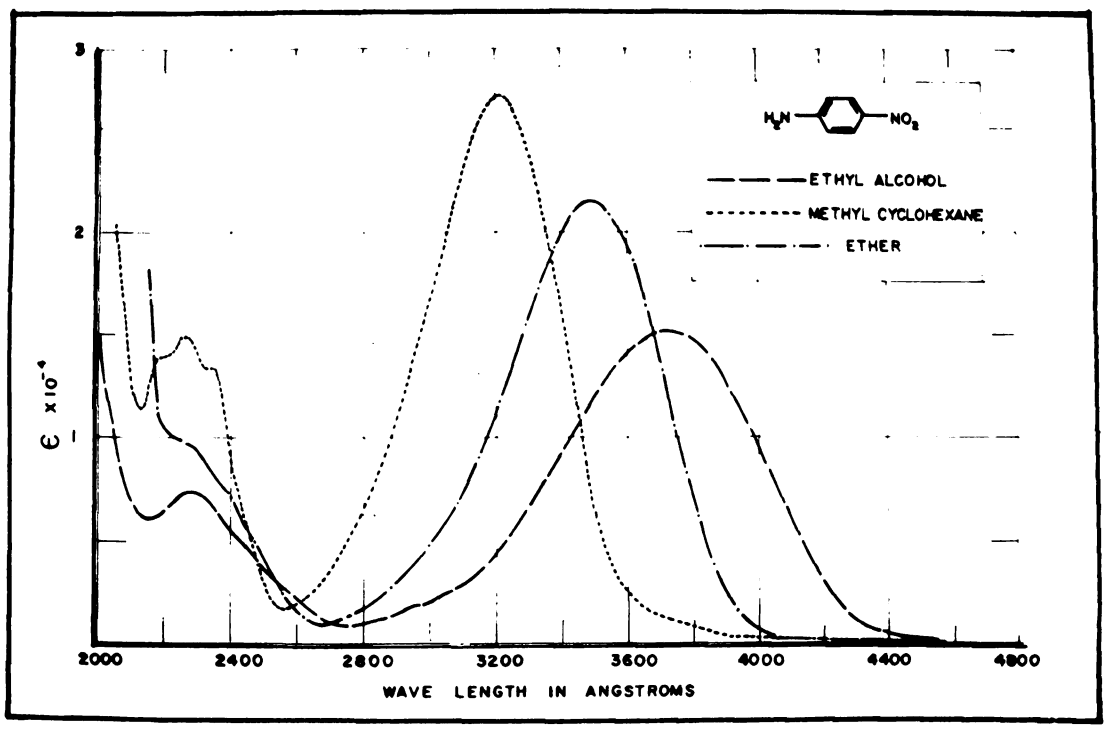

Figure 29. Room temperature absorption spectra of p-nitroaniline in different solvents: (...) methyl-cyclohexane, (-·-·-) ether, and (----) ethanol (concentration in alcohol = 6.52 x 10^{-5} gm moles lit^{-1}.).

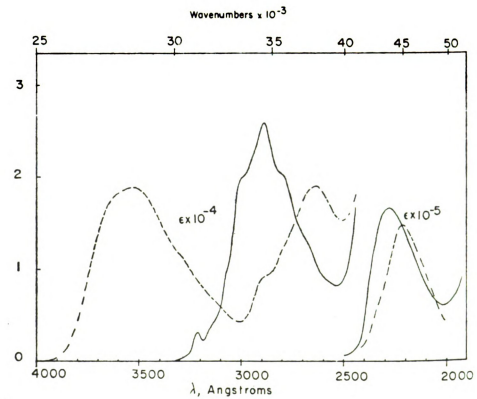

Figure 30. Room temperature absorption spectrum of tri-1-naphthylboron in methylcyclohexane (dashed line); and same after bubbling in dry ammonia gas (solid line).[172]

reason is that it allows a correlation between the absorption bands of various substituted benzenes. The CT state energies can be calculated by using the equation:

$$E_{CT} = I_D - E_A - C$$

where I_D is the ionization potential of the donor, E_A is the electron affinity of the acceptor and C is the Coulombic attraction energy between the electron and the hole.

In monosubstituted benzenes symmetric and antisymmetric CT states result, due to the degeneracy of the highest filled and lowest vacant benzene orbitals, their energies are different due to the difference in the electrostatic term. In disubstituted benzenes of the type D- 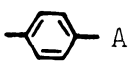 A, one can use two modifications.[173] The first is the use of the ionization potential of D- rather than that of benzene. The second arises from the realization that the degeneracy of the highest filled benzene orbitals is removed as a result of substitution. The highest filled MO of benzene is doubly degenerate, but this is not the case in phenol or aniline (Figure 31).

In para disubstituted benzene the transition to the symmetric state is allowed but it is forbidden for the antisymmetric state, due to the zero coefficient of the wave function on the carbon atom which is linked to the substituent. The CT band observed for the para isomer

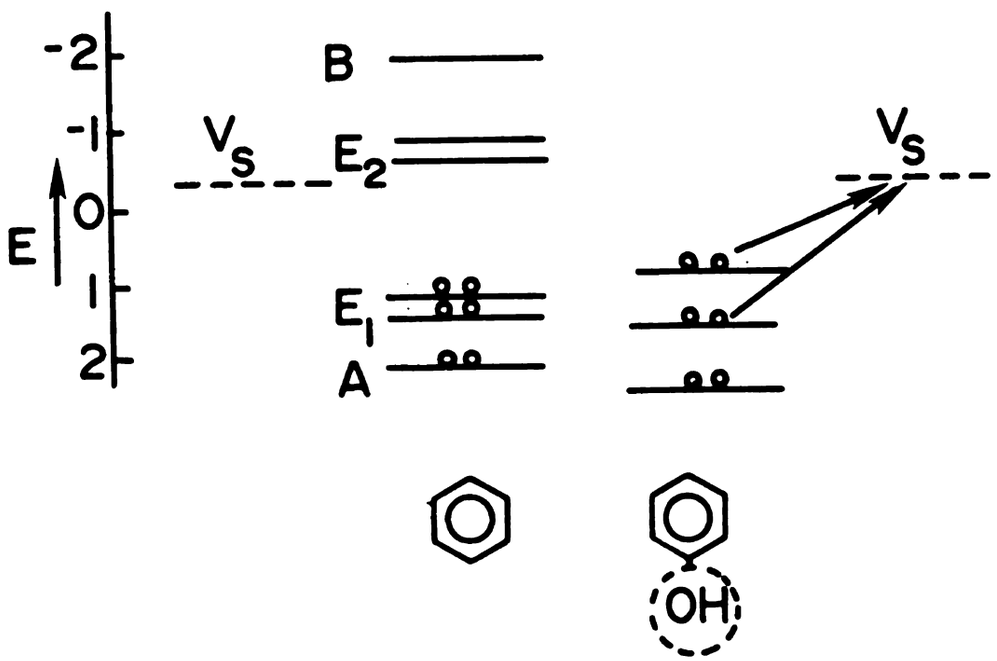

Figure 31. Qualitatively molecular orbital energy level for benzene, phenol and lowest vacant orbitals of substituent.

corresponds to the symmetric CT state and it borrows most of its intensity from $^1B_{1u}$ band. For meta and ortho di-substituted benzene both transitions are symmetry allowed.

Let us consider the absorption spectra of salicylic acid (SA) in different media (Figure 32). For SA in its neutral form there exist two CT bands, one at 302 nm and the other at 237 nm. These bands are due to a transition to a CT state in which the hydroxyl group acts as an electron donor and the carboxyl group acts as an electron acceptor. The n-π and B_{2u} bands of benzene are hidden under the intense CT band at 302 nm, but the higher energy CT band at 237 nm of the ortho and meta isomers borrows most of its intensity from the $^1B_{1u}$ LE band of benzene. The intensity of the $^1B_{1u}$ band is approximately 10 fold greater than that of the $^1B_{2u}$ band and therefore the band at 302 nm has greater CT character. When we remove a proton from the carboxyl group, the two CT bands are shifted to the blue because of the lower electron affinity of the carboxylate anion compared to that of the carboxyl group. The removal of the phenolic proton causes a red shift for both CT bands, because of the lower ionization potential of the phenolate anion with respect to that of the phenol group. The red shifts for the doubly-charged anion for the two CT bands are smaller than that of methylated salicylic acid. This reflects the electron repulsion of these two negative charges which forces the carboxyl group

Fluorescence Intensity x
2

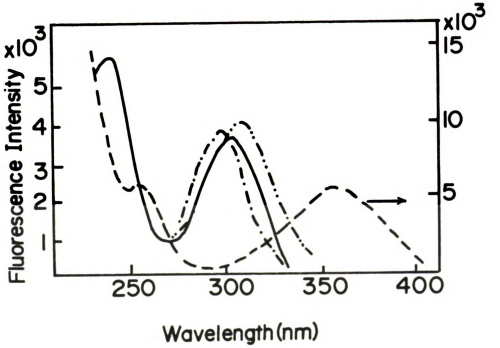

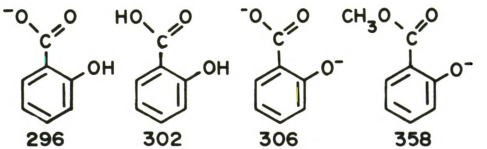

Figure 32. Room temperature absorption spectra of salicylic acid (SA) in different media: (——) N/10-HCl; (-.-.-) N/20-NaOH; (-.....-) 5-n NaOH; and methyl salicylate in (----) N/20-NaOH.

to be out of plane. The spectrum in this case is very similar to the spectrum of the phenolate anion.

1. Solvent Effect on the Absorption Spectra of PAS and PASE

Environmental factors affecting the absorption spectra can be conveniently divided into three types: intermolecular hydrogen-bonding between solute molecules only; intermolecular hydrogen-bonding between solute and solvent molecules; and environmental effects not involving the formation of hydrogen bonds such as dipole-dipole effects. All of our experiments were performed for very low concentrations of the compound in order to eliminate the possibility of intermolecular hydrogen bonding between solute molecules.

Absorption spectra of dilute solutions (5×10^{-5} M) of PAS has been taken in different media and are shown in Figure 33. The energies of the two near UV absorption bands in different media and their spectral shifts with respect to 3-methylpentane (3MP) are listed in Table 3. Depending on the solvent, an intramolecular hydrogen bond or intermolecular hydrogen bond can be formed. In 3MP, one expects that the predominant species will have intramolecular hydrogen bonds involving the hydroxyl and carboxyl groups. We have assigned the 275.5 nm absorption

Absorbance
08
07
06
05
04
03
02
01
200

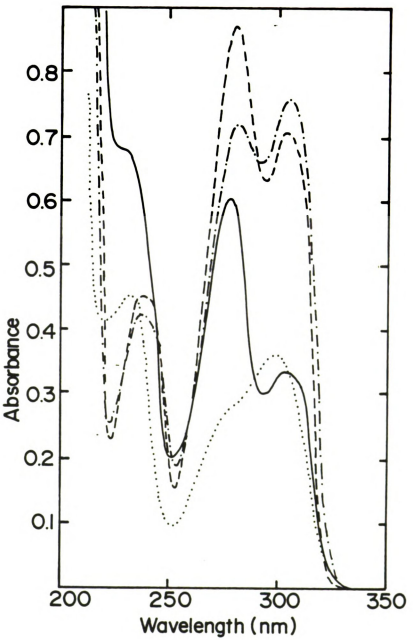

Figure 33. Room temperature absorption spectra of PAS in different solvents: (———) 3MP, (----) ether, (-·-·-) ethanol, and (....) H_2O (pH = 2).

Table 3. Room Temperature Absorption Maxima (nm) and Spectral Shifts (cm^{-1}) Relative to 3MP for PAS in Different Solvents.

Solvent	λ(nm) (N)CT	$\Delta\bar{\nu}(cm^{-1})$	λ(nm) (O)CT	$\Delta\bar{\nu}(cm^{-1})$
3MP	275.5	0	302	0
Ether	278	-327	302	0
EtOH	280	-584	303.5	-164
H_2O(PH=2)	279	-456	299	+332

- red shift + blue shift

band to a transition to a charge transfer state in which the amino group acts as an electron donor and the aromatic ring as an electron acceptor, (N)CT band. The 302 nm band is assigned as a charge transfer band involving the hydroxyl as an electron donor and the carboxyl group as an electron acceptor, (O)CT band. Of course, this is a zeroth-order description of the electronic states since mixing between locally-excited and charge transfer states occurs. If the transition involves mainly an electron transfer from the highest filled orbital of the donor group to the lowest vacant orbital of the acceptor, then one would expect that the band would disappear if the energy of the highest filled orbital of the donor group becomes much deeper in energy as a result of protonations.

Charge transfer transitions involving promotion of an electron from a π-orbital "lone pair"* which has π-symmetry and can therefore conjugate with the benzene molecule, virtually disappear as a result of protonation. The absorption spectrum of PAS at a low pH value (0.85) is consistent with our assignments since the 275.5 nm band attributed to a charge-transfer band involving the amino group, disappears when the amino group is protonated and the spectrum becomes nearly the same as that of salicylic acid (Figure 35). The fact that neutral salicylic acid exhibits an absorption band at ∿302 nm and that p-amino benzoic acid exhibits an absorption band at ∿270 nm supports our assignment.

In ether, where intermolecular hydrogen bonds involving the hydroxyl and amino groups are formed, the spectrum is very similar to that in 3MP where an intramolecular hydrogen band is formed. Dipole-dipole interactions contribute to the observed transition energies in ether.

In ethanol, in addition to the previously mentioned interactions, there are intermolecular hydrogen bonds

---

*The 2p π orbitals on the nitrogen atom of aniline and pyrrole are π-orbitals while the 2p orbitals on the aza-nitrogen of pyridine and on the oxygen atom of the carbonyl group are n-orbitals.

involving the proton of ethanol. The net result is that both absorption bands are shifted slightly to the red compared with those in ether.

In water, at pH 2, the spectrum shown in Figure 33 corresponds to the neutral form and is similar to that in alcohol. However, the relative intensities of the two absorption bands are reversed and the bands occur at slightly higher energies. Hydrogen bonding involving the protons of water with the amino group lone-pair is probably responsible for these effects. In water the intensity of the (N)CT band decreases due to H-bonding with the amino nitrogen lone-pair which if carried to the extreme situation, would be the addition of H^+ which would eliminate the amino CT band. In water we expect a larger red shift, but the hydrogen bond between the amino group lone-pair and the alcohol proton is weakened as a result of CT excitation and will cause a blue shift which is superimposed on the red shift due to dipole-dipole interactions. This effect is more pronounced in water than in alcohol because of the higher acidity of water. Hydrogen bonds formed between the amino group hydrogen atoms and the solvent molecules become more stable in the CT state and lead to a red shift.

The absorption spectra of PASE (5×10^{-5} M) have been measured in different media and the results are shown in Figure 34. Absorption maxima and spectral shifts are

08
07
06
05
04
03
02
01
20
Absorbance

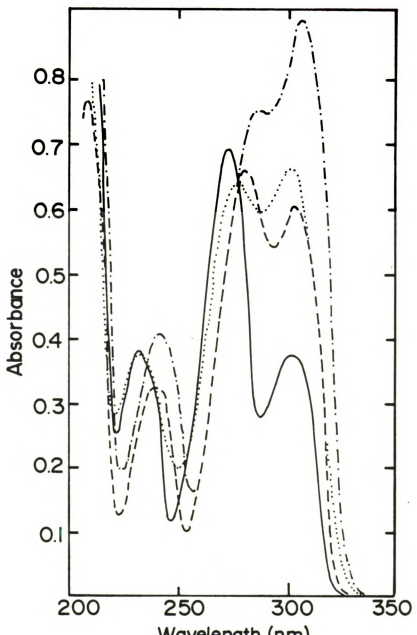

Figure 34. Room temperature absorption spectra of PASE in different solvents: (——) 3MP, (----) ether; (-·-·-) ethanol; and (-···-··) H_2O.

summarized in Table 4. The results are very similar to that of PAS.

Table 4. Room Temperature Absorption Maxima (nm) and Spectral Shifts (cm^{-1}) Relative to 3MP for PASE in Different Solvents.

Solvent	λ(nm) (N)CT	$\Delta\bar{\nu}(cm^{-1})$	λ(nm) (O)CT	$\Delta\bar{\nu}(cm^{-1})$
3MP	273	0	302	0
Ether	281	-1043	303	-110
EtOH	285	-1542	306	-433
H_2O	276	-398	301	+110

2. pH Effect on the Absorption Spectra of PAS and PASE

We have studied the effect of pH on the absorption spectra of PAS and its ester (PASE) in order to determine the absorption characteristics of different species which may exist in the ground state. The results are summarized in Tables 5 and 6 and in Figures 35 and 36. For PAS at pH 0.85, the cation exhibits only one charge transfer band involving the hydroxyl group as an electron donor since the amino group is protonated at this pH value.

Table 5. Room Temperature Absorption and Emission Maxima for PAS at Different pH Values, Ground and Excited States Species.

pH	Absorption Maxima (nm)		Ground State Species	Excited State Species	Emission Maxima (nm)
0.85	---	299	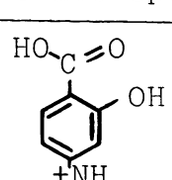	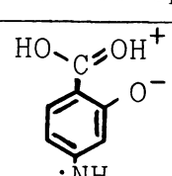	~440
2.00	279	299	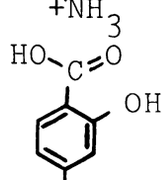	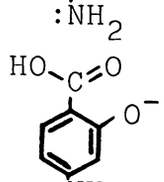	414
5.60	264	298	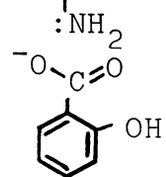	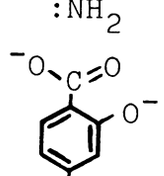	~400
13.10	262	300	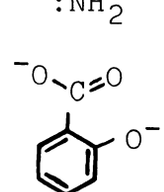	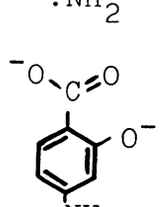	400

Table 6. Room Temperature Absorption and Emission Maxima for PASE at Different pH Values, Ground and Excited States Species.

pH	Absorption Maxima (nm)		Ground State Species	Excited State Species		Emission Maxima (nm)
1.3	---	298	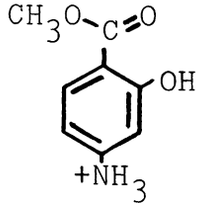	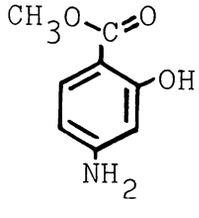	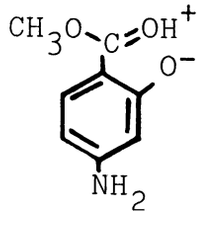	365 451
5.9	276	301	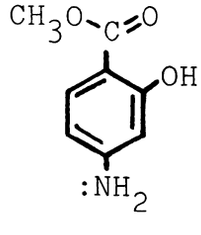	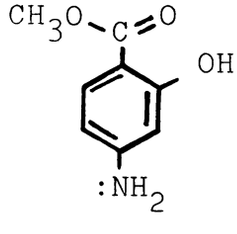	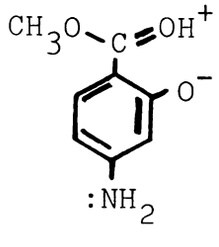	365 450
11.0	272	320	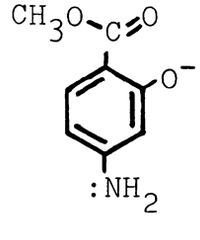	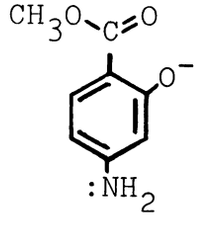		409

08
07
06
05
04
03
02
01
Absorbance
200

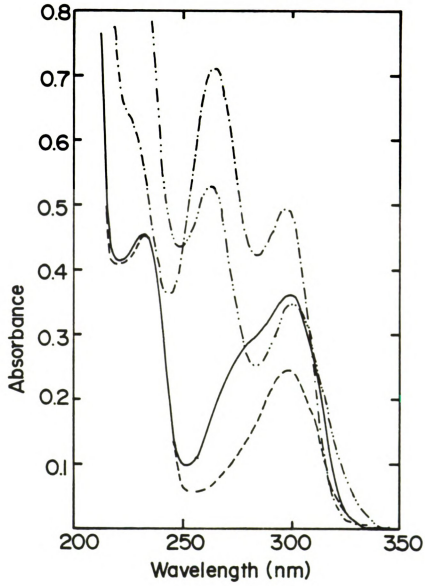

Figure 35. Room temperature absorption spectra of PAS at different pH values: (----) 0.85, (———) 2.0, (-·-·-) H_2O (2.9-12.1); and (-··-··-) 13.1.

07
06
05
04
03
02
01
00
Absorbance
200

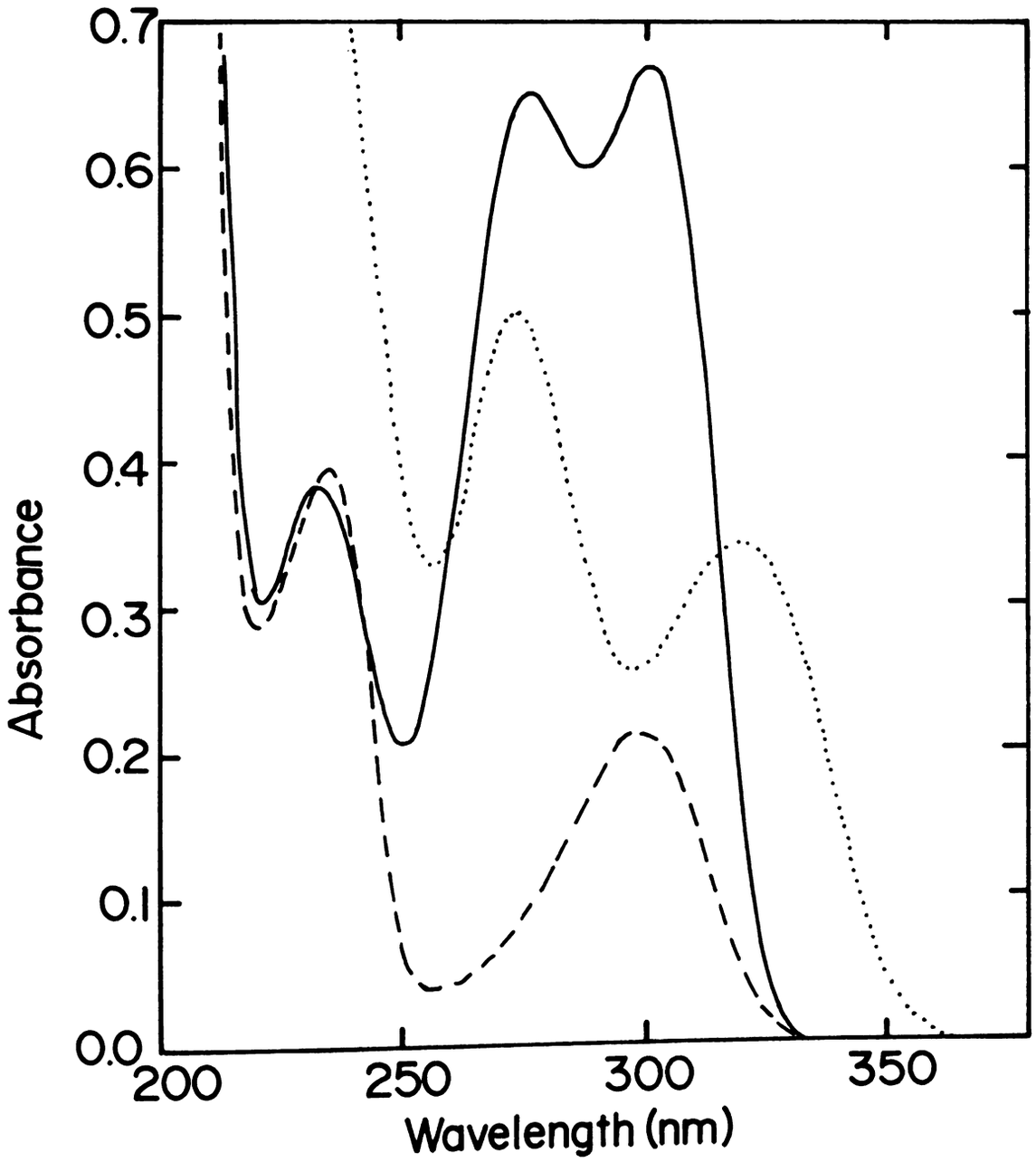

Figure 36. Room temperature absorption spectra of PASE at different pH values: (----) 1.3; (——) H_2O (2.3-10.3); and (....) 11.0.

At pH 2, the PAS exists in the neutral form, and two absorption bands comparable in intensity are observed. At pH range 2.9-12.1, PAS exists as an anion, the (N)CT absorption band occurs at higher energy (264 nm) compared with its value for the neutral form. This is due to the lower electron affinity of the carboxylate anion compared with the carboxyl group. The intensity of the band is increased relative to that of neutral PAS, probably due to more charge migration from the amino group to the carboxyl group and to the planar structure. At pH 13.1, the doubly-charged anion spectrum shows a decreased intensity of both bands, probably reflecting a partially twisted carboxylate group due to electron repulsion involving the O^- group.

For PASE, the results are very similar to those for PAS. An exception is that in the case of the PASE species, no carboxylate anions or doubly-charged anions are formed, instead the phenolate anion is formed at higher pH values. The absorption spectrum of the phenolate anion lies at longer wavelengths than that of the doubly-charged anion of PAS, supporting the notion that repulsion in the doubly-charged anion of PAS forces the carboxyl group out of plane.

3. Emission Spectra of PAS and PASE as a Function of pH at Room Temperature

The room temperature emission spectra of PAS and its ester (PASE) at selected pH values are shown in Figures 37 and 38. The excitation wavelengths are 286 and 280 nm for PAS and PASE, respectively, which correspond to the first absorption bands. The ground and excited state species at a given pH value are shown in Tables 5 and 6.

In water at pH 2, where PAS exists predominantly in its neutral form in the ground state, the emission band occurs at 414 nm. This band is due to intermolecular proton transfer from the hydroxyl group to the solvent molecules, producing the phenolate anion as shown in Table 5. The emission of PASE in ethanol in the presence of sodium hydroxide shows a band at ∿414 nm which provides further support to this conclusion. At a pH value of 5.6 where the dominant species in the ground state is the carboxylate anion, the emission maximum occurs at 400 nm. Under such conditions the spectrum is identical to the emission observed at pH 13.1 where the dominant species in the ground state is the doubly-charged anion. This indicates that the species produced in the excited state under these conditions is the doubly-charged anion. Further confirmation of this conclusion comes from the observation that the emission spectrum of PAS in ethanol in the presence of sodium hydroxide and that of PAS in

Intensity
350

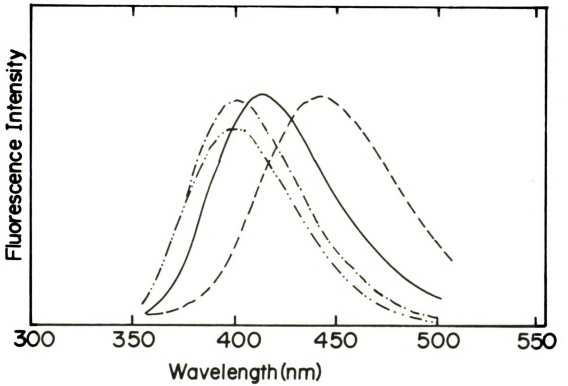

Figure 37. Room temperature fluorescence spectra of PAS at different pH values: (----) 0.85, (———) 2.0, (-·-·-) H_2O, and (-··-··-) 13.1.

350

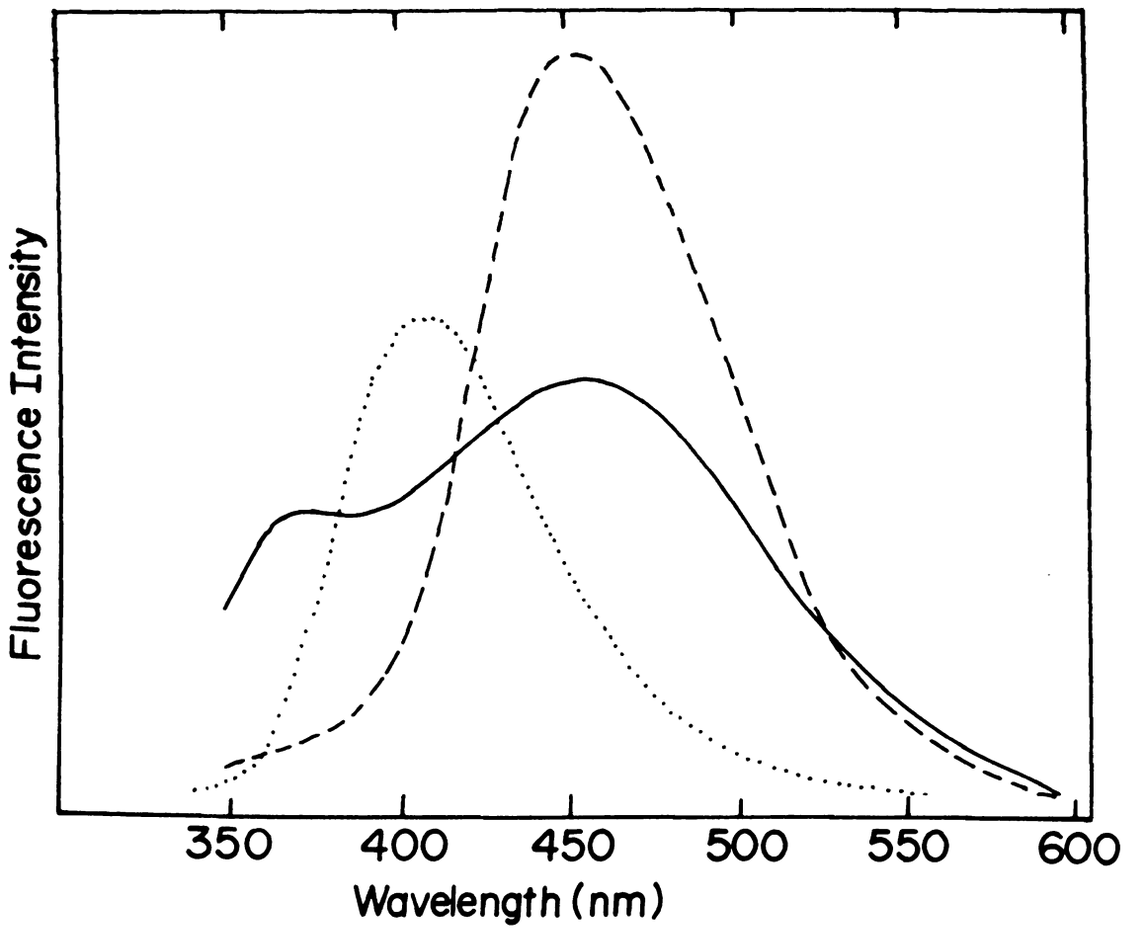

Figure 38. Room temperature fluorescence spectra of PASE at different pH values: (----) 1.3, (——) H_2O, and (....) 11.0.

3MP in the presence of pipyridine are both nearly the same as that observed in water at pH 5.6.

The emission of the phenolate anion occurs at longer wavelengths than that of the doubly-charged anion, probably due to a smaller electron affinity of the carboxylate anion and the non-planar configuration of the doubly-charged species. At pH 0.85, where the amino group is protonated in the ground state, emission occurs at 440 nm which is due to the zwitterion formed upon the excitation of PAS at this pH value. This emission occurs at longer wavelength compared to the singly-charged anion emission. The dissociation of the hydroxyl group and the protonation of the carboxyl group both stabilize the excited state. PAS in 3MP where an intramolecular hydrogen bond is formed in the ground state gives a similar emission band at 450 nm. Here an intermolecular double proton transfer involving the solvent molecules occurs in the excited state. At this pH value the amino group loses the proton in the excited CT state because of more charge migration to the carboxyl group.

For PASE at pH 1.3 two emission bands are observed, one at ∿365 nm which appears as a shoulder and one at ∿450 nm. The 365 nm band emission is assigned to the neutral form of PASE, but the long wavelength emission band (∿450 nm) is assigned to the zwitterion formed during the lifetime of the PASE excited state. The emission of

the zwitterion of PASE is red shifted compared to that of PAS, the same is true for methyl salicylate (MSA) and salicylic acid (SA). In the case of PAS at low pH values we have observed only one emission band at ∿440 nm. The results for PAS and PASE at low pH are very similar to the results of SA and its ester (MSA) at low pH values.

The phototautomerization of methyl salicylate in aqueous solutions shows[85] an acidity dependence which indicates that phototautomerism in aqueous solutions is biprotonic involving diffusion-limited protonation of the carboxyl group in the excited state, followed by dissociation of the hydroxyl group by the solvent, the former step is slow and incomplete in dilute acid resulting in some of the excited MSA fluorescing from the neutral molecular form. The biprotonic process in methyl salicylate is complete during the lifetime of the excited state in moderately concentrated acid solutions.[85]

In the case of PASE, the observation of short wavelength emission could be interpreted as in MSA.

Excitation of PASE in 3MP is very similar to that of PAS giving rise to a 450 nm emission band of the zwitterion which results from an intramolecular proton transfer during the lifetime of its excited state.

When the neutral form of PASE is excited, two emission bands are observed. One corresponds to the excited neutral form (∿365 nm) and the other corresponds to the zwitterion

(∿450 nm). In the case of PAS, excitation of the neutral form gives rise to one band at 414 nm corresponding to emission from the phenolate anion. In the PASE case, the carboxyl oxygen is more basic and tends to be protonated in the excited state. Therefore intermolecular proton transfer occurs in the excited state giving rise to a zwitterion emission band. At high pH values PASE exists mainly in the phenolate anion form in the ground state and exhibits an emission maximum at ∿410 nm.

4. Fluorescence Spectra of PAS and PASE in Different Solvents at Room Temperature

The room temperature fluorescence spectra of PAS and PASE in different solvents are shown in Figures 39 and 40 and the emission band maxima in different solvents are summarized in Tables 7 and 8.

In 3MP where there is an intramolecular hydrogen bond involving the hydroxyl and the carboxyl groups of PAS, we have observed two emission bands, one at ∿340 nm and the other with a large Stoke shift (10890 cm^{-1}) at ∿450 nm. The short wavelength band at ∿340 nm corresponds to the normal fluorescence of the molecule from its lowest singlet excited state. But the long wavelength emission band at 450 nm is due to intramolecular proton transfer from the hydroxyl group to the carboxyl group which occurs during the lifetime of the excited state giving rise to the

Fluorescence Intensity
250
30

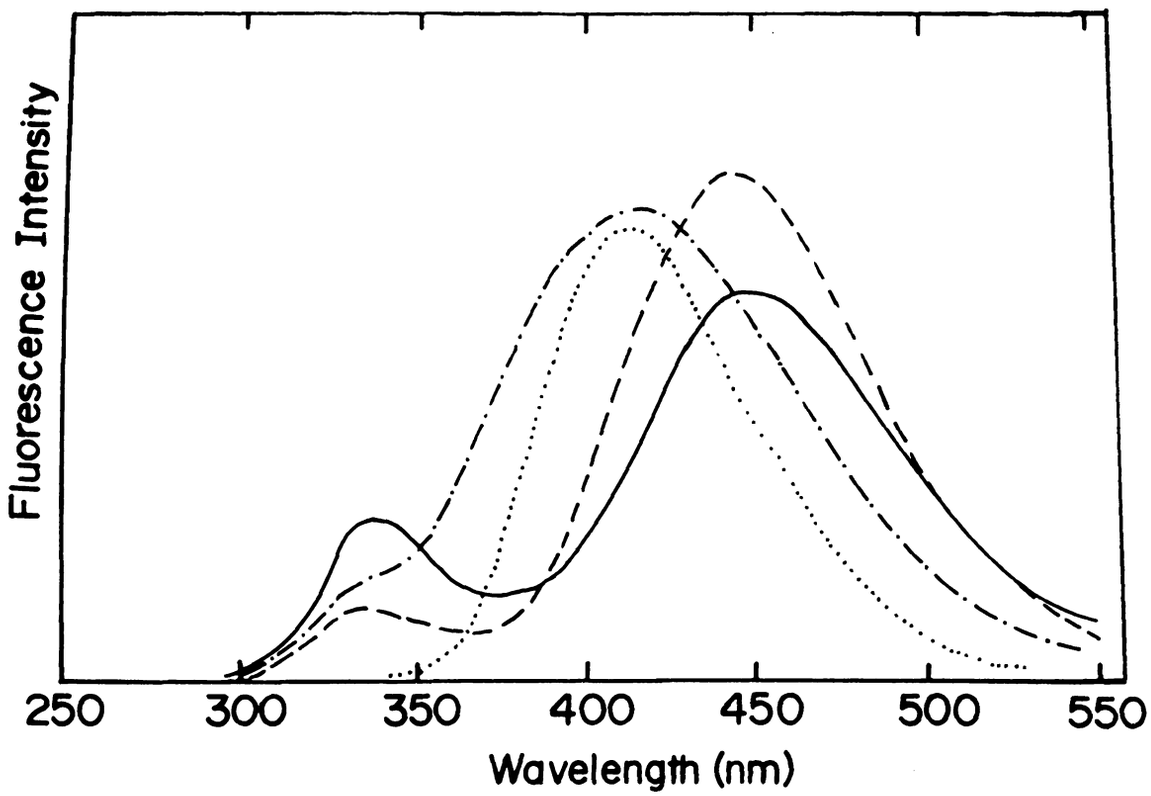

Figure 39. Room temperature fluorescence spectra of PAS in different media: (——) 3MP; (----) ether; (-·-·-) ethanol; and (....) H_2O (pH = 2).

Fluorescence Intensity
250
30

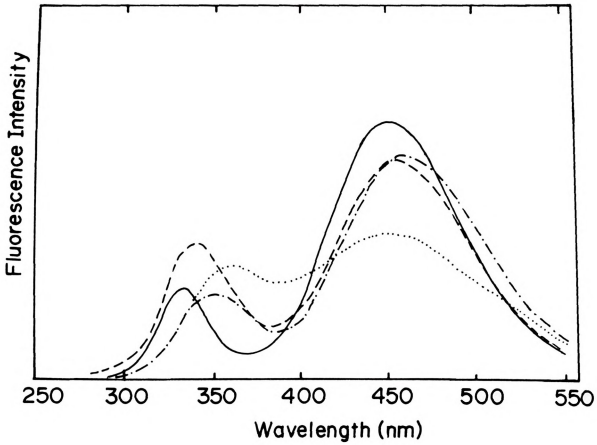

Figure 40. Room temperature fluorescence spectra of PASE in different media: (——) 3MP; (----) ether; (-·-·-) ethanol; and (....) H_2O.

Table 7. Emission Maxima in nm for PAS in Different Solvents.

Solvent	Emissions Maxima in nm		
3MP	340		450
Ether	338		448
EtOH	340	416	---
H_2O (pH=2)	---	414	---

Table 8. Emission Maxima in nm for PASE in Different Solvents.

Solvent	Emissions Maxima in nm	
3MP	334	450
Ether	342	452
EtOH	350	458
H_2O	365	450

HO

formation of a zwitterion.

The observation of these two bands is probably due to an excited state equilibrium between the neutral form and zwitterion according to:

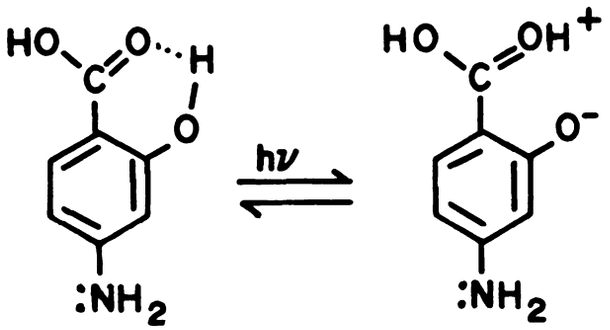

(I)

Alternatively, they may have originated from a ground state equilibrium between different conformers followed by a rapid intramolecular proton transfer in the excited state. It seems that the latter process is more probable than the first. This is because picosecond time resolved spectroscopy for MSA showed[96] that the rate of intramolecular proton transfer is greater than 10^{11} s^{-1} even at 4°K, whereas the interconversion between cis and trans conformers is slow. The rate constants found[94] in neat MSA between cis and trans forms, at 25°C were k_f = 9.5×10^5 and k_b = 2.6×10^7 s^{-1}. If excited MSA in cyclohexane solution has a similar value of k_b, the formation of the cis form, a prerequisite for the intramolecular proton transfer, cannot efficiently take place during the

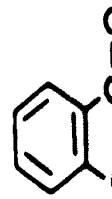

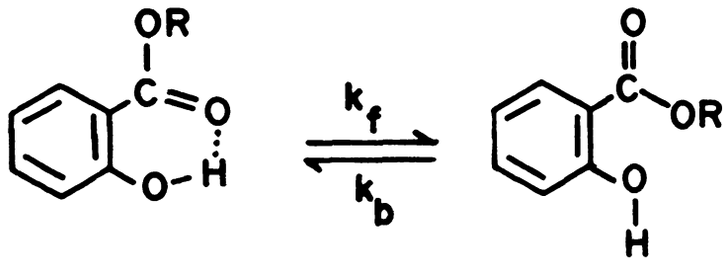

(II)

lifetime of the excited state trans form. In air saturated solutions this lifetime is probably less than 10^{-8} s. It might well be that the proton transfer in excited cis form molecules is very efficient, i.e., that equilibrium (I) (which is similar to that of MSA) is almost totally displaced to the right. The temperature effect on equilibrium (II) should then be the main cause of the fluorescence temperature dependence in methylcyclohexane solution found by Weller. The lifetime measurement of MSA showed[96] that the neutral excited species has a fluorescence lifetime three times larger than the excited zwitterion at room temperature. Rapid formation of 450 nm emission and the very different lifetime of the fluorescence components would also indicate that the two species are formed immediately after absorption of a photon. Perhaps they originate from different ground state molecules. In the case of MSA this is suggested by the observation of differences in the excitation spectrum of the two emissions in methylcyclohexane. One would expect in hydrocarbon solvents where there is an intramolecular hydrogen

bond (cis conformer) and not an intermolecular hydrogen bond between solute and solvent molecules, to get emission at longer wavelengths due to the zwitterion, whereas for both MSA and PAS we see the short wavelength emission also. The interpretation is as follows: Fluorescence quenching measurements[90] on the short wavelength emission band of MSA indicated that the short wavelength emission may contain contributions from two "slowly" interconverting ground state conformers that are not equally quenched and which upon excitation, give rise to an emission in the short wavelength band. The suggested conformers were ones in which the phenolic proton is H-bonded to the "ether" oxygen atom of the ester group (41a), and a nonintramolecularly H-bonded, or "open-ring", trans conformer (41b). The latter is stabilized in hydroxylic solvents by solute-solvent H-bonding. Excited-state prototropism depends in part on an increase in the basicity upon excitation, of the carbonyl oxygen, no such change in basicity is expected for the ether oxygen. Preliminary fluorescence decay measurements using single-photon counting appears to verify the results of the quenching experiments in MSA.[108] In a third conformer (41c), cis form, in which the phenolic proton is H-bonded to the carbonyl oxygen, intramolecular proton transfer occurs upon excitation, giving rise to a zwitterion which emits at 450 nm.

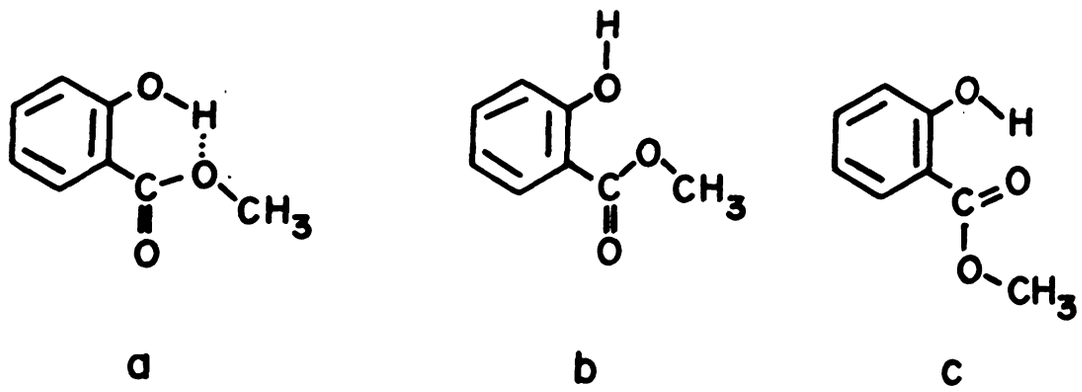

Figure 41. Ground-state conformers of methyl salicylate: (a) "ether bonded", (b) "open-ring" (trans), and (c) "closed ring" (cis).

The observation of a nonexponential fluorescence decay and two fluorescence lifetimes (τ_1 = 23.3±0.2 ns, and τ_2 = 5.1±0.9 ns) for the normally Stoke shifted emission of methyl 3-hydroxy-2-naphthoate[12] in cyclohexane also was interpreted in terms of more than one excited state (originating from excitation of distinct ground state conformers) emitting within the two fluorescence band. Therefore, the observation of the short wavelength emission in MSA and PAS could be mainly due to the existence of the stable ether bonded conformer in the ground state.

In ether the results are very similar to those in 3MP. There are two emission bands, one at ∿338 nm corresponding to the neutral form of PAS and the other at ∿446 nm, corresponding to the zwitterion. In ether, intramolecular hydrogen bonds are formed in PAS.

In ethanol there are mainly intermolecular hydrogen

bonds between the hydroxyl group and solvent molecules in the ground state. Here we observed two emission bands, one at ∿416 nm and the other at ∿344 nm. The short wavelength emission band at ∿344 nm arises from the neutral form of PAS after excitation. The long wavelength emission band can be attributed to a species produced by an intermolecular proton transfer from the hydroxyl group to the solvent ethanol molecule producing a singly-charged anion (phenolate anion). In order to prove this assignment we produced this species in the ground state by using sodium hydroxide and found that the emission occurs at the same wavelength. Therefore, in ethanol, the phenolate anion is created after excitation of a neutral molecule ground state rather than by direct excitation of a ground state phenolate anion.

In water at pH 2, where PAS exists in its neutral form in the ground state, there is only one emission band at ∿414 nm, which again corresponds to a species produced via an intermolecular proton transfer between the hydroxyl group and solvent molecules. The shift in emission is due to a solvent effect. In ethanol and in water the ground state equilibria between different conformers play an important role in determining the emission properties.

In the case of PASE in all four solvents two emissions are observed. One occurred at shorter wavelengths and corresponds to emission from the excited neutral form. The wavelength of this emission is solvent dependent as with

H_2N-

MSA.[94] The long wavelength emission occurs at nearly the same wavelength (∿452 nm) and corresponds to a zwitterion emission. The zwitterion results from intramolecular proton transfer in the case of 3MP and ether and from intermolecular proton transfer in the case of ethanol and water. Again, one could consider the ground state equilibrium between conformers to be the origin of the two emission bands in different solvents. Depending on the solvent and which conformer is more stable in the solvent we have inter- or intramolecular proton transfer.

C. Excited State Proton Transfer in the Solid Phase of P-Amino Salicylic Acid (PAS)

The crystal structure of PAS has been investigated[166] by x-ray diffraction. The packing of the molecules in the unit cell, the intermolecular distances, the bond distances and the positions of the hydrogen atoms were all consistent with the following scheme for the hydrogen bond system in PAS.

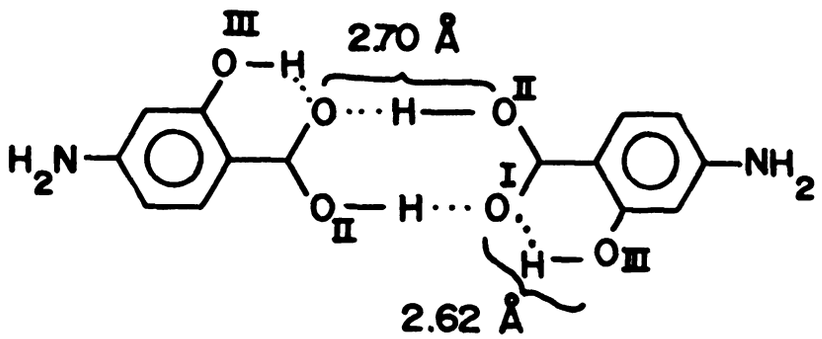

The different band distances found for $C\text{-}O_1$ and $C\text{-}O_{II}^{H}$ and the positions of the hydrogens show clearly that these groups are not equivalent. O_1 forms two hydrogen bonds, an intramolecular one with the phenolic OH and an intermolecular one with the carboxylic OH of a second molecule related by a center of symmetry. The intramolecular H-bonds are stronger than the intermolecular H-bonds ($d_{O_I\text{-}O_{III}} = 2.62$ Å and $d_{O_1\text{-}O_{II}} = 2.70$ Å). The intermolecular bridge is responsible for the relatively high melting point and low solubility of PAS, while the intramolecular hydrogen bridge might well explain the fact that the dipole moment of p-amino-benzoic acid does not change appreciably when the OH group of PAS is introduced.(174)

In contrast to the results obtained for aliphatic amino acids, a hydrogen bridge between the carboxyl groups is preferred in this case to that between an amino group and the carboxyl group. This can be explained by the fact that the NH_2 group is conjugated with the benzene ring and therefore zwitterion cannot be formed. Thus, the molecules are uncharged in the crystal.

Assuming that the four formulas shown on the following page contribute to the ground state of PAS, the best agreement between measured and calculated distances was obtained(166) by assuming the following contributions:

I 58%, (III) 20%, (IV) 13% and (II) 9%.

The Kekulé formulas account for only about 60% of the

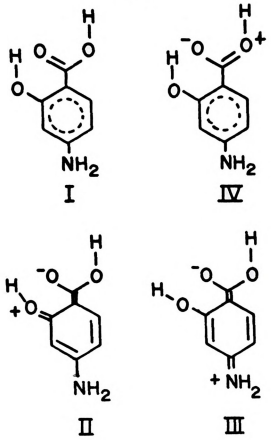

total contribution, and this may explain several properties of this substance such as the high rate of decarboxylation, the low pK value, corresponding to the ionization of the amino group, and the marked variation of the absorption spectrum with pH.

The existence of intramolecular hydrogen bonds in PAS in the solid phase encouraged us to look for intramolecular proton transfer in the excited state. For this reason we measured the fluorescence spectrum of PAS in a KCl pellet. We observed a broad emission band with a maximum in the visible region (~440 nm) (Figure 42). Excitation at 300 nm and 370 nm gives the same emission spectrum. The observation of this emission band in the solid phase may be rationalized as due to proton transfer

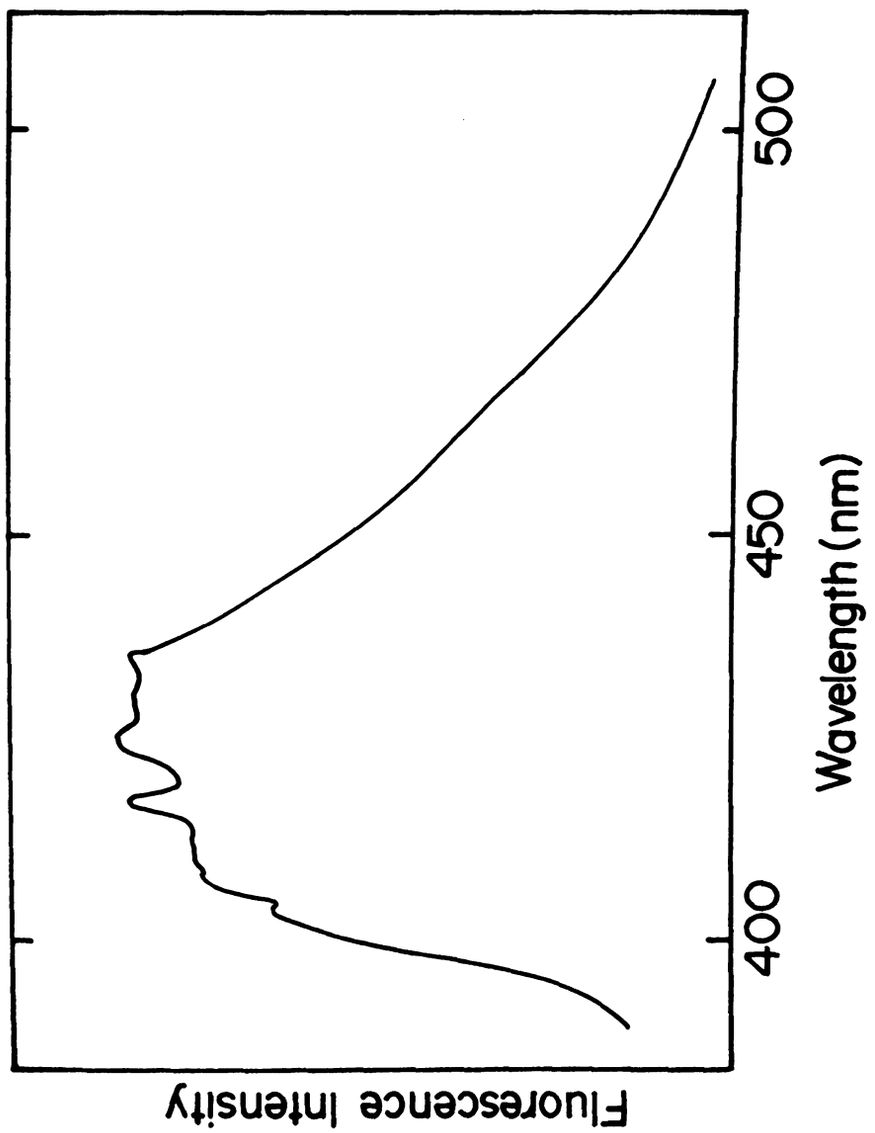

Figure 42. Room temperature fluorescence spectrum of PAS in KCl pellet.

occurring in the excited state of the solid phase since excitonic emission cannot account for such a large Stakes shift. Our fluorescence spectral measurements of PAS in solutions under various conditions such as the effect of solvent and pH, support the suggestion that the emission at ∿440 nm originates from the zwitterion species which is produced in the excited state via an intramolecular proton transfer from the hydroxyl group to the oxygen of the carboxyl group.

The study of fluorescence spectra of MSA in solution made it clear that the ground state equilibrium between different conformers is important in understanding the observed emission. Thus, in non hydrogen bonding solvents the closed ring conformer (cis form) and hence the zwitterion emission was the most predominant one. However, in hydrogen bonding solvents a longer excitation wavelength gives rise to emission from the zwitterion while a shorter excitation wavelength gives rise to a normal fluorescence emission band reflecting the existence of at least two conformers. Since the crystal structure shows that all of the molecules exist in an intramolecular hydrogen-bonded form, i.e. that the most predominant conformer in the solid phase is the intramolecular hydrogen banded cis form, one would expect only zwitterionic species at ∿440 nm. Excited state intermolecular proton transfer cannot occur in the solid phase of PAS since the proton of the carboxyl groups are involved in intermolecular hydrogen bonds and the acidity of this

proton does not increase substantially upon excitation. The absence of the normal fluorescence band in the UV region which is due to neutral PAS in Solution is due to the type of inter- and intramolecular hydrogen bonds present in the solid phase of PAS.

D. Excited State Proton Transfer in N,N-Dimethyl P-Amino Solicylic Acid (DPAS) and Its Methyl Ester (DPASE)

1. Solvent Effect on The Absorption Spectra DPAS and DPASE

The room temperature absorption spectra of DPAS (2.5×10^{-5} M) have been measured in different solvents and are shown in Figure 43. The energies of the two near UV absorption bands in different solvents are summarized in Table 9. In water at pH 2.4 the spectrum shown in Figure 43 corresponds to the neutral form. Depending on the solvent intramolecular or intermolecular hydrogen bonds are formed. The results are similar to that of PAS with a very important exception; namely, an energy-level reversal of the two charge-transfer states. The N,N-Dimethyl amino group has a lower ionization potential than the amino group, which lowers the energy level corresponding to the charge-transfer state in which the N,N-dimethyl amino group acts as an electron-donor. In fact, the electronic transition to this state is lower in energy than C.T. transition in

0.6
0.5
0.4
0.3
0.2
0.1
Absorbance

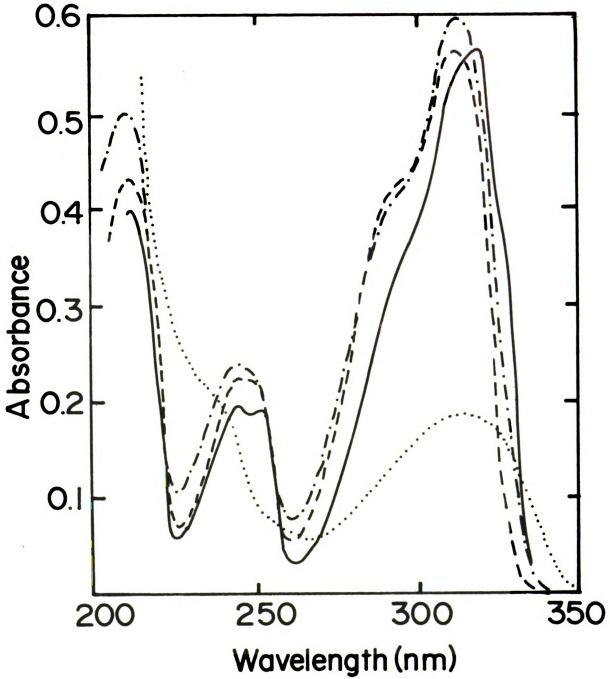

Figure 43. Room temperature absorption spectra of DPAS in different solvents: (——) 3MP; (----) ether; (-·-·-) ethanol; and (....) H_2O (pH = 2.4).

Table 9. Room Temperature Absorption Maxima (nm) and Spectral Shifts (cm^{-1}) Relative to 3MP for DPAS in Different Solvents.

Solvent	λ(nm) (O)CT	$\Delta\bar{\nu}(cm^{-1})$	λ(nm) (N)CT	$\Delta\bar{\nu}(cm^{-1})$
3MP	295	0	319	0
Ether	291	+466	311	+806
EtOH	292	+349	313	+601
H_2O	295	0	313	+601

Table 10. Room Temperature Absorption Maxima (nm) and Spectral Shifts (cm^{-1}) Relative to 3MP for DPASE in Different Solvents.

Solvent	λ(nm) (O)CT	$\Delta\bar{\nu}(cm^{-1})$	λ(nm) (N)CT	$\Delta\bar{\nu}(cm^{-1})$
3MP	294	0	309	0
Ether	295	-116	313.5	-464
EtOH	295	-116	316	-716
H_2O	290	+469	318	-915

which the hydroxyl group acts as an electron-donor. The room temperature absorption spectra of P-amino benzoic acid (PAB) and its N,N-dimethyl derivative (DPAB) have been measured in water at a pH value of 2.4 where the amino group is not protonated. For these two compounds the only charge-transfer transitions occur from the amino group to the aromatic ring. This charge transfer band lies at ∿277 nm for PAB and at ∿315 nm for the N,N-dimethyl derivative. The comparison of the spectra of the neutral forms of DPAS (∿290, 313), DPAB (315), and SA (∿302), (in SA there is only one charge transfer band due to hydroxyl group) supports our assignments of the charge transfer bands (Figure 44). Another confirmation of our assignment has been obtained from the study of the absorption spectra of DPAS in ethanol and in water at different pH values. This energy level-reversal has an important consequence to the emission properties of DPAS which will be discussed later.

The absorption spectra of DPASE (2.5×10^{-5} M) have been measured in different solvents and are shown in Figure 45. Absorption maxima and spectral shifts are summarized in Table 10. The results are very similar to those of DPAS.

2. pH Effect on The Absorption Spectra of DPAS and DPASE

The spectra of various species of DPAS have been identified by studying the effect of pH on the absorption

Absorbance
0.4
0.3
0.2
0.1
20

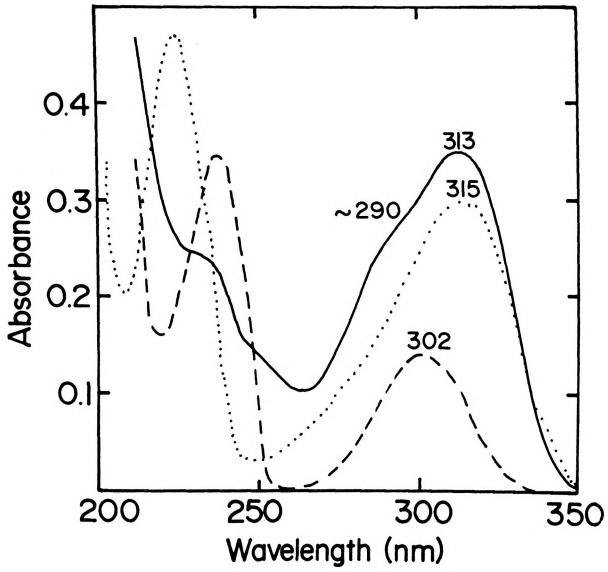

Figure 44. Room temperature absorption spectra of (——) N,N-dimethyl p-amino salicylic acid, (....) N,N-dimethyl p-amino benzoic acid, and (----) salicylic acid in their neutral form in H_2O.

Molar Absorbability x 10^3
24
20
16
12
8
4
200

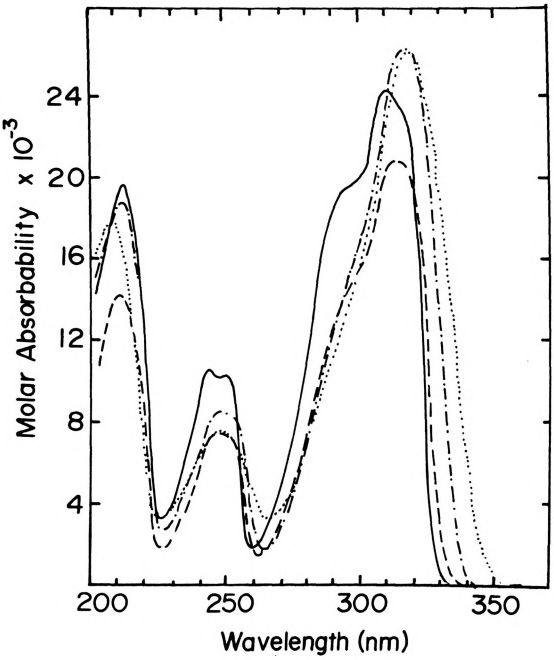

Figure 45. Room temperature absorption spectra of DPASE in different solvents: (——) 3MP; (----) ether; (-·-·-) ethanol; and (-···-) H_2O.

spectra and the results at selected pH values are shown in Table 11 and Figure 46.

At pH 0.8, where the amino group is protonated, there is only one charge-transfer band at ∿300 nm involving the hydroxyl group. The spectrum in this case is very similar to that of salicylic acid at the same pH value. At pH 2.4 in which DPAS exists in its neutral form, the charge-transfer band due to the amino group appears at 313 nm while a shoulder appears at 290 nm. In the pH range 4.1-12.5 DPAS exists as an anion and the whole spectrum is shifted to higher energies compared to the neutral form. This probably reflects the lower electron affinity of the carboxylate anion compared with the carboxyl group giving rise to an increase in the energies of both charge transfer states. At pH 13.6 DPAS exists as a doubly-charged anion and the charge-transfer band due to the carboxylate anion is shifted to higher energies compared to the same form of PAS or SA. The repulsion of the two negative charges is probably greater in this molecule, reflecting the higher electron density of the carboxylate group in DPAS.

The effect of pH on the absorption spectra of DPASE are shown in Figure 47 and the results are summarized in Table 12. The spectra of the cation as well as the neutral form are very similar to those observed for DPAS. In this case, neither carboxylate nor doubly-charged anions are formed. Instead we have the hydroxylate anion formed at high pH values. The absorption spectrum of the phenolate

Table 11. Room Temperature Absorption and Emission Maxima for DPAS at Different pH Values, Ground and Excited States Species.

pH	Absorption Maxima (nm)		Ground State Species	Excited State Species	Emission Maxima (nm)
0.8	300	---	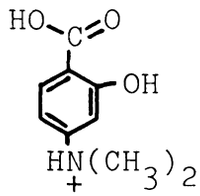	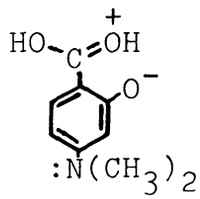	450
2.4	290	313	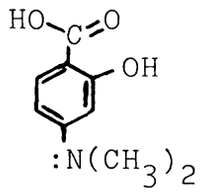	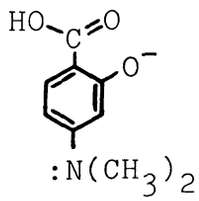	414
5.2	284	306	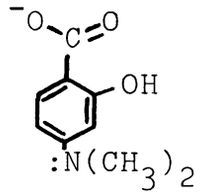	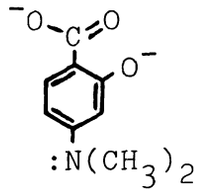	410
13.6	280	307	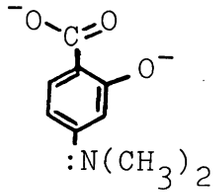	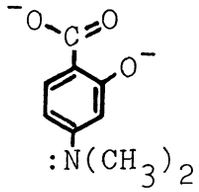	408

0.8
0.7
0.6
0.5
0.4
0.3
0.2
0.1
0.0
Absorbance

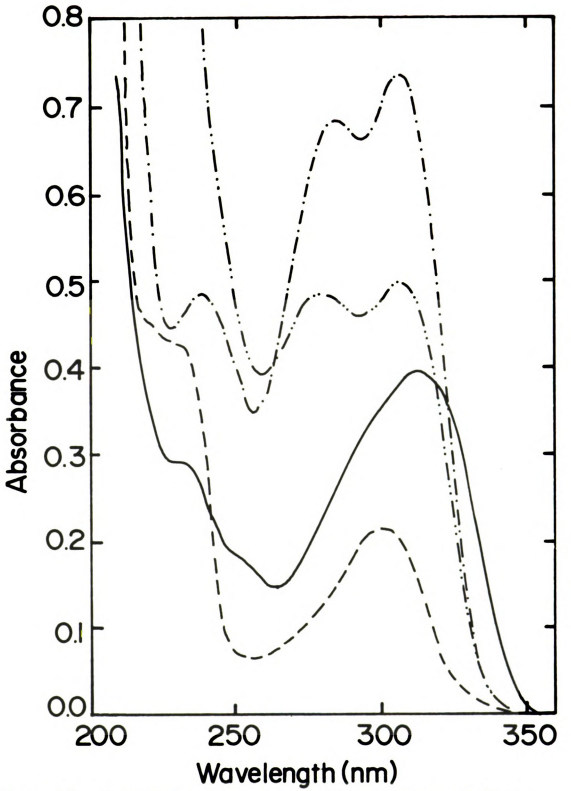

Figure 46. Room temperature absorption spectra of DPAS at different pH values: (----) 0.8; (———) 2.4, (-·-·-) H_2O (4.1-12.5) and (-··-··-) 13.6.

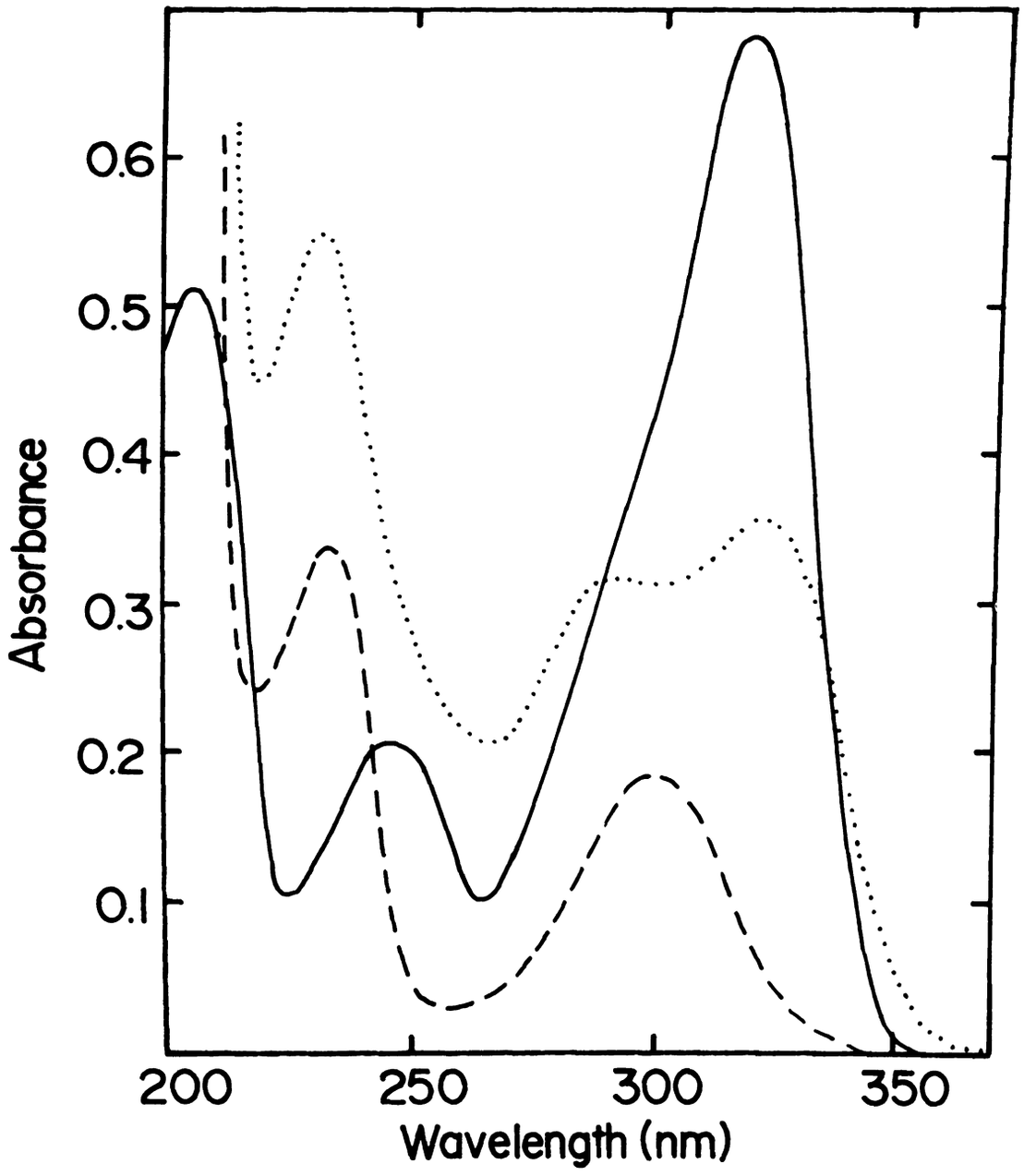

Figure 47. Room temperature absorption spectra of DPASE at different pH values: (----) 1.1, (——) H_2O; and (....) 11.9.

Table 12. Room Temperature Absorption and Emission Maxima for DPASE at Different pH Values, Ground and Excited States Species.

pH	Absorption Maxima (nm)		Ground State Species	Excited State Species	Emission Maxima (nm)
1.1	300	---	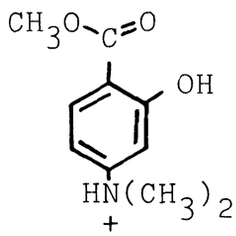	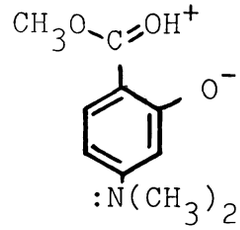	450
5.4	290	318	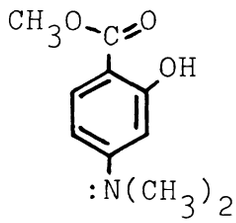	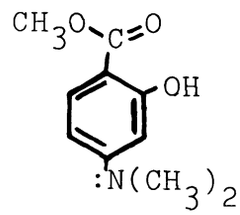	380
11.9	290	322	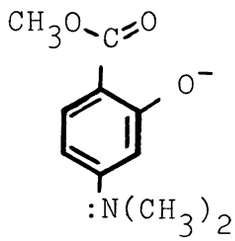	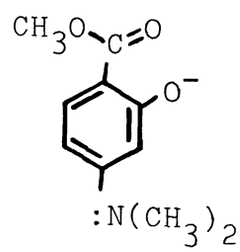	424

anion lies at longer wavelengths than that of the doubly-charged anion, reflecting a larger electron affinity of the carboxyl group.

3. Emission Spectra of DPAS and DPASE As A Function of pH at Room Temperature

The room temperature emission spectra of DPAS in water at different pH values are shown in Figure 48. The excitation wavelength is 290 nm which corresponds to the first absorption band. The ground state and excited state species at given pH values are shown in Table 11. The results are very similar to those of PAS.

The results of the pH effect on the emission spectra of DPASE are shown in Figure 49 and Table 12. At pH 1.1, there is only one emission band at 450 nm which is attributed to the zwitterion formed during the lifetime of the DPASE excited-state via a double-Proton Transfer process involving two solvent molecules. This is in contrast to PASE at about the same pH region, where a very weak, short wavelength shoulder is seen. When the neutral form is excited, there is only one emission band at ∿380 nm which is probably due to the neutral form, but in the case of PASE the excitation of the neutral form results in emission at two wavelengths, one at ∿367 nm which is due to the neutral form, and the other at 450 nm which is due to the zwitterion. At pH 11.9 where DPASE exists in the anion form emission occurs at

Fluorescence Intensity

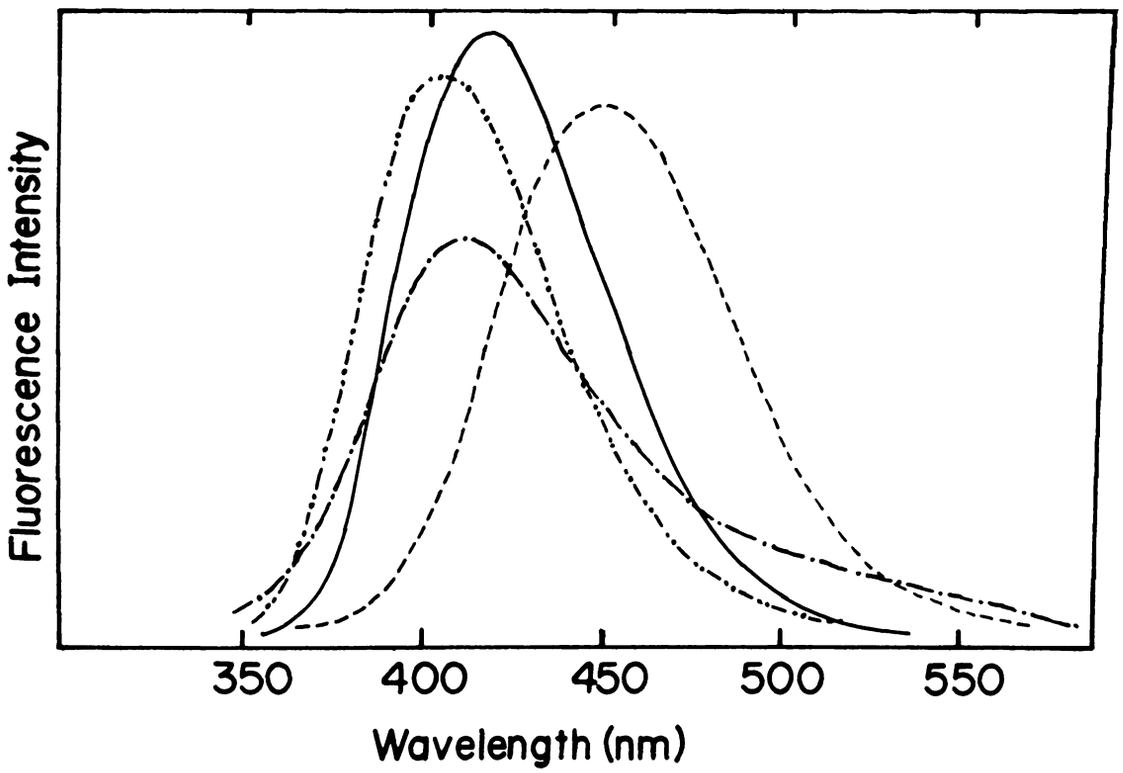

Figure 48. Room temperature fluorescence spectra of DPAS at different pH values: (----) 0.8, (——) 2,4, (-·-·-) H_2O, (-·-·-·-) 13.6

Fluorescence Intensity

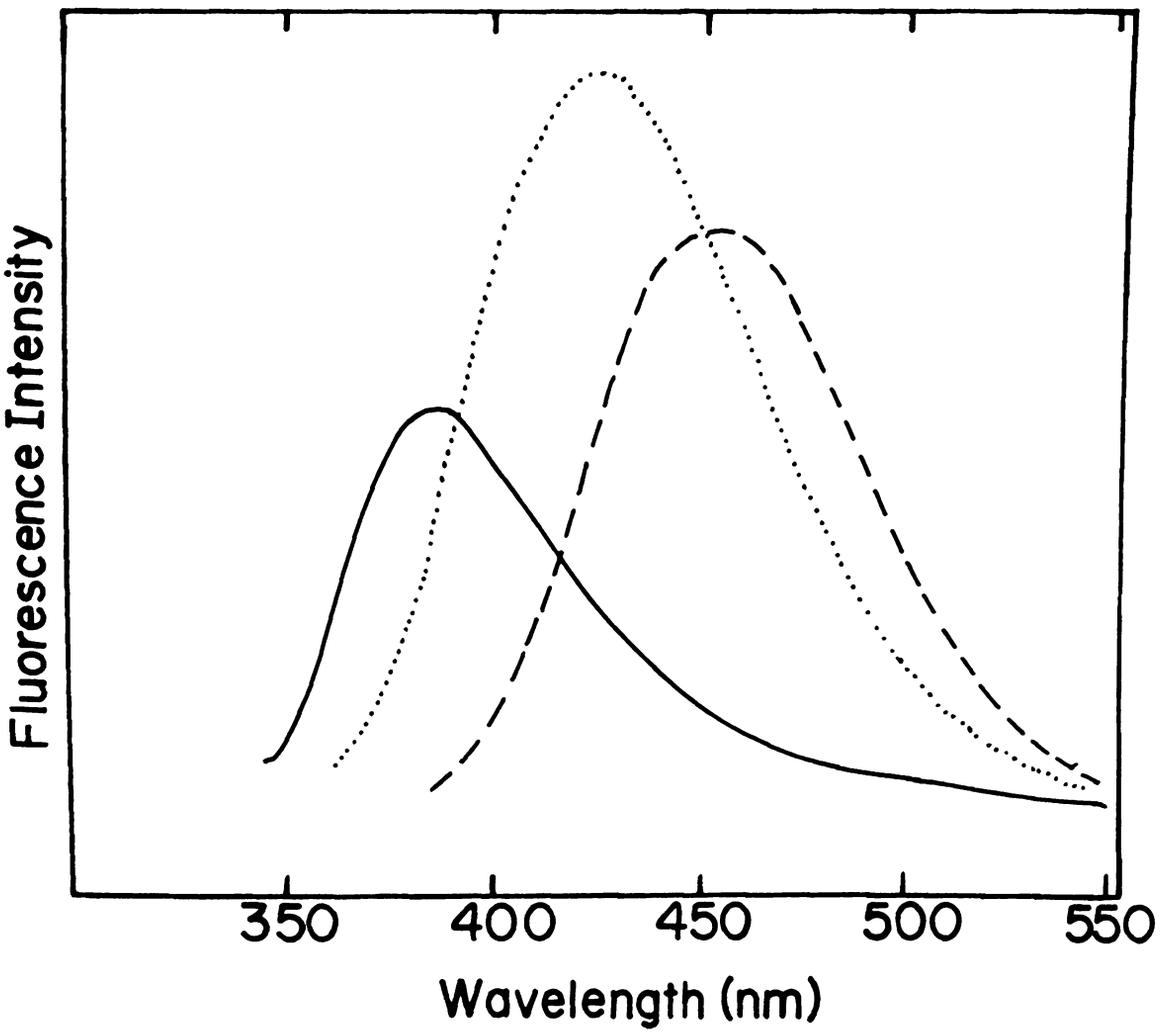

Figure 49. Room temperature fluorescence spectra of DPASE at different pH values: (----) 1.1, (———) H_2O, and (....) 11.9.

420 nm which is at longer wavelengths than that of the doubly-charged anion of DPAS (∿410 nm).

4. Fluorescence Spectra of DPAS and DPASE in Different Solvents at Room Temperature

The room temperature fluorescence spectra of DPAS in different media are shown in Figure 50, and the emission maxima in Table 13. There are two emission bands in 3MP and ether, one at ∿460 nm which is attributed to a zwitter-ion produced via an intramolecular Proton Transfer from the hydroxyl group to the carboxyl group, which occurs during the lifetime of the excited state. The other emission band at 354 nm corresponds to the neutral form of DPAS.

Table 13. Room Temperature Emission Maxima in nm for DPAS in Different Solvents.

Solvent	Emission Maxima in nm		
3MP	354		460
Ether	354		458
EToH	-	400	460
H_2o (2.4)		414	

In ethanol there are two emission bands, one at ∿400 nm due to a species produced via an intermolecular Proton

Fluorescence Intensity
250

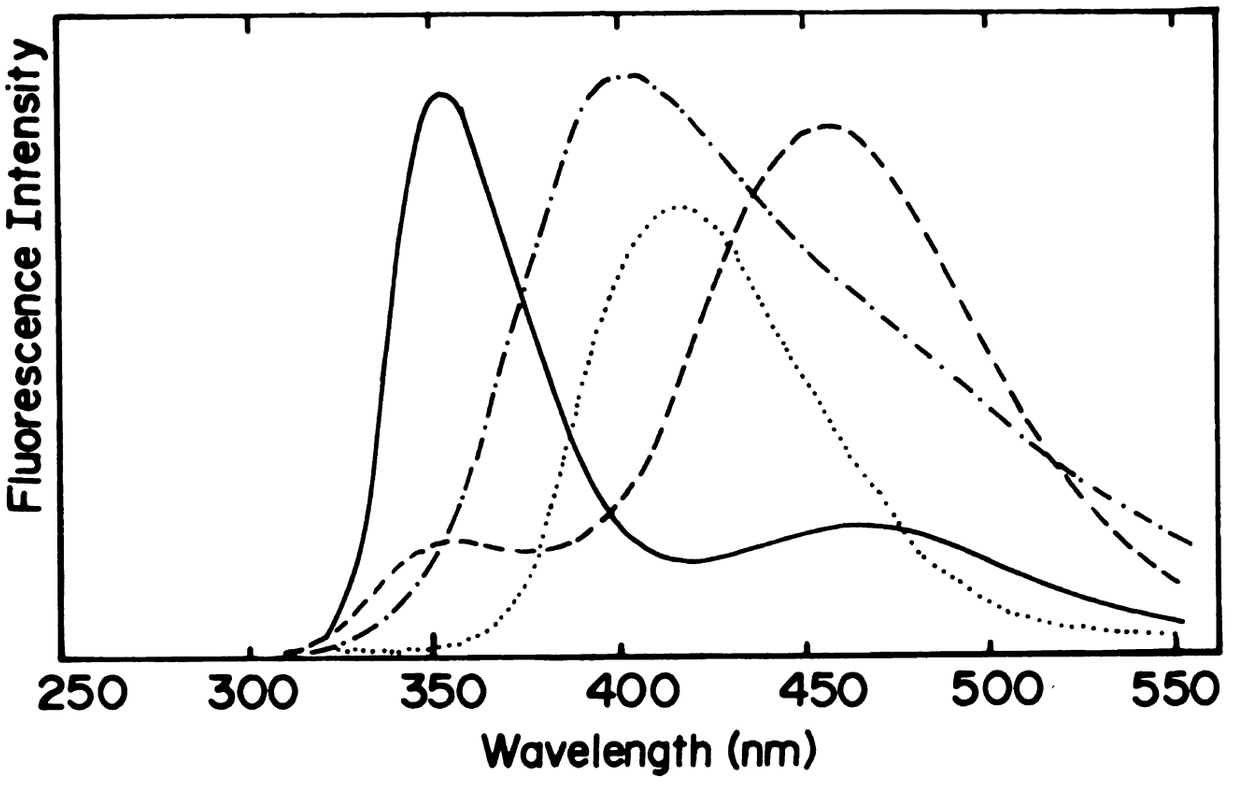

Figure 50. Room temperature fluorescence spectra of DPAS in different solvents: (———) 3MP; (----) ether; (-.-.-) ethanol, (....) H_2O (pH = 2.4).

Transfer from the hydroxyl group to a solvent ethanol molecule producing a singly-charged anion, and the long wavelength emission band at ∿460 nm which is a shoulder and is attributed to the zwitterion produce via an intermolecular double proton transfer between the solute and the solvent. One important difference between PAS and its N,N-dimethyl derivative is that in DPAS the carboxyl oxygen is more basic than in the case of PAS and tends to be protonated in the excited state. In the case of PAS in ethanol we have two emission bands, one due to the neutral form (∿344 nm) and the other due to the phenolate anion (∿416 nm). In water at pH 2.4, where DPAS exists in its neutral form, there is only one emission band at 414 nm which is due to a singly-charged anion as was observed in PAS in the same pH region.

The fluorescence spectra and emission maxima of DPASE in different solvents are shown in Figure 51 and Table 14.

Table 14. Room Temperature Emission Maxima in nm for DPASE in Different Solvents

Solvent	Emission Maxima in nm	
3MP	350	468
Ether	360	454
EtOH	366	492
H_2O	380	

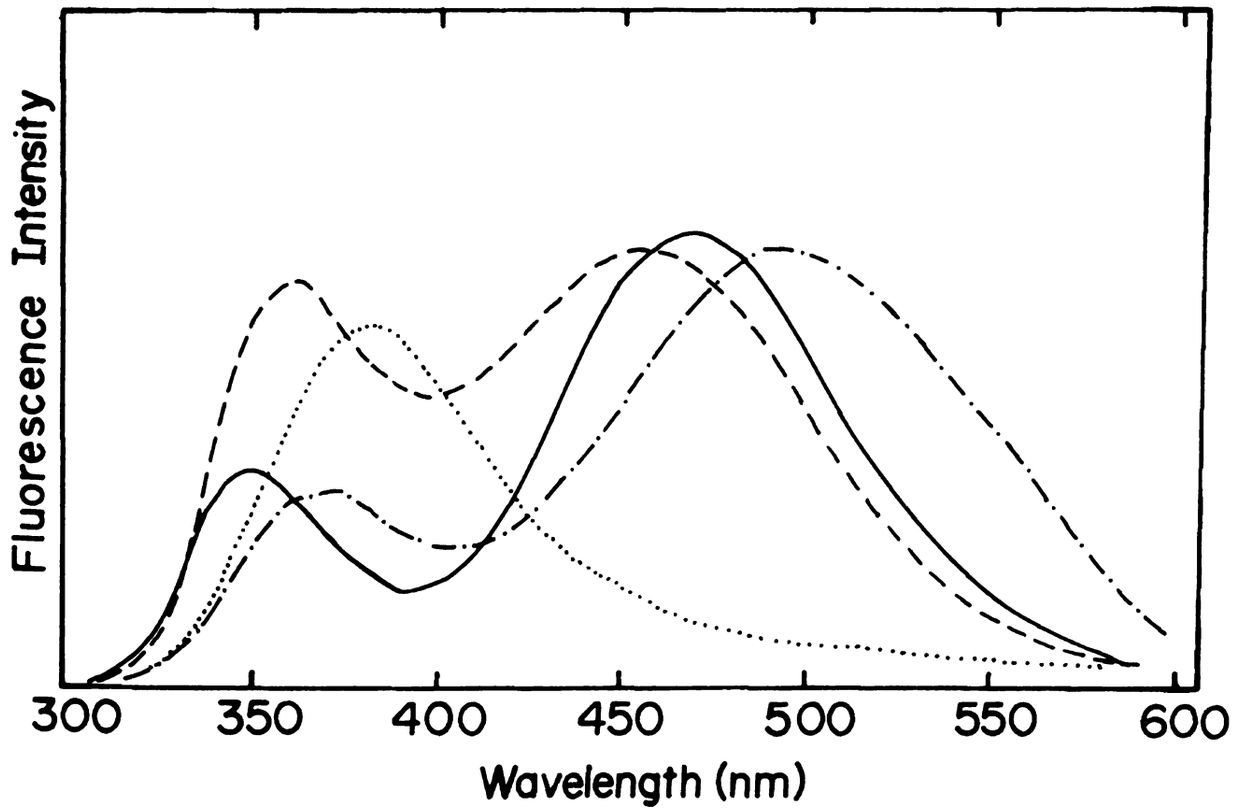

Figure 51. Room temperature fluorescence spectra of DPASE in different solvents: (——) 3MP; (----) ether; (-·-·-) ethanol; and (....) H_2O.

In 3MP, ether and ethanol there are two emission bands, one at short wavelengths with a normal Stokes' shift and is due to the neutral form. The other occurs at long wavelengths with a large Stokes' shift due to the zwitterionic species. In 3MP and ether, intramolecular proton transfer occurs whereas in ethanol intermolecular proton transfer occurs. In water, as we mentioned earlier, there is only one emission band due to the neutral form of the molecule.

E. A Unique Excitation Wavelength Dependence of Excited-State Proton-Transfer

A comparison of the relative intensities of the short (354 nm) and long ($\sim$ 460 nm) wavelength emission bands of DPAS in 3MP indicates that the intensity of the 354 nm emission band is higher than that of the 460 nm emission band which is the reverse of the situation with PASE and MSA. The high intensity of the short-wavelength emission band relative to that of long wavelength emission band prompted us to investigate whether the energy-level reversal of the two charge transfer states in DPAS could be responsible for this observation.

To verify this suggestion we studied the fluorescence spectra of DPAS in 3MP at two different excitation wavelengths (Figure 52). Excitation at the 330 nm band gave mainly the emission at 354 nm, while excitation at 300 nm gave two emission bands, one at 354, the other at $\sim$460 nm.

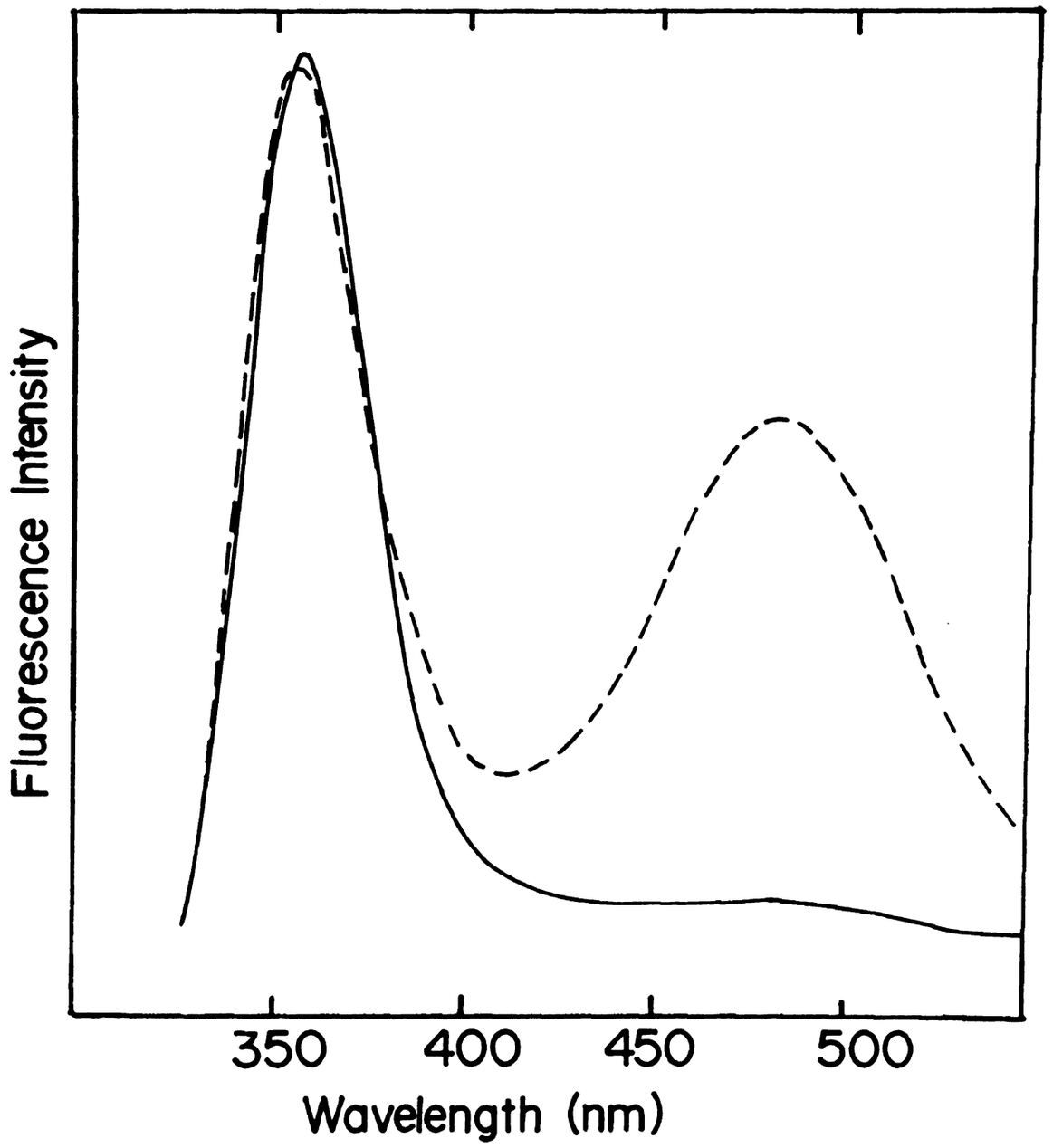

Figure 52. Room temperature fluorescence spectra of DPAS in 3MP at two different excitation wavelengths: (----) λ_{ex} = 300; (——) λ_{ex} = 330.

It is most interesting that at a longer excitation wavelength (330 nm) the emission occurs at 354 nm while a shorter excitation wavelength (300 nm) gives rise to an emission at 460 nm as well as at 354 nm. It is important to note that in the case of MSA, shorter excitation wavelengths gave mostly an emission at 340 nm while longer excitation wavelengths gave mainly emission at 450 nm. To interpret these data, we have constructed an energy level diagram for DPAS (Figure 53a). From the absorption maxima we calculated that the energy of the (O) charge transfer state lies at roughly 2600 cm^{-1} above that of the (N) charge transfer state.

In the (N) C.T state where the amino group acts as the electron donor, the basicity of the oxygen of the carboxyl group is expected to be larger than that of the ground state, but the acidity of the hydroxyl group is not expected to change appreciably. In this case, no proton transfer is expected for the hydroxyl group as a result of excitation of the (N) C.T state. In contrast, an excitation of the (O) C.T state where the hydroxyl group acts as an electron donor, both the acidity of the phenol group and the basicity of the oxygen of the carboxyl group are expected to be increased relative to their values in the ground state. Thus excited state proton transfer is expected to occur as a result of excitation to the (O) C.T state unless other deactivation processes are much faster than the rate of proton transfer. One can therefore expect two possible

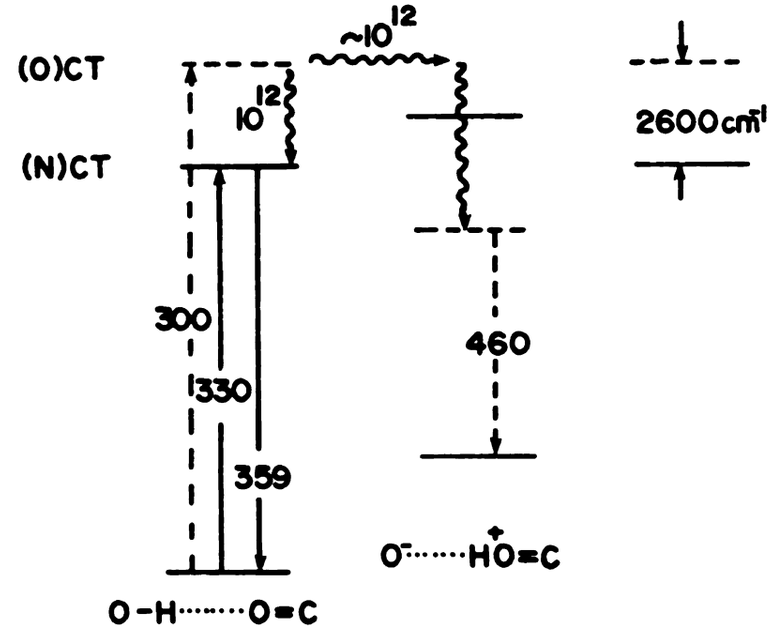

Figure 53(a). Energy level diagram for DPAS (change in emission due to excitation of different electronic state of the same conformer).

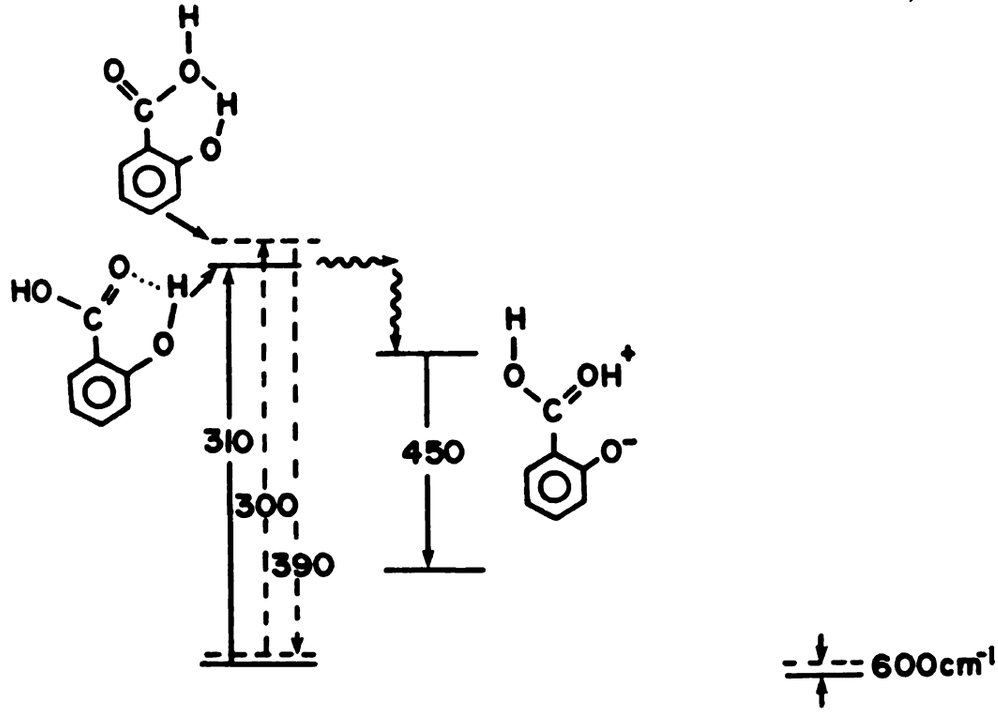

Figure 53(b). Energy level diagram for two conformers of MSA (change in emission due to excitation of different conformers).

pathways depending on the excitation wavelength. If the (O) CT state is excited radiationless transition will occur with a rate constant of 10^{12} sec^{-1} to the lowest excited singlet state, (N) CT, giving rise to emission at 354 nm. However, excited state proton transfer may occur during the lifetime of the (O) CT state giving rise to the zwitterion species in the excited state and leading to an emission at 460 nm. The intensity of the 460 nm band indicates that the rate constant for proton transfer must be of the order of 10^{12} sec^{-1}. Excitation of the (N)CT band will give rise to 354 nm emission only.

Figure 53b also shows the energy level diagram of MSA. The diagram shows an energy gap of 600 cm^{-1} for the two ground state conformers. This value is obtained from theoretical calculations[100]. In this case excitation to the lower level corresponding to the cis conformer leads to proton transfer with a rate constant of 10^{11} sec^{-1} resulting in an emission band at 450 nm. However, excitation to the higher energy level, i.e., excitation of the ether bonded conformer where no proton transfer may occur gives rise to an emission band at 340 nm.

A comparison of the two energy level diagrams clearly shows that in the case of DPAS, we are dealing with excitation of two different electronic states of the same conformer. In contrast, the emission of MSA is varied as a result of excitation of different conformers which are at equilibrium in the ground state.

Consistent with our suggestion, we expected different excitation spectra for these two emission bands. The excitation spectra monitored at two different emission wavelengths are shown in Figure 54. The excitation maximum corresponding to the 354 nm emission occurs at 310 nm while the excitation maximum corresponding to the 464 nm emission occurs at 300 nm. In the case of MSA[96], emission at 340 nm gives an excitation maximum at 308 nm and emission at 450 nm gives an excitation maximum at 311 nm. Our experiments also support our earlier assignments of charge transfer states, and to our knowledge, this result is the first example of this unique excitation wavelength dependence.

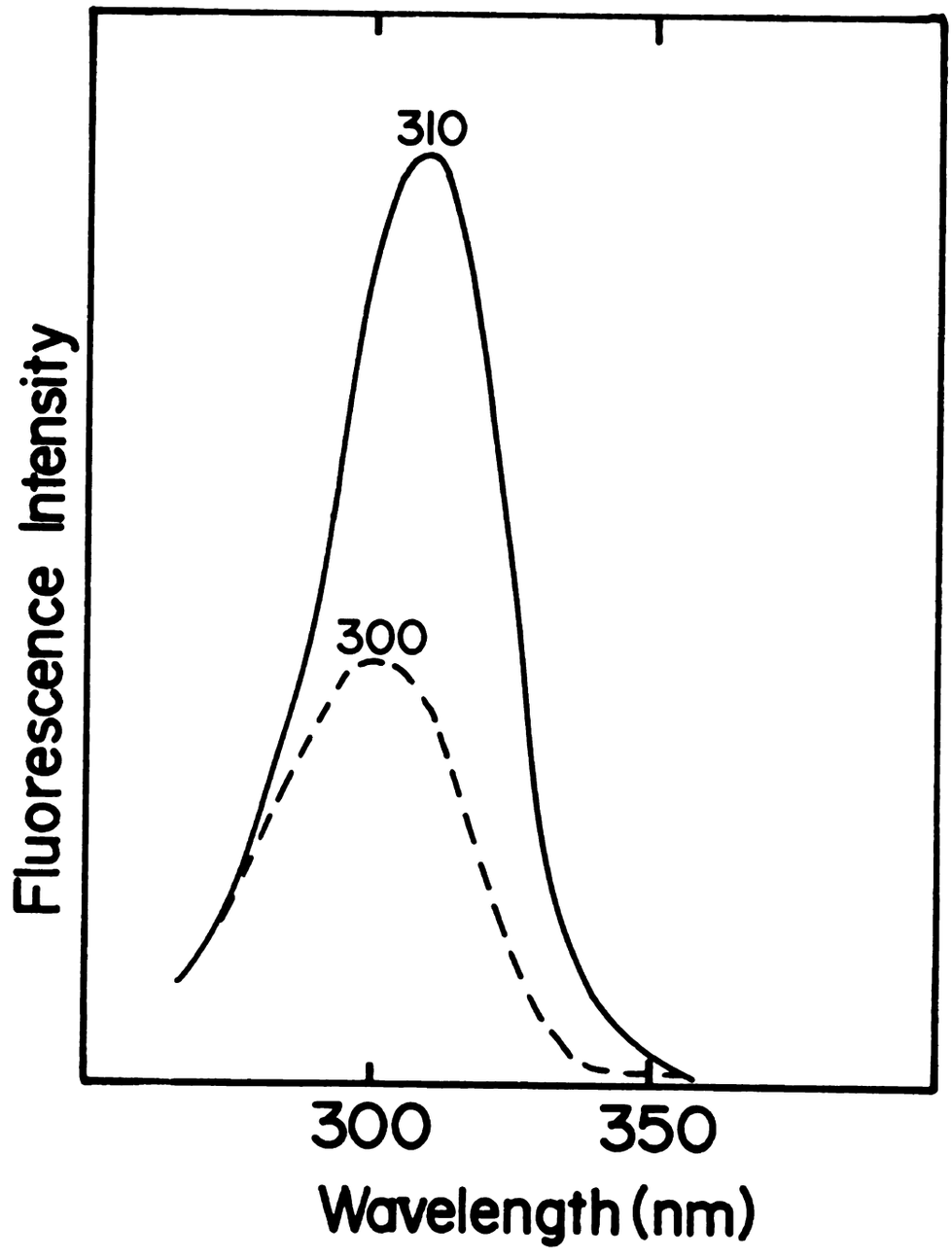

Figure 54. Room temperature excitation spectra of DPAS in 3MP (uncorrected spectra) (——) represents the 354 nm band, while (----) represents the 464 nm fluorescence.

CHAPTER III

EXCITED STATE DOUBLE PROTON TRANSFER IN 1-AZACARBAZOLE HYDROGEN BONDED DIMERS ITS ACETIC ACID COMPLEX AND IN THE SOLID PHASE

A. Introduction

Both 1-azacarbazole hydrogen bonded dimers and the 1-azacarbazole-acetic acid complex were shown[175] to undergo photoinduced double proton transfer reactions in their lowest excited singlet state. An emission band with a maximum at 510 nm arises from a tautomer formed in the excited state as a result of the double proton transfer process.

Studies of 1-azacarbazole in the solid phase also show that excited state double proton transfer accounts for the observed emission. The crystal structure, determined by x-ray diffraction methods[176], shows that the crystal contains cyclic dimers only. Spectral measurements of 1-azacarbazole in solution under various conditions provide further details regarding the mechanism of excited state proton transfer. The absorption and emission properties of 1-azacarbazole were reexamined under various conditions.

1. Excited State Double Proton Transfer in 1-AZA Carbazole Hydrogen-Bonded Dimers

Dilute solutions of 1-azacarbazole in 3-methylpentane (3MP) exhibit a fluorescence band with a maximum near 367 nm. Concentrated solutions of 1-azacarbazole in 3MP, in addition to the normal fluorescence (F_1) at 374 nm with a small contribution from the dimer, exhibit a second fluorescence band (F_2) with a maximum at about 510 nm (Figure 55). The relative intensities of F_1 and F_2 depend on the concentration, excitation wavelength and temperature.

The room temperature absorption spectrum of 1-aza carbazole in 3MP (Figure 56) exhibits an absorption band covering the range from 300 to 350 nm. This band corresponds to the $^1A_1 \rightarrow {}^1A_1$ (^1L_a) transition of carbazole which has a transition moment along the short axis of the molecule. Such an assignment was obtained from polarized absorption of carbazole in a single-crystal matrix of fluorene at about 15 K[177]. An emission polarization study[178] of stretched polyvinylalcohol films confirmed this result. The same study showed that the second absorption band with a maximum at 296 nm corresponds to the $^1A_1 \rightarrow {}^1B_2$ (^1L_b) transition of carbazole and is polarized along the long axis of the molecule. These results are consistent with relative polarizations obtained from luminescence polarization studies of frozen solutions[179].

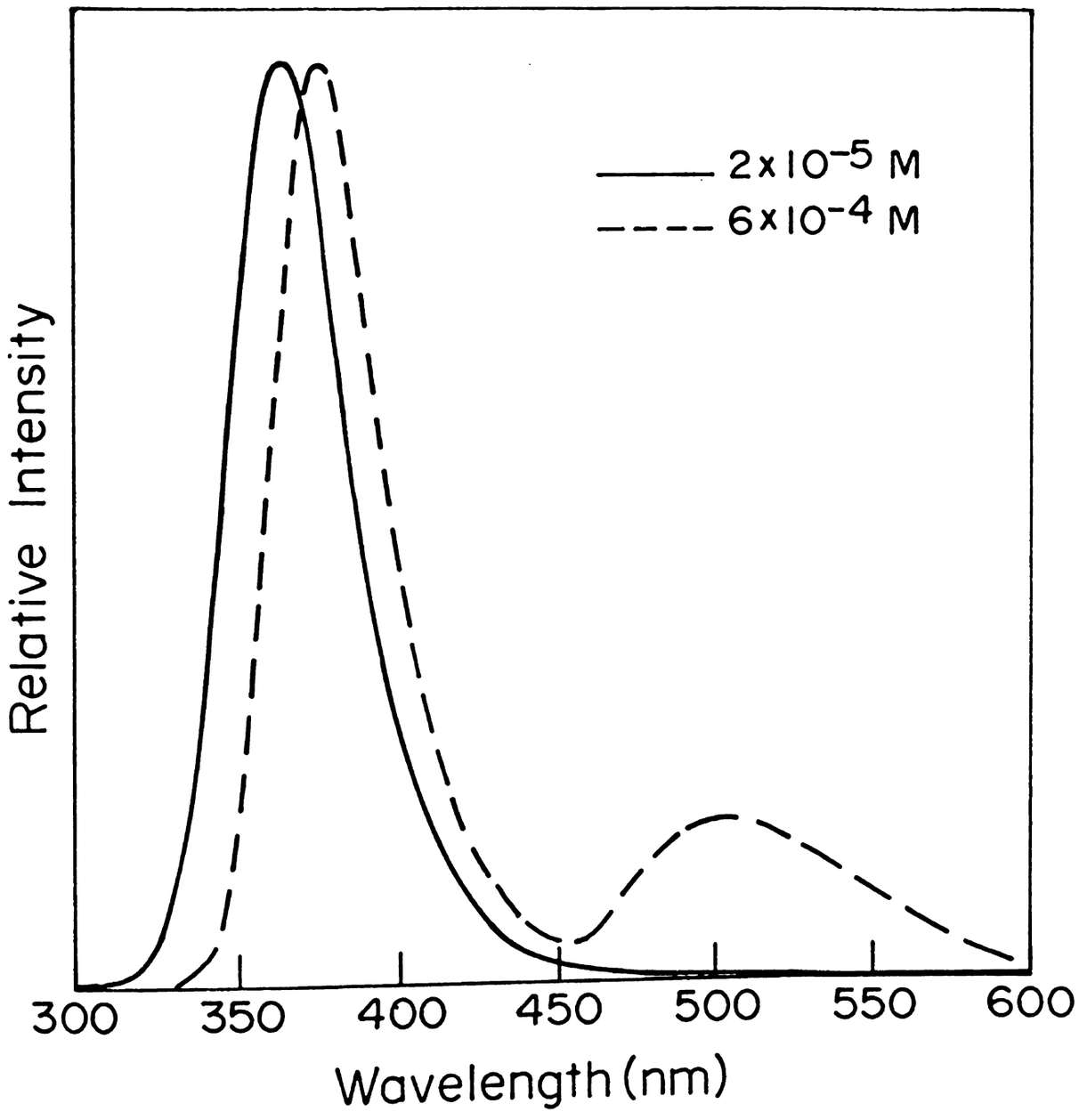

Figure 55. Room temperature fluorescence spectra of 1-azacarbazole in 3MP at two different concentrations.

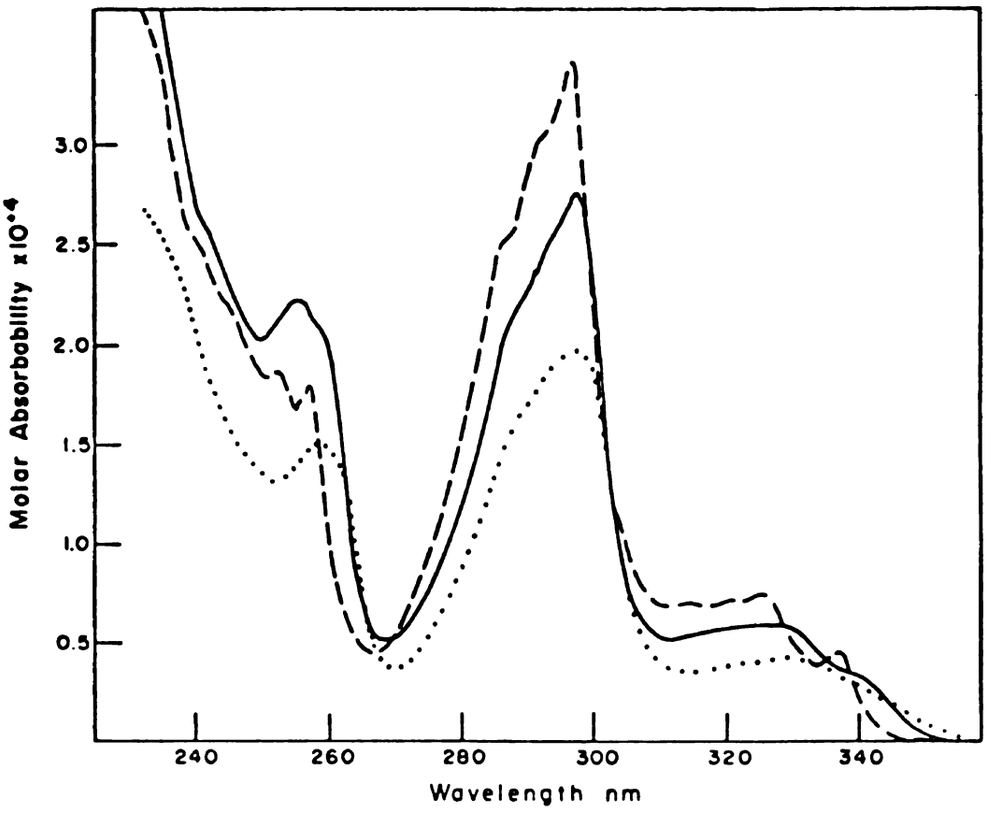

Figure 56. Room temperature ultraviolet absorption spectra of 1-azacarbazole (2 x 10^{-5} M) in different media: (----) cyclohexane; (——) ether; and (....) ethanol.

Solvent effects on the absorption spectrum of 1-aza carbazole indicate that the hydrogen bond energy has the following order: $^1L_a > {}^1L_b > {}^1A$. Analysis of the spectral shifts due to change in medium leads to the qualitative conclusion that the acidity of the pyrrolic proton and the basicity of the aza-nitrogen of 1-azacarbazole are both enhanced, particularly in the ^1L_a state, the lowest excited singlet state. Figure 57 clearly shows the large red shift of ^1L_a band of dilute solution of 1-azacarbazole in 3MP at 77 K. Solvent effects on the emission spectrum of 1-aza carbazole also are consistent with a larger dipole moment in the ^1L_a state compared with that of the ground state. The ground and excited state dipole moments of carbazole were found[180] to be 1.7 and 3.6 D respectively.

If equilibrium is established during the excited state lifetime, then the pK_a^* and pK_b^* can be determined in a way analogous to the spectraphotometeric determination of the ground state pK's, by fluorometric titration. For this reason we have repeated earlier measurements of the fluorescence and absorption intensity of 1-azacarbazole in water as a function of pH. In the range from 7 to 13, neither the absorption spectra nor the emission spectra show any change. Above a pH value of 13, the absorption spectra remain the same; however, the emission spectrum exhibits the 400 nm band as well as a shoulder around the 500 nm region (See Figure 58). The new emission band can be clearly identified as the emission of the anion of 1-aza

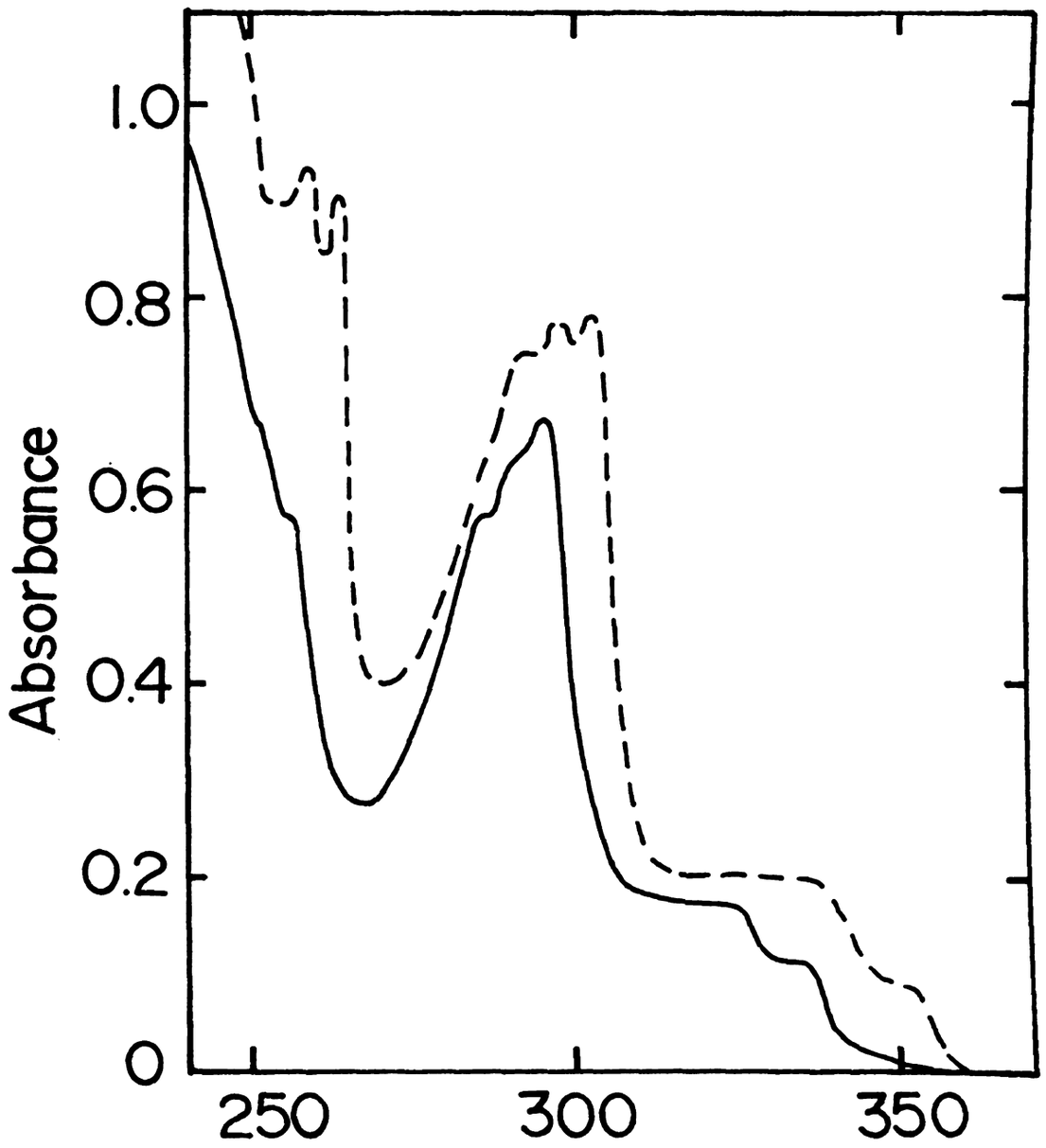

Figure 57. Ultraviolet absorption spectra of 1-azacarbazole (2.5×10^{-5} M) in 3-methylpentane at room temperature (——); 77°K (----).

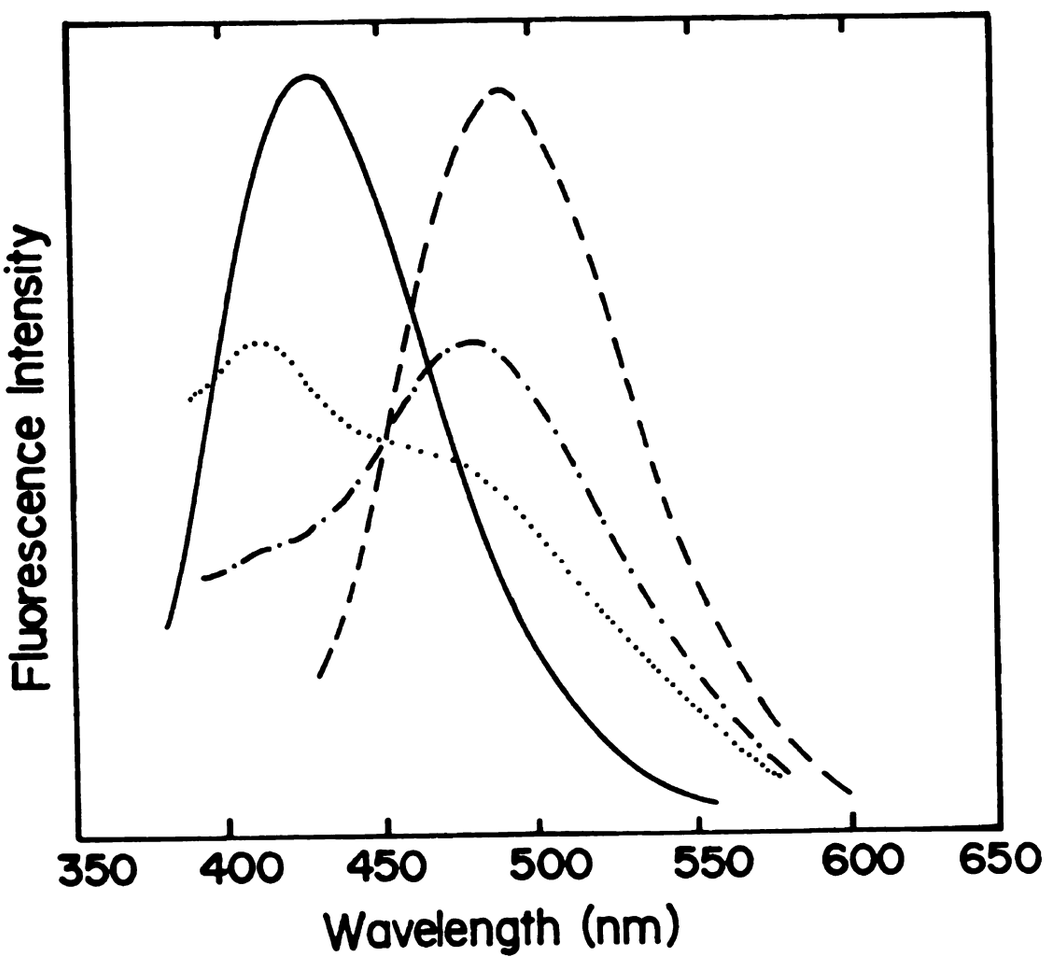

Figure 58. Room temperature fluorescence spectra of 1-azacarbazole at different pH values: (——) 4-13), (....) 13.5, (-·-·-) 13.7, (----)>13.7.

carbazole which exists in pH $\geq$ 14 solution. From the above discussion, we can conclude that the acidity increases upon excitation to the L_a state. In other words, the proton will dissociate more easily in the lowest excited singlet state than the ground state. Other evidence that supports our idea is the dramatic decrease of the fluorescence quantum yield around pH 13.5 (see Figure 59) which is due to the proton dissociation of the pyrrolic nitrogen and production of the weakly emitting anion. From the midpoint of the fluorescence and absorption titration curves we obtain a $pK_b^* = 12.12$ and $pK_b = 13.42$ for the excited and ground states respectively which show that indeed the acidity of pyrrolic hydrogen increases by 1.3 pK unit. In the same way we get $pK_a^* = 4.2$ and $pK_a = 2.4$ at low pH due to protonation of the aza nitrogen which indicates that the basicity of the aza nitrogen increases by 1.8 pK unit. The actual magnitude of the pK value change due to excitation has been estimated (by using the Förster cycle) to be $\Delta pK_b = 1.6$ and $\Delta pK_a = 4.9$ for the pyrrolic hydrogen and aza nitrogen respectively.

Hydrogen bonded dimer formation of 1-azacarbazole has been studied by comparing the ultraviolet absorption spectra at different concentrations in 3MP at room temperature (Figure 60). A shoulder appears at 353 nm in the more concentrated solution which corresponds to the dimer. The association constant of dimer formation as obtained from absorption spectra at different concentrations is

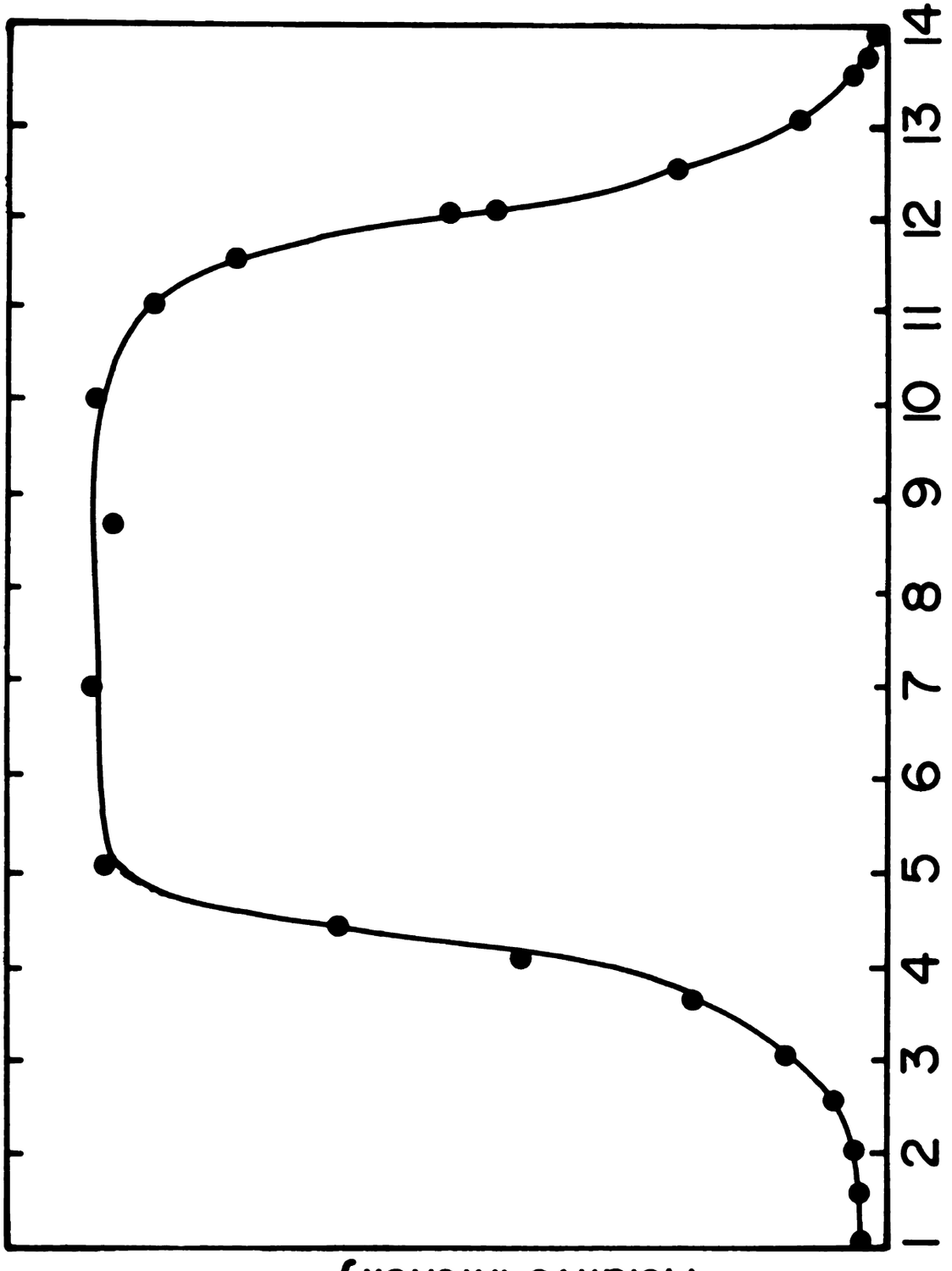

Figure 59. Effect of pH on the fluorescence spectra of 1-azacarbazole at room temperature.

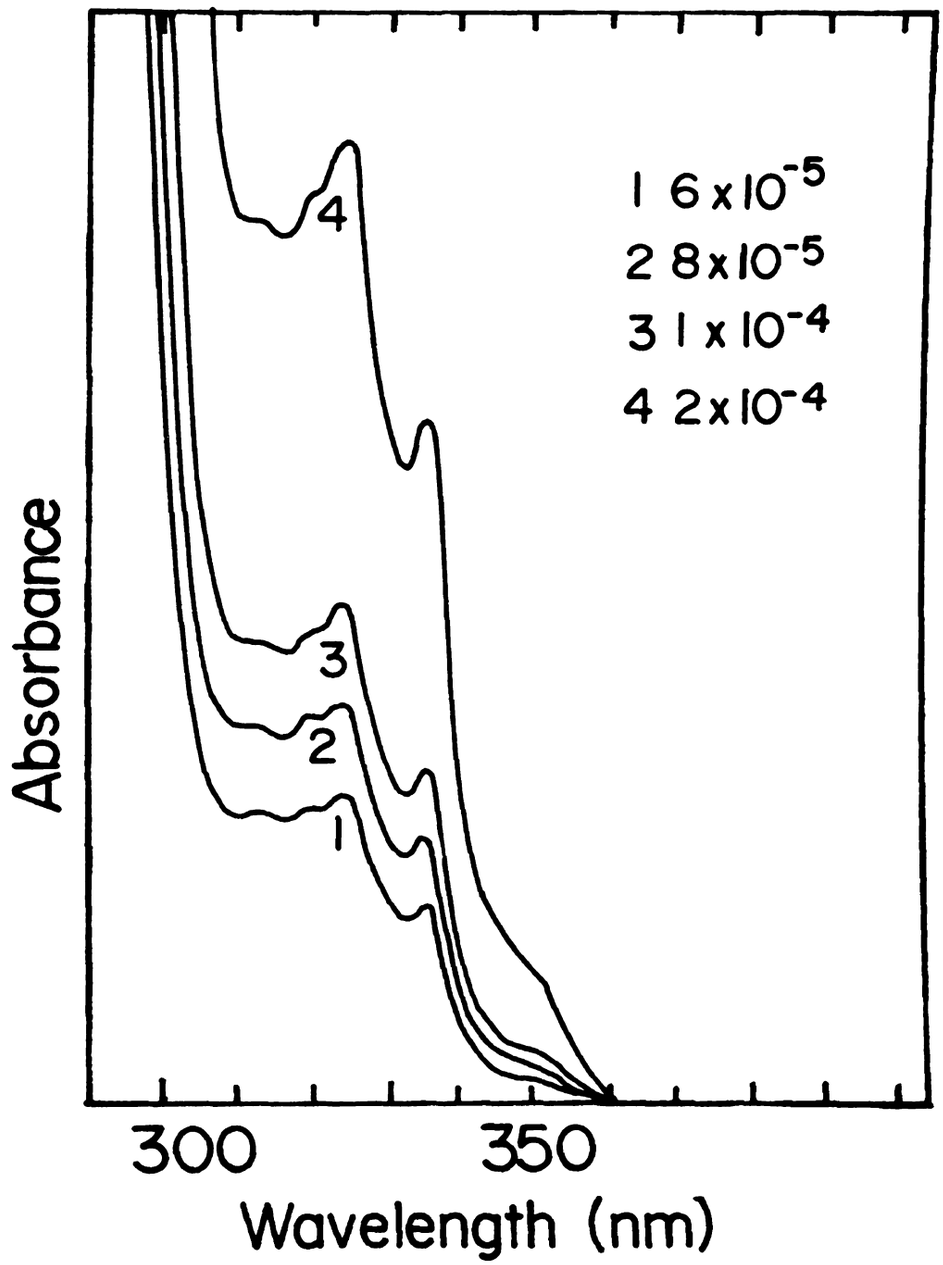

Figure 60. Room temperature absorption spectra of 1-azacarbazole in 3-methylpentane at different concentrations.

$(6.8\pm0.7)\times10^{2}$ M^{-1} at room temperature (21°C). This corresponds to a ΔG value of 3.8 Kcal $mole^{-1}$ at room temperature $(8.1\pm0.8)\times10^{3}$ M^{-1} at 0°C and $\sim10^{8}$ M^{-1} at 77°K. The association constant in 3MP as a function of temperature resulted in an estimate of -18.25 Kcal $mole^{-1}$ for ΔH and -49 eu for ΔS. The large negative value of the enthalpy change means the system is energetically favorable towards dimerization at low temperature.

The excitation spectrum ($\sim10^{-4}$M) for the F_2 band is shifted to longer wavelengths compared with that for the F_1 band indicating that the F_2 fluorescence band arises from excitation of the hydrogen bonded dimer which absorbs at longer wavelength compared to the monomer. The F_1 fluorescence band arises mainly from monomer excitation.

The assignment of the F_2 band as being due to a tautomer formed as a result of double proton transfer in the excited state of the 1-azacarbazole hydrogen-bonded dimer has been further confirmed by studying the emission spectrum of the N_1-methyl tautomer of 1-azacarbazole (I) which we have synthesized.

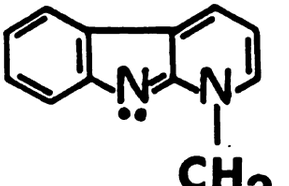

I

This molecule has the same π-electron system as the proposed tautomer. Its emission spectrum in ethanol occurs at the

same energy and exhibits similar fine structure to the F_2 band observed by excitation of the 1-azacarbazole hydrogen-bonded dimer.

By using nanosecond time resolved spectroscopy[181], the rate constants of double deuteron transfer has been estimated at 77°K to be $k_f^d = 6.1 \times 10^7$ and $k_b^d = 2.1 \times 10^7$ sec^{-1}. The large rate of the double deuteron transfer points to a very low barrier energy for the process. The energy barrier for excited-state proton transfer in the 1-aza carbazole hydrogen-bonded dimer can be estimated by studying the temperature effect on the F_2/F_1 intensity ratio. An estimated energy barrier is about 3 Kcal $mole^{-1}$. A potential energy diagram which qualitatively describes the energetics of the double proton transfer process is shown in Figure 61. Potential energy is plotted versus a reaction coordinate associated with the simultaneous motion of the two protons in the dimer. It is assumed that the tautomer is unstable in the ground state.

By using an activation energy of 3 Kcal $mole^{-1}$ and $k_{pt} = 6.1 \times 10^7$ sec^{-1} one may obtain a value of 10^{13} for the frequency factor A in the equation for the absolute rate constant, which is similar to the expected theoretical value $10^{12} \sim 10^{13}$.

2. Phosphorescence of 1-Azacarbazole

In the case of 7-azaindole where photo-induced double proton transfer occurs in concentrated solution in 3MP[79],

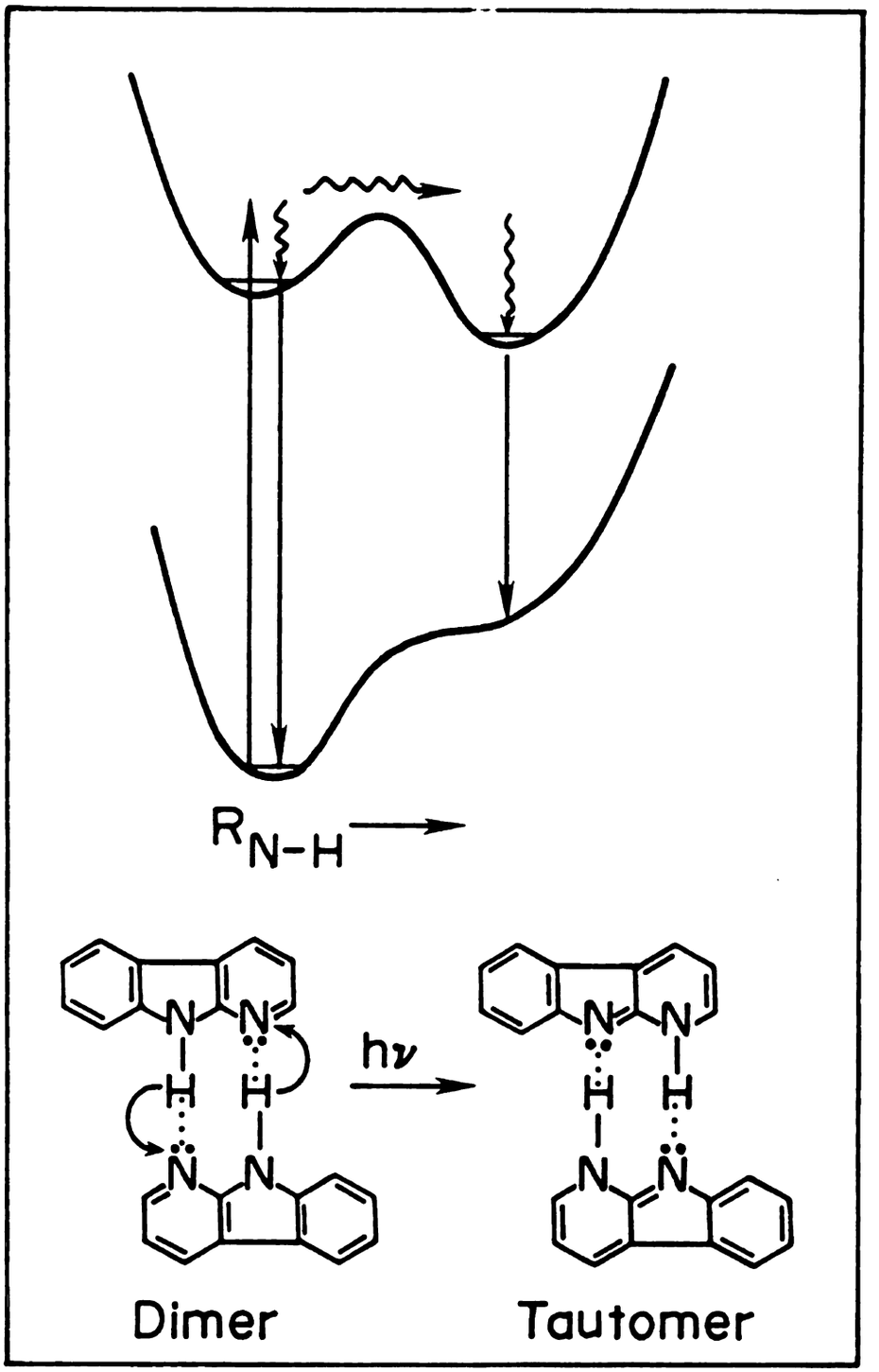

Figure 61. Qualitative double minimum potential energy diagram illustrating excited-state double proton transfer in 1-azacarbazole hydrogen-bonded dimers.

the low temperature fluorescence spectrum overlaps with the isoenergetic monomeric phosphorescence[127]. This coincidence makes it difficult to remove ambiguities regarding the temperature dependence of the two fluorescence bands and makes the mechanism of proton transfer less certain.

The phosphorescence spectrum of 1-azacarbazole was measured at 77°K and is shown in Figure 62. The maximum of the phosphorescence band occurs at 440 nm while the fluorescence band due to the excited state double proton transfer of hydrogen-bonded dimers occurs at 510 nm. Thus, in the case of 1-azacarbazole no ambiguity is present.

3. Excited State Double Proton Transfer in the 1-Azacarbazole-Acetic Acid Complex

1-Azacarbazole forms a complex with acetic acid. The room temperature absorption spectra of a dilute solution in hexane, 2×10^{-5} M of 1-azacarbazole in the presence of various amounts of acetic acid are shown in Figure 63. The absorption at 353 nm is due primarily to the complex and can be used to determine the association constant of the complex. A value of $4 \times 10^{5} M^{-1}$ has been estimated for the association constant of the complex. It should be noted that the association constant for the 1-azacarbazole acetic acid complex is much larger than that for the 1-azacarbazole dimer ($6.8 \times 10^{2} M^{-1}$).

The room temperature emission spectra of 1-azacarbazole in the presence of excess acetic acid exhibits only the F_2

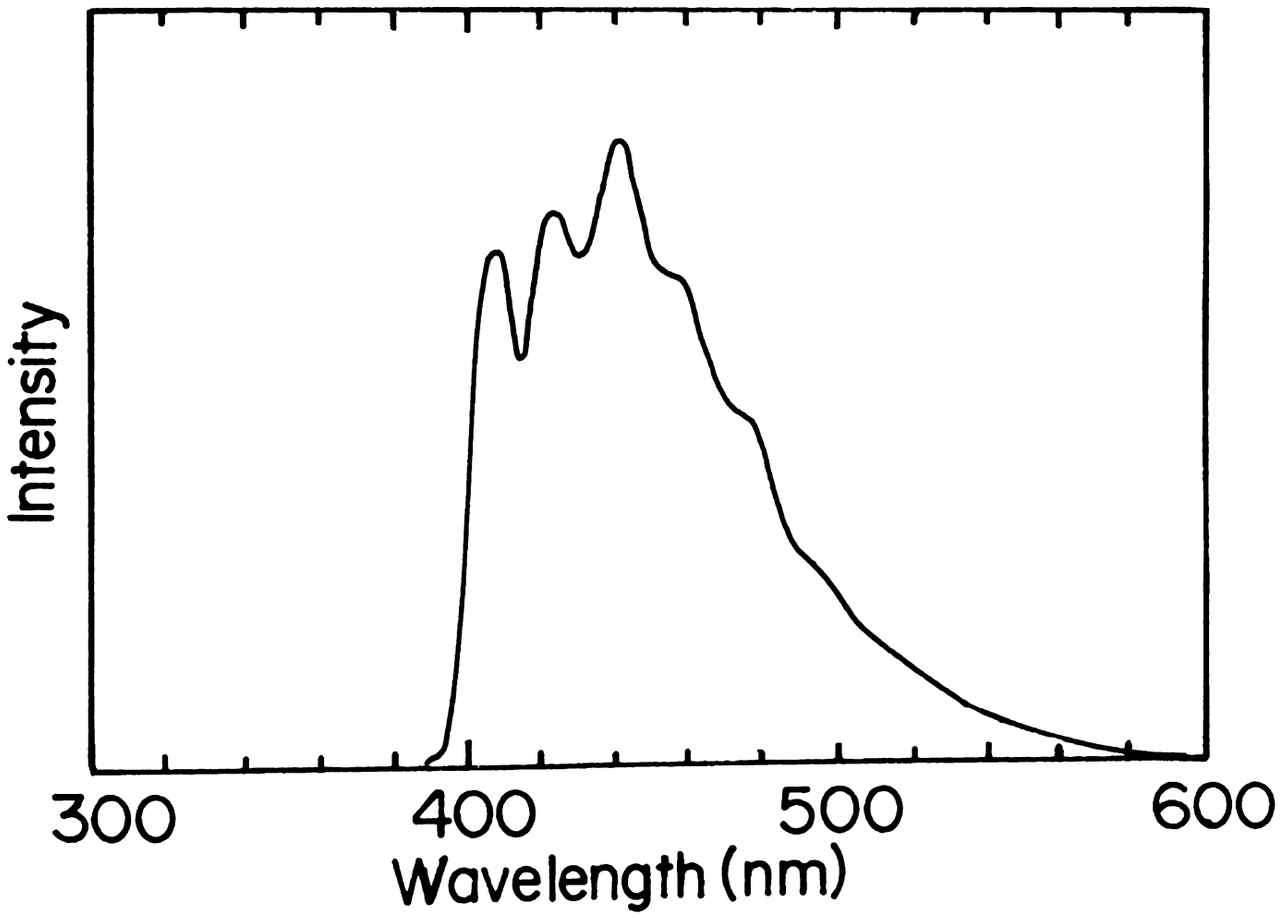

Figure 62. Phosphorescence spectrum of 1-azacarbazole (6×10^{-4} M) in ether at 77°K excited at 330 nm.

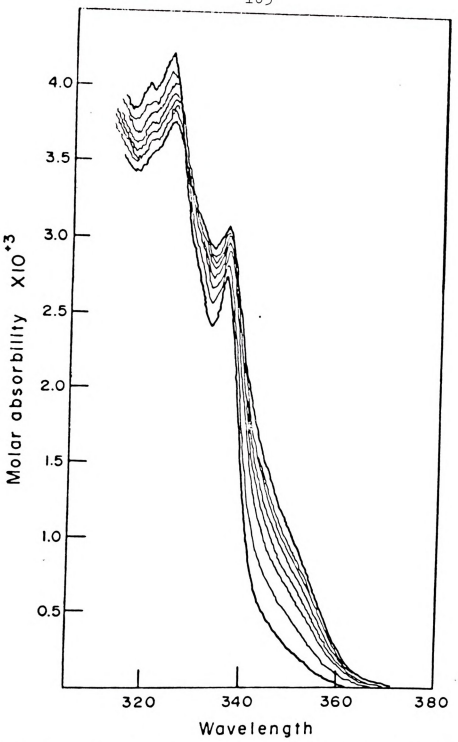

Figure 63. Room temperature absorption spectra of 1-azacarbazole (2×10^{-5} M) in hexane, in the presence of variable amounts of acetic acid, 0, 1.66×10^{-6}, 3.32×10^{-6}, 4.98×10^{-6}, 6.64×10^{-6}, 8.30×10^{-6}, 9.96×10^{-6}, 1.16×10^{-5} M in 10 cm cell.

band as shown in Figure 64. Similarly, at 77°K only F_2 emission is observed. This means that the proton transfer is much faster than the fluorescence rate of 1-azacarbazole The estimated value for k_{pt} is 1.4 x 10^9 sec^{-1}, so that the activation energy in the excited state must be less than 0·16 Kcal $mole^{-1}$ and consequently, the thermal energy at 77°K is enough to overcome the barrier.

4. Excited State Double Proton Transfer in 1-Aza Carbazole in the Solid Phase

Crystallographic data

The crystal structure of 1-azacarbazole has been determined[176] by x-ray diffraction. Crystals of 1-azacarbazole are monoclinic and belong to the space group $P2_1/n$; the dimensions of the unit cell are: a = 13.516(4), b = 5.526 (2), c = 11.336(5)Å, β = 95.77(3)°; Z = 4, M = 168.20, ρ_c = 1.326 g cm^{-3}. Lattice dimensions were determined using a Picker FACS-I diffractometer and MoKα_1 (λ = 0.70926 Å radiation. Intensity data were measured by using MoKα radiation ($2\theta_{max}$ = 55°) yielding 1940 total unique data points and, based on I>3σ(I), 1236 observed data points. The data were reduced[182], the structures were solved by direct methods[183], and the refinement was by full-matrix least squares techniques[184]. The final R. value was 0.035. The final difference Fourier map showed densities ranging

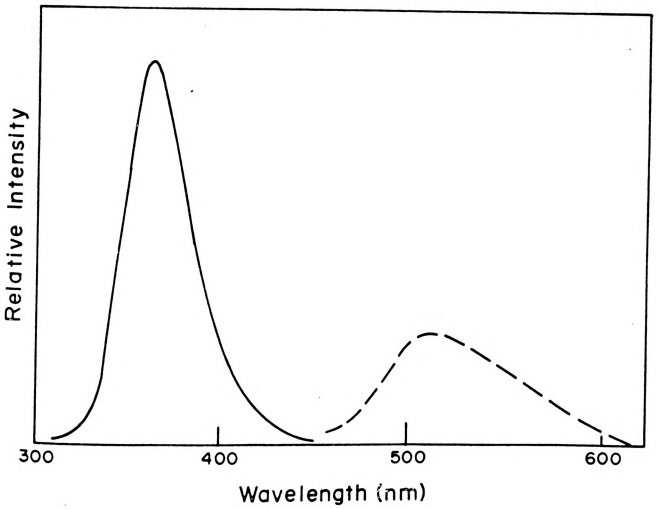

Figure 64. The emission of 5×10^{-4} M of 1-azacarbazole in 3-methylpentane in the absence (——), presence of excess acetic acid (----).

from +.19 to -.28 with no indication of missing or incorrectly placed atoms.

The planes of the three rings individually are flat to within ±0.01Å. The plane of the three rings together is parallel to the plane of the equivalent molecule joined by hydrogen-bonds and related by a crystalographic center of symmetry, but these two planes are not coincident. The distance between the two planes is ∿0.51Å and the angle between either plane and the plane of 4 nitrogen atoms involved in the H-bond is 10.25°. Figure 65 shows stereoscopic view[185] of a hydrogen-bonded dimer molecule. The stereoscopic views of the packing of the dimer molecules into the unit all are shown in Figure 66. The intermolecular distances, the bond distances and the positions of the hydrogen atoms were all consistent with doubly hydrogen-bonded 1-aza carbazole dimers in the crystal.

Room Temperature Absorption and Fluorescence Spectra of 1-Aza Carbazole in the Solid Phase

The absorption spectrum of 1-azacarbazole in a nujol mull at room temperature is shifted to the red similar to that observed for concentrated solutions in 3MP, which indicates the existence of hydrogen-bonded dimers in the solid phase of 1-azacarbazole.

The infrared spectrum was measured in the region of 4000 cm^{-1} to 2000 cm^{-1} in two different media, a nujol mull and

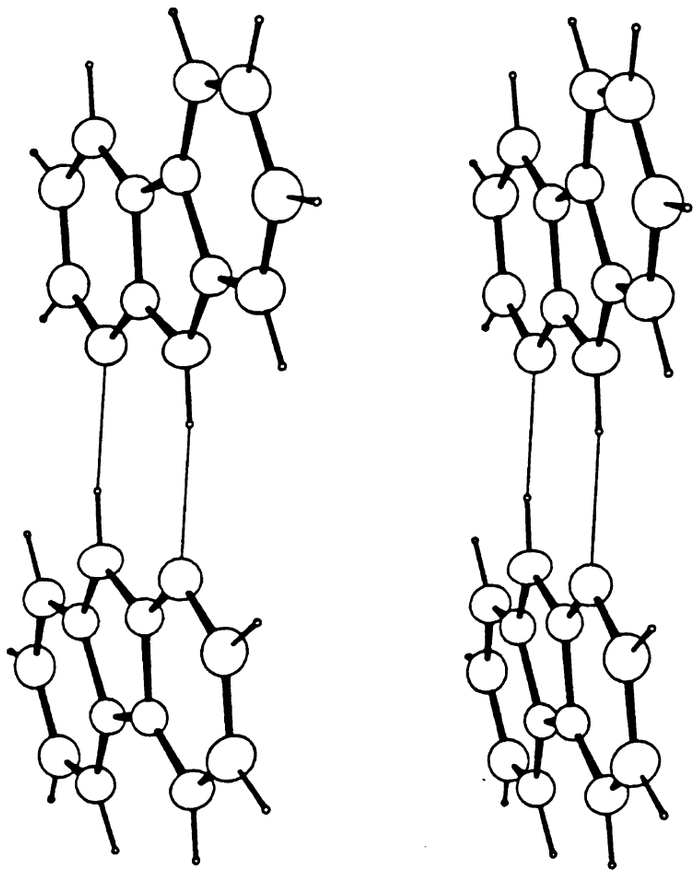

Figure 65. Stereoscopic view of a hydrogen-bonded dimer molecule.

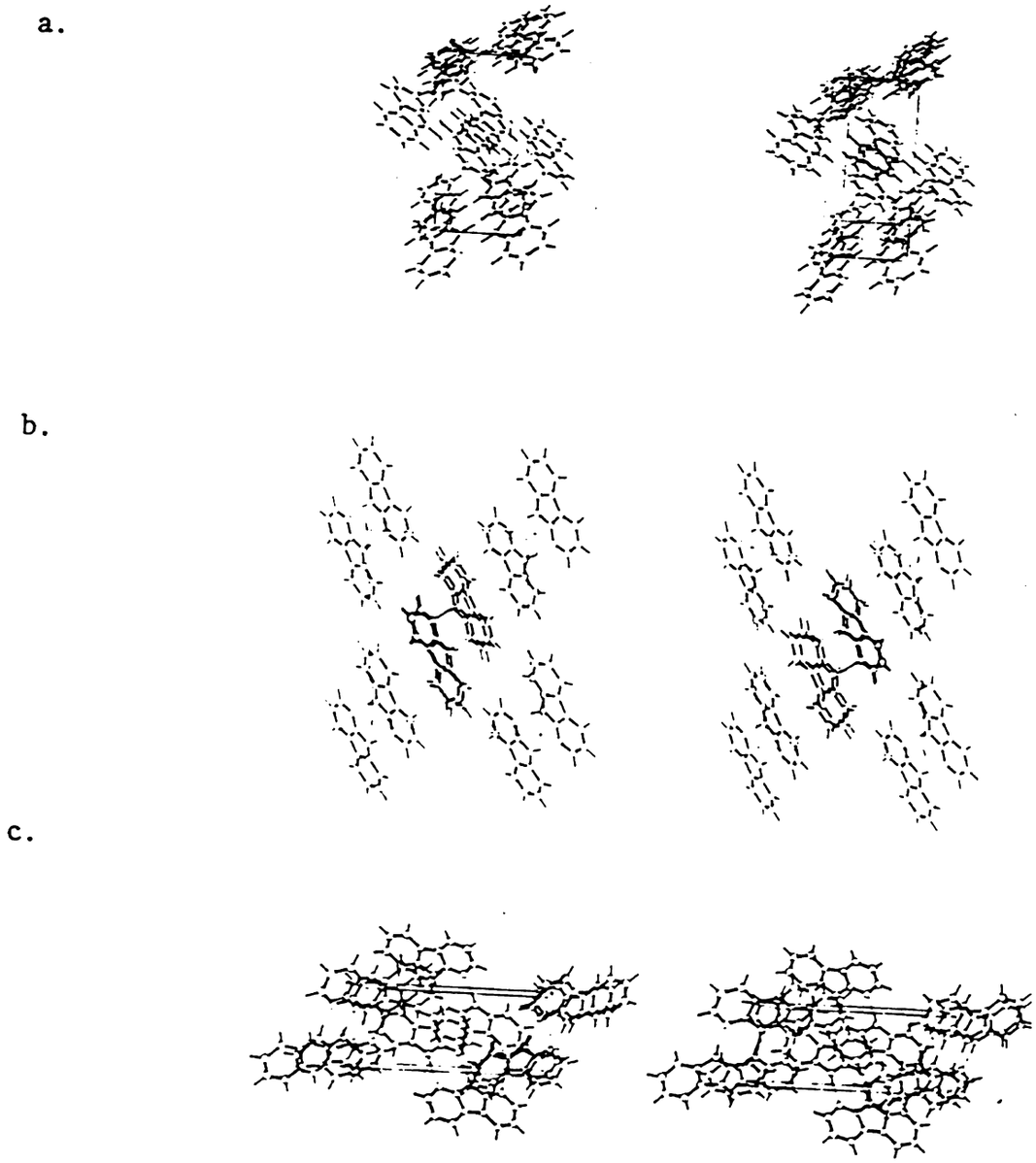

Figure 66. Stereoscopic views of the packing of dimer molecules into the unit cell.

a. Viewed down the a* axis with +b to the right and +c towards the top of the page.
b. Viewed down the b axis with +c to the right and +a towards the top of the page.
c. Viewed down the c* axis with +a to the right and +b towards the top of the page.

a KBr pellet. In both cases the free N-H stretching vibration ($\sim$3480 cm^{-1}) is absent.

The room temperature fluorescence spectrum of a single crystal of 1-azacarbazole which has been grown by slowly cooling the liquid is shown in Figure 67. The spectrum shows clearly that an emission band occurs at $\sim$500 nm which is similar to the band observed in concentrated solution of 1-azacarbazole. The emission is therefore interpreted as being due to a tautomer formed via double proton transfer in the excited state. This result is what is expected from the fact that the crystal consists of hydrogen bonded dimers.

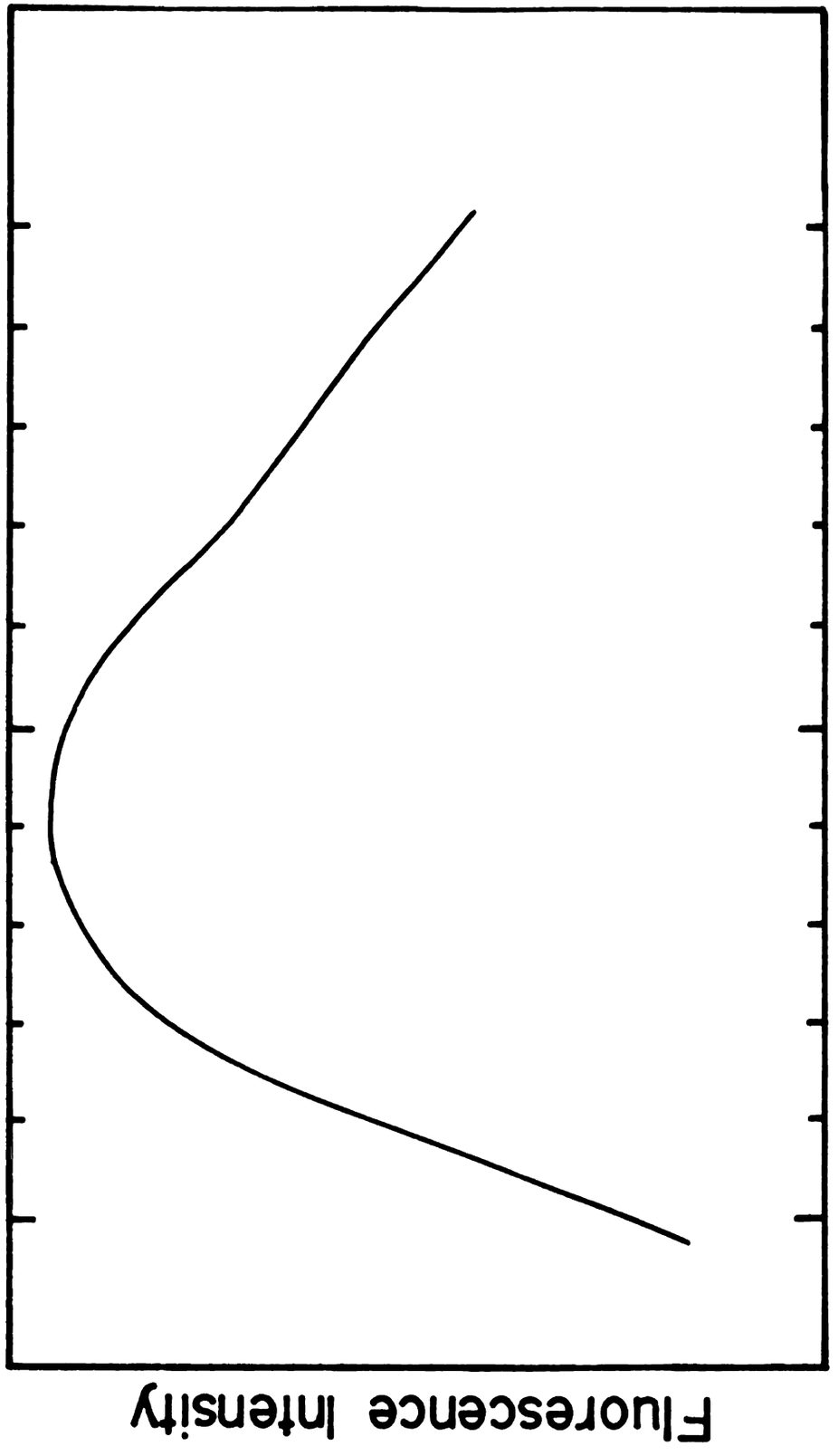

Figure 67. Room temperature fluorescence spectrum of 1-azacarbazole in the solid phase.

CHAPTER IV

EXPERIMENTAL

A. Experimentally Studied Molecules

1. Para Amino Salicylic Acid (PAS)

PAS was obtained from Aldrich Chemical Company, and was further purified by crystallization from ethanol M.W. = 153.14, MP = 144-145 (dec.)

2. Methyl Para Amino Salicylic Acid (PASE)

PASE was synthesized by using the method of selective esterification of aromatic carboxylic acids which have other reactive groups by using a Boron Trifluoride Etherate-Alcohol reagent[186] and was purified by crystallization from ethanol. Confirmation of the identity of the compound was done by measuring the melting point (120°C), the mass spectrum (MW= 167.14), and NMR and infrared spectra (in a KBr disk). The UV absorption spectrum is almost identical to that of PAS.

3. N,N Dimethyl Para Amino Salicylic Acid (DPAS)

DPAS was purchased from Aldrich Chemical Company, and was crystallized from ethanol, MW = 181.19, MP = 140 (dec.)

4. Methyl N,N Dimethyl Para Amino Salicylic Acid (DPASE)

DPASE was synthesized in the same way as PASE. Characterization of the compound was done by melting point 85°C, and by obtaining the mass spectrum (M.W. = 195.19), NMR and infrared (in KBr) spectra. The u.v. absorption spectrum is almost identical to that of DPAS.

5. 1-Azacarbazole (1AC)

1AC was synthesized by using the method of L. Stephenson and W. K. Warburton[187] with more attention to the effect of light, and purification of starting materials. It was recrystalized from ethanol several times. Confirmation of the identity of the compound was done by measuring the melting point (217°C) and from the mass spectrum. The pyrrolic hydrogen was identified by N.M.R. with $\tau = -1.79$. The UV absorption spectrum is almost identical to that of carbazole. The expected $n \rightarrow \pi^*$ transition must be completely hidden by the more intense $\pi \rightarrow \pi^*$ absorption band.

6. N_1-Methyl 1-Azacarbazole Tautomer

After dissolving 1 gm of 1AC in toluene, we added 1.5 ml. dimethylsulfate. The solution was then refluxed for 10 hours, and cooled down. The solid was filtered and recrystalized from acetone and methanol. The white crystals have been identified as α-carbolium methylsulphate. After dissolving in acetone, it was neutralized by adding NaoH solution. The yellow precipitate was separated. The final

bright yellow crystals with m.p. 130 to 132°C have been identified as the N_1-methyl 1-azacarbazole tautomer by Mass, NMR, and UV, spectra.

B. Solvents

1. 3-Methylpentane (3MP)

A modified version of the purification method of Potts (188) was used. Phillips pure grade 3-methylpentane (3MP) was mixed with a 50:50 mixture of concentrated sulfuric acid and concentrated nitric acid, then stirred for two days. Then it was separated and stirred with concentrated sulfuric acid for several hours until the dark red color disappeared and the acid layer became yellowish brown. After separation, it was stirred with a dilute solution of sodium carbonate for one hour until CO_2 production ceased. The 3MP was then stirred several times with distilled water until the water remained clear compared to the initial yellow color it attained after the first stirring. After drying the 3MP overnight over anhydrous sodium sulfate, the solution was refluxed over sodium wires for two days and distilled. The vapor was passed through a four foot vacuum-jacketed column and condensed at a speed of two drops per minute. The purity was checked by obtaining the absorption spectrum. Passing the distillate through a 1m column of activated silica gel did not alter its absorption characteristics so this was not required in the purification process.

2. Ethanol

Absolute ethanol was fractionally distilled through a 1 meter vacuum jacketed column. The distillation rate was adjusted so that a very slow rate (about 5 drops per minute) was maintained. Distillation continued until the benzene-alcohol azeotrope was no longer present as determined by an absorption spectrum of the distilled alcohol in a 10 cm cell. That is, the characteristic benzene UV absorption was no longer apparent. Ethanol was then distilled and used as needed.

3. Ether

Ether was distilled over sodium hydroxide.

4. Water

Only doubly-distilled water was used.

5. Cyclohexane

Aldrich Chemical Company (spectra grade).

6. Hexane

This solvent was slowly refluxed over benzophenone and sodium wire until the blue color turned to white. Dry hexane was used after distillation.

C. Spectral Measurements

1. Absorption Spectra

All reported absorption spectra were run on a Cary Model 17 spectrophotometer.

2. Emission Spectra

Most of the fluorescence spectra were obtained with an Aminco-Bowman spectrofluorometer equipped with a high pressure Xenon arc lamp and an EMI 9781 R photomultiplier tube.

To obtain better resolved emission spectra, a multi-component system was used. A high intensity Xenon lamp (500W) was used as the light source, the excitation wavelengths were reflected by a Bausch & Lomb 10 cm grating glazed at 300 Å in a B & L 500 mm monochromator (which provides a narrow excitation band width). The excitation illumination was focused on the sample by using quartz lenses, and emission was detected at a right angle relative to excitation. The emission monochromator was a Spex 1700-II which utilized a 10 cm B & L grating glazed at 5000Å. The emission spectrum was detected with an EMI 9558 QA photomultiplier tube. The tube's input voltage was maintained by a Fluke 412B power supply which was normally operated at 1100V. Signals from the detected emission were fed to a Princeton Applied Research HR-8 Lock-in Amplifier whose reference was provided by a light chopper. Finally, the

amplified emission signal was displayed on a strip-chart recorder. Phosphorescence spectra were obtained with Amino SPF 500 equipped with a rotating can (SLM Instruments Inc) chopper.

3. Infrared Spectra

Infrared spectra were obtained by using a Perkin-Elmer 457 Grating Infrared spectrophotometer. Calibration of frequency reading was made with a polystyrene film. Samples were examined as KBr disks.

4. Mass Spectra

Mass spectra were taken with a Finnigan EI.CI gas chromatograph-mass spectrometer.

5. NMR Spectra

NMR Spectra were run on a varian T-60 NMR Spectrometer system.

CHAPTER V

CONCLUSION AND FUTURE WORK

Absorption spectra of dilute solutions of PAS have been measured in different media. Depending on the solvent, an intramolecular hydrogen bond or intermolecular hydrogen bonds are formed. The interpretation of the absorption spectra which are dominated by "charge-transfer" transitions has been obtained by studying the effect of medium, pH and substituents effect and comparison with the related compounds. The absorption and emission characteristics of different species which may exist in the ground and excited states have been obtained by studying the effect of pH on the absorption and emission spectra of PAS and its methyl ester (PASE). This study has revealed the occurrence of excited state proton transfer in both PAS and PASE. The fluorescence spectra of PAS in 3MP and ether consist of two bands, one at 340 nm which is due to the neutral form, and the other at 450 nm and is due to zwitterion species produced via an intramolecular PT in the excited state (S_1). In ethanol and water we have intermolecular proton transfer from hydroxyl group to the solvents molecule. In all solvents PASE exhibit two emission bands, the long wavelength emission band in

3MP and ether arises from intramolecular PT. The short wavelength emission band is solvent dependent.

The observation of these two emission bands is probably due to an equilibrium between the ground state conformers. Further study is needed specifically for these compounds of three functional groups to account for ground state conformers. Excitation wavelength dependence in both hydrocarbon and hydrogen bonding solvents could confirm such possibility. To identify different species in the excited state and to measure the rate of excited state proton transfer, picosecond time-resolved studies are required.

The crystal structure of PAS shows intra- and intermolecular hydrogen bridges. We measured the fluorescence spectrum of PAS in the solid phase. Information from the solution spectra of PAS helped to interpret the emission band in the solid phase of PAS in terms of an excited state intramolecular proton transfer. Further studies including the effect of temperature and time resolved technique may reveal interesting information about excited state proton transfer (EPT), in the solid phase.

Absorption and luminescence properties of DPAS and its methyl ester DPASE also have been investigated under various conditions. The results of absorption spectra of DPAS in different solvents are similar to that of PAS with a very important exception, namely, an energy-level reversal of the two charge-transfer states. The emission spectra clearly reveal the occurrence of PT in the excited state (S_1). Excited state PT occurs either intramolecularly or

intermolecularly depending on the medium. For DPAS in 3MP, the intensity of the short wavelength (354 nm) emission band is higher than that of the 460 nm emission band which is the reverse situationwith PASE and MSA. Excitation wavelength dependence clearly demonstrates that at a longer excitation wavelength (330 nm) the emission occurs at 354 nm while a shorter excitation wavelength (300 nm) gives rise to an emission at ∿460 nm as well as at 354 nm. In the case of DPAS, depending on the electronic state excited two pathways are possible. Excitation of the (O) C.T. state, may lead to radiationless transition to the lowest excited singlet state, (N) C.T., giving rise to an emission at 354 nm or an excited state proton transfer may occur giving rise to the zwitterion species and leading to an emission at 460 nm. Excitation of the (N) CT band on the other hand, will give rise to 354 nm emission only. In the case of DPAS, we are dealing with excitation of two different electronic states of the same conformer. In contrast, the emission of MSA is varied as a result of excitation of different conformers which are at equilibrium in the ground state. Further studies such as temperature effect and time-resolved spectroscopy will be very helpful in revealing more information about the mechanism and the rate of P.T. in this molecular system.

Solutions of 1-azacarbazole in 3MP at concentrations where hydrogen-bonded dimers are formed (6×10^{-4}m) exhibit both F_1 and F_2 fluorescence. The relative intensities of F_1 and F_2 depend on the concentration, excitation wavelength and

temperature. All these studies as well as the study of model compounds indicates that the record fluorescence band originates from a tautomer formed by excited state double P.T. within a hydrogen bonded dimer. The enhanced acidity of the pyrrolic proton and basicity of the aza-nitrogen in the lowest excited state of 1-azacarbazole (^1L_a state) makes the proton transfer process favorable. A preliminary study for the rate of P.T. set 6.1×10^7 sec^{-1} for the rate of P.T. and the energy barrier is estimated to be 2.95 Kcal $mole^{-1}$. The 1-azacarbazole-acetic acid complex undergo also an excited state proton transfer that is much more efficient than in 1-azacarbazole dimer. The phosphorescence spectrum of this compound occurs at $\sim$440 nm which is far from F_2 emission band. This system is ideal to study the temperature and deuterium-isotope effect in order to determine whether a tunneling proton transfer mechanism is operative at low temperature. A study of the dynamics of excited-state proton transfer in 1-azacarbazole using picosecond time resolves spectroscopy is also needed.

The crystal structure as determined by x-ray diffraction methods shows that the crystal contains cyclic dimers only. We have also measured the UV absorption and infrared spectra of this molecule in nujol mull and in KBr pellets; both are consistent with the existence of hydrogen bonded dimer in this system. A preliminary study of the fluorescence spectrum of a single crystal shows an emission band at $\sim$500 nm which is similar to the band observed for concentrated

solution of 1-azacarbazole. This indicates that excited state proton transfer occurs in the crystal.

REFERENCES

REFERENCES

1. J. N. Brönsted and K. J. Pederson, Z. Phys. Chem. 108, 185 (1928).

2. M. Eigen and L. deMaeyer, Z. Electrochem. 59, 986 (1955).

3. For this theory, P. Mitchell has been awarded the Nobel Prize in Chemistry for 1978; see A. L. Lehninger, Biochemistry (Worth, NY, 1970).

4. A. J. Kresge, Accts. Chem. Res. 8, 354 (1975).

5. Isotopes in Organic Chemistry, E. Buncel and C. C. Lee, ed. (Elsevier, Amsterdam 1976).

6. R. A. Marcus, Faraday Symp. 10, 60 (1975).

7. M. Eigen, Angew. (Chem. Int. Ed. Eng. 3, 1 (1964)) and references therein.

8. E. Grunwald and E. K. Ralph, Accts. Chem. Res. 4, 107 (1971).

9. A. Weller, Progress in Reaction Kinetics 1, 189 (1961).

10. M. R. Loken, J. W. Hayes, J. R. Gohlke, and L. Brand, Biochem. J., 11, 4779 (1972).

11. G. Weber and K. Rosentieck, Biochem. Symp. 1, 333 (1964).

12. G. Weber, D. J. R. Laurence, Proc. Biochem. J., 56, (1954).

13. M. Deluca, L. Brand, T. A. Cebula, H. H. Seliger, and A. F. Makula, Time-resolved Proton-Transfer, 246, 6702 (1971).

14. P. A. Kollman, and L. C. Allen, Chem. Rev., 72, 283 (1972).

15. J. E. DelBene, J. Chem. Phys., 58, 3139 (1973).

16. C. A. Coulson, and V. Danielson, Arkiv, Kysik. 8, 205 (1955).

17. S. Bratoz, Symp. Forces Intermoleculaires, Bordeaux, 1965.

18. G. M. Barrow, J. Am. Soc., 78, 5802 (1956).

19. H. Baba, A. Matsuyama, and H. Kokubum, J. Chem. Phys., 41, 895 (1964).

20. M. Arrio-DuPont, Biochem. Biophys. Research Communications 44, 653 (1971).

21. G. L. Bell and G. M. Barrow, J. Chem. Phys., 31, 1158 (1959).

22. G. M. Barrow, Spectrochim. Acta 16, 799 (1960).

23. Kreuger, Can. J. Chem., 42, 201 (1964).

24. G. E. Bacon, in D. Hadzi (editor), Hydrogen Bonding, Pergamon London, 1959, p. 23.

25. A. Piekara, J. Chem. Phys., 36, 2145 (1962).

26. A. R. Ubbelohde, and K. J. Gallagher, Acta Cryst., 8, 71 (1955).

27. Y. Imry, I. Pelah, and E. Wiener, J. Chem. Phys., 43, 2332 (1965).

28. S. Ganesan, Nature, 185, 757 (1960).

29. A. Grimson, J. Phys. Chem., 67, 962 (1963).

30. C. C. Costain, and G. P. Srivastava, J. Chem. Phys., 41, 1620 (1964).

31. R. Blinc, and M. Pintar, J. Chem. Phys., 35, 1140 (1961).

32. J. L. Wood, J. Mol. Structure, 13, 141 (1972).

33. R. Blinc, D. Hadzi, and A. Novak, Z. Elektrochem., 64 567 (1960).

34. R. Blinc, and D. Hadzi, Spectrochim. Acta, 16, 852 (1960).

35. D. Hadzi, Pure and Appl. Chem., 11, 435 (1965).

36. E. Clementi, J. Mehl, and W. von Niesen, J. Chem. Phys., 54, 508 (1971).

37. P. O. Löwdin, Rev. Mod. Phys., 35, 724 (1963).

38. M. Kasha, Disc. Faraday Soc., 9, 14 (1950).

39. N. S. Bayliss and E. G. McRae, J. Phys. Chem., 58, 1002 (1954).

40. G. C. Pimentel, J. Am. Chem. Soc., 79, 3323 (1957).

41. K. Weber, Z. Phys. Chem., B15, 18 (1931).

42. A. Weller, Z. Physik. Chem., 3, 238 (1955).

43. A. Weller, Z. Elektrochem., 56, 662 (1952).

44. A. Weller, Z. Physik. Chem., 15, 438 (1958).

45. T. Förster, Naturwiss. 36, 186 (1949).

46. T. Förster, Z. Elektrochem. 54, 42 (1950).

47. T. Förster, Z. Elektrochem., 54, 531 (1950).

48. E. Z. Lippert, Naturforsch, 109, 541 (1955).

49. E. Z. Lippert, Elektrochem., 61, 962 (1957).

50. A. Weller and W. Urban, Angew Chem. 66, 336 (1954).

51. H. Kokubun, Naturwiss, 44, 233 (1957).

52. A. Weller, Z. Elektrochem., 58, 849 (1954).

53. A. Weller, Z. Elektrochem., 61, 956 (1957).

54. A. Weller, Z. Physik. Chem., 18, 163 (1958).

55. G. Jackson, and G. Porter, Proc. Roy. Soc., (London), A260, 13 (1961).

56. E. Vander Donckt, Progr. Reaction Kinetics, 5, 273 (1970).

57. J. F. Ireland, and P. A. H. Wyatt, Adv. Phys. Org. Chem., 12, 131 (1976).

58. C. Parker, "Luminescence of Solution", 1970.

59. Albert and E. P. Sargent, "Ionization Constants of Acids and Bases", Methuen, London, 1962.

60. S. G. Schulman, P. T. Tidwell, J. J. Cetroelli, and J. D. Winefordner, J. Am. Chem. Soc., 93, 3179 (1971).

61. S. G. Schulman, and I. Pace, J. Phys. Chem., 76, 1966 (1972).

62. T. C. Werner, and D. M. Hercules, T. Phys. Chem., 74, 1030 (1970).

63. E. L. Wehry, and L. B. Rogers, Spectrochim. Acta, 21, 1976 (1965).

64. E. Lippert, W. Lüder and F. Möll, Spectrochim. Acta, 15, 858 (1959).

65. E. Vander Donckt, and G. Porter, Trans. Faraday Soc., 64, 3215 (1968).

66. H. H. Jaffe and H. Lloyd Jones, J. Org. Chem., 30, 964 (1956).

67. S. Udenfriend, "Fluorescence Assay in Biology and Medicine", S. Schulman, and H. Gershon, J. Phys. Chem., 72, 3297 (1968).

68. C. A. Parker, "Photoluminescence of Solutions", Elsevier, London (1968).

69. R. Argauer, and C. E. White, "Fluorescence Analysis", Dekker, New York (1970), Academic Press, NY (1962).

70. Li. L. Yang, M. S. Thesis, Michigan State University, 1974.

71. E. Vander Donckt, Bull. Soc. Chim. Belges, 78, 69 (1969).

72. G. Yagil, J. Phys. Chem., 71, 1034 (1967).

73. J. W. Bridges, and R. T. Williams, Biochem. J. 107, 225 (1968).

74. D. D. Rosebrook, and W. W. Brandt, J. Phys. Chem., 70, 3857 (1966).

75. N. Mataga and Y. Kaifu, Mol. Phys., 7, 137 (1963).

76. A. Weller, Z. Elektrochem., 60, 1144 (1956).

77. K. Hirota, Z. Phys. Chem. N. F., 35, 222 (1962).

78. D. L. Williams and A. Weller, J. Phys. Chem., 74, 4473 (1970).

79. K. C. Ingham and M. A. El-Bayoumi, J. Amer. Chem. Soc. 96, 1674 (1974).

80. M. A. El-Bayoumi and P. Avouris and W. R. Ware, J. Chem. Phys., 62, 2499 (1975).

81. W. Klöpffer, Adv. Photochem., 10, 311 (1977).

82. W. Bartok, P. J. Lucchesi, and N. U. Snider, J. Am. Chem. Soc., 84, 1842 (1962).

83. A. Weller, Naturwissenshaften, 42, 175 (1955).

84. G. M. Gantz, and W. G. Summer, Textile Rev. J., 27, 244 (1957).

85. P. J. Kovi, C. L. Miller, and S. G. Schulman, Anal. Chim. Acta, 61, 7 (1972).

86. W. Klöpffer and G. Naundorf, J. Luminescence, 8, 457 (1974).

87. IU. V. Naboikin, E. N. Pavolva, and B. A. Zaborozhnyi, Opt. Spectrosc. (Engl. Transl.), 6, 231 (1959).

88. G. J. Woolfe and P. J. Thistlethwaite, J. Am. Chem. Soc., 102, 6917 (1980).

89. P. J. Thistlethwaite and G. J. Woolfe, J. Chem. Phys. Lett., 63, 401 (1979).

90. D. Ford, P. J. Thistlethwaite, and G. J. Woolfe, J. Chem. Phys. Lett., 69, 246 (1980).

91. K. Z. Ismail, Ph.D. Thesis, Michigan State University 1982.

92. H. Beens, K. H. Grellman, M. Gurr and A. H. Weller, Disc. Faraday Soc. 39, 183 (1965).

93. E. M. Kosower and Hanna Dodiuk, J. Luminescence, 11, 249 (1975/76).

94. K. Sandros, Acta. Chem. Scand., A30, 761 (1976).

95. T. Yasunaga, N. Tatsumoto, H. Inoue and M. Miura, J. Phys. Chem., 73, 477 (1969).

96. K. K. Smith and K. J. Kaufmann, J. Phys. Chem., 82, 2286 (1978).

97. H. Shizuka, K. Matsui, Y. Hirata, and I. Tanaka, J. Phys. Chem., 80, 2070 (1976).

98. H. Shizuka, K. Matsui, Y. Hirata, and I. Tanaka, J. Phys. Chem., 81, 2243 (1977).

99. N. Mori, Y. Asano, T. Irie and Y. Tsuzuki, Bull. Chem. Soc., Japan, 42, 482 (1969).

100. J. Catalan and J. I. Fernandez-Alonso, Chem. Phys. Lett., 18, 37 (1973).

101. E. Canadell, J. Catalan and J. I. Fernandez-Alonso, Advance in Molecular Relaxation and Interaction Processes, 12, 265 (1978).

102. S. G. Schulman, P. J. Kovi and J. F. Young, J. Pharm., Sci., 62, 1197 (1973).

103. Iu. V. Naboikin, and B. A. Zadorozhnyi, Opt. Spectrosc. (Engl. Transl.), 8, 347 (1960).

104. W. R. Ware, P. R. Shukla, P. J. Sullivan, and R. V. Bremphis, J. Chem. Phys., 55, 4048 (1971).

105. Iu. V. Naboikin, B. A. Zadorozhnyi, and E. N. Pavlova, Opt. Spectrosc. (Engl. Transl.), 6, 312 (1959).

106. M. Oki, M. Hirota, and S. Hirofuji, Spectrochim., Acta. 22, 1537 (1966).

107. E. D. Bergmann, Y. Hirshberg, and S. Pinchas, J. Chem. Soc., 2351 (1950).

108. G. J. Woolfe, and P. J. Thistlethwaite, J. Am. Chem. Soc., 103, 3849 (1981).

109. P. T. McTigue, and P. T. Renowden, J. Chem. Soc., Faraday Trans. I., 71, 1784 (1975).

110. P. J. Kovi, and S. G. Schulman, Anal. Chem., 45, 989 (1973).

111. S. G. Schulman, P. J. Kovi, Anal. Chim. Acta, 67, 259 (1973).

112. S. Nagakura, and M. Gouterman, J. Chem. Phys., 26, 881 (1957).

113. (a) E. Lippert, Z. Naturf., 109, 541 (1955).

(b) E. Lippert, Z. Elektrochem., 61, 962 (1957).

113. (c) N. Mataga, Y. Kaifu, and M. Koizumi, Bull. Chem. Soc. Japan, 28, 690 (1955).

(d) N. Mataga, Y. Kaifu, and M. Koizumi, Bull. Chem. Soc. Japan, 29, 465 (1956).

(e) J. Czekalla, Z. Elektrochem., 64, 1221 (1960).

114. A. Weller, Z. Elektrochem. 56, 662 (1952).

115. (a) N. Mataga, Y. Kaifu, and M. Koizumi, Bull. Chem. Soc. Japan, 29, 115 (1956).

(b) N. Mataga, Bull. Chem. Soc. Japan, 31, 481 (1958).

116. (a) Th. Förster, Naturwissenschaften, 36, 108 (1949).

(b) Th. Förster, Z. Elektrochem., 54, 42 (1950).

(c) Th. Förster, Z. Elektrochem., 54, 531 (1950).

(d) A. Weller, Z. Elektrochem., 64, 55 (1960).

117. N. Mataga and Y. Kaifu, J. Chem. Phys., 36, 2804 (1962).

118. A. Matsuzaki, Nagakura, and K. Yoshihara, Bull. Chem. Soc. Japan, 47, 1152 (1974).

119. O. Stern, and M. Volmer, Phys. Z., 20, 183 (1919).

120. "Handbook of Chemistry and Physics", ed. by C. Hodgmon, Chemical Rubber, Cleveland, OH (1962), pp. 2258-2264.

121. A. Weller, Z. Phys. Chem. N. F., 17, 224 (1958).

122. M. V. Smoluchowski, Z. Phys. Chem., (Leipzig), 92, 129 (1917).

123. W. R. Ware and J. S. Novros, J. Phys. Chem., 70, 3246 (1966).

124. C. A. Taylor, M. A. El-Bayoumi, and M. Kasha, Proc. Nat. Acad. Sci. U.S., 63, 253 (1969).

125. M. A. El-Bayoumi, Ph.D. Thesis, Florida State University, 1961.

126. K. C. Ingham, M. Abu-Elgheit and M. A. El-Bayoumi, J. Amer. Chem. Soc., 93, 5023 (1971).

127. H. Bulska, and A. Chodkouska, J. Am. Chem. Soc., 102, 3259 (1980).

128. K. B. Eisenthal, K. Gnaedig, W. M. Hetherington, M. Crawford, and R. H. Micheels, Springer Ser. Chem. Phys. 4 (Picosecond Phenom.), 34-9 (1978).

129. W. M. Hetherington III, R. H. Micheels and K. B. Eisenthal, Chem. Phys. Lett., 66, 230 (1979).

130. P. Avouris, L. L. Yang, and M. A. El-Bayoumi, Photochemistry and Photobiology, 24, 211 (1976).

131. C. A. Taylor, Masters Thesis, Florida State University, 1969.

132. W. A. Van Hook in Isotope Effects in Chemical Reactions, eds., J. C. Collins and N. S. Bowman, ACS Monograph 167, Van Nostrand Reinhold, New York (1971). Earlier reviews are cited in this reference.

133. C. G. Swain, E. C. Stivers, J. F. Reuwer, Jr., and L. J. Schaad, J. Amer. Chem. Soc., 80, 5885 (1958).

134. E. S. Lewis and J. K. Robinson, J. Amer. Chem. Soc., 90, 4337 (1968).

135. M. J. Stern and P. C. Vogel, J. Amer. Chem. Soc., 93, 4664 (1971); M. J. Stern and R. E. Weston, Jr. J. Chem. Phys., 60, 2815 (1974).

136. J. Bigeleisen, Tritium in the Physical and Biological Sciences, IAEA, Vienna, Vol. 1 (1962), p. 161.

137. R. P. Bell, The Proton in Chemistry, 2nd Ed., Chapman and Hall (1973).

138. E. F. Caldin, Chem. Revs., 69, 135 (1969).

139. A. J. Kresge, Pure Appl. Chem., 8, 243 (1964).

140. V. Gold, Adv. Phys. Org. Chem., 7, 259 (1969).

141. P. M. Laughton, and R. E. Robertson, Can. J. Chem. 34, 1714 (1956).

142. R. E. Robertson, Can. J. Chem., 35, 613 (1957).

143. R. E. Robertson, and P. M. Laughton, Can. J. Chem., 35, 1319 (1957).

144. F. D. Rossini, J. W. Knowlton, and H. L. Johnston, J. Res. Natl. Bur. Stand., 24, 369 (1940).

145. W. M. Jones, J. Chem. Phys., 48, 207 (1968).

146. C. G. Swain, and R. F. W. Bader, Tetrahedron, 10, 182 (1960).

147. C. G. Swain, A. D. Ketley, and R. F. W. Bader, J. Am. Chem. Soc., 18, 2353 (1959).

148. F. Hund, Z. Physik, 43, 805 (1927).

149. E. P. Wigner, Z. Phys. Chem. (Leipzig), B19, 203 (1932).

150. D. M. Dennison, and G. E. Uhlenbeck, Phys. Rev., 41, 313 (1932).

151. E. Grunwald, in "Progress in Physical Organic Chemistry".

152. Cohen, Streitwieser, and Taft, eds. Wiley, NY 1965 Vol. 3.

153. H. S. Johnston, Adv. Chem. Phys., 3, 131 (1961).

154. E. F. Caldin, Chem. Rev., 69, 135 (1969).

155. C. Haas, and D. F. Horning, J. Chem. Phys., 32, 1763 (1960).

156. G. M. Barrow, Spectrochim. Acta. 16, 799 (1960).

157. D. Hadzi, J. Chem. Phys., 34, 1445 (1961).

158. P. O. Löwdin, Adv. Quantum Chem., 2, 213 (1965).

159. J. K. Marsh, J. Chem. Soc., 125, 418 (1924).

160. W. Klöpffer and G. Kaufmann, J. Luminescence, 20, 283 (1979).

161. B. A. Zadorozhnyi and I. K. Ishchenko, Opt. Spectry. (English. Transl.) 19, 306 (1965).

162. H. Kokubun, Z. Physik. Chem., 13, 386 (1957); Naturwissenschaften 44, 233 (1957); Z. Elektrochem. 62, 599 (1958).

163. A. N. Terenin and A. V. Karyakin, Doklady Akad. Nauk SSSR 8, 425 (1947); Nature 159, 115 (1947).

164. A. V. Sheblya and A. N. Terenin, Optika. Spektr. 10, 617 (1961).

165. Yu. N. Sheinker and I. Ya. Partovskii, Zhur. Fiz. Khim. 32, 394 (1958).

166. F. Bertinotti, G. Giacomello and A. M. Liquori, Acta Cryst. 7, 808 (1954).

167. R. S. Mulliken, J. Am. Chem. Soc., 74, 811 (1952).

168. S. P. McGlynn, Chem. Rev., 58, 1113 (1958).

169. G. Briegleb, Elektronen-Donator-Acceptor Komplexe Springer-Verlag, Berlin-Gottingen-Heidelberg, 1961.

170. J. N. Murrel, Quart. Rev., 15, 191 (1961).

171. R. S. Mulliken and W. B. Person, Ann. Rev. Phys. Chem. 13, 107 (1962).

172. B. Ramsey, M. A. El-Bayoumi, and M. Kasha, J. Chem. Phys., 35, 1502 (1961).

173. J. N. Murrell, The Theory of Electronic Spectra of Organic Molecules, Wiley (1963).

174. L. Lannelli, P. Giordano Orsini and G. Daniele, R. C. Accad. Napoli, 20, 1 (1953).

175. C. Chang, N. Sharbestury and M. A. El-Bayoumi, J. Chem. Phys. Lett. 75, 107 (1980).

176. X-ray structure was determined by D. L. Ward, Michigan State University in 1978.

177. A. Bree and R. Zwarick, J. Chem. Phys., 49, 3355 (1968).

178. K. R. Popov, L. V. Smirno, L. A. Nakhimovskaya and V. L. Grebneva, Opt. i Spektroskopiya 31, 363 (1971).

179. H. U. Schuett and H. Zimmermann, Ber. Bunsenges. Physik. Chem. 67, 54 (1963).

180. A. Marty and P. Viallet, J. Photochem., 1 (6), 443 (1973).

181. C. Chang, Ph.D. Thesis, Michigan State University, 1978.

182. K. T. Wei and D. L. Ward, Acta Crystallographica, B32, 2768 (1976).

183. G. G. Multan, P. Main and M. M. Woolfson, Acta Crystallographica, A27, 368 (1971).

184. A. Zalkin, private communication (1974).

185. C. K. Johnson (1965). "ORTEP. A FORTRAN Thermal-Ellipsoid Plot Program for Crystal Structure Illustrations", Report ORNL-3794, Oak Ridge National Laboratory, Oak Ridge, Tennessee.

186. P. K. Kadaba, J. Pharm. Sci., 63, 1333 (1974).

187. L. Stephenson, and W. K. Warburton, J. Chem. Soc. (c), 1355 (1970).

188. N. S. Potts, J. Chem. Phys., 20, 809 (1952).

MICHIGAN STATE UNIVERSITY LIBRARIES
3 1293 03146 0342